PHASE TRANSITIONS

AND DIVERSIFICATION

IN COMPLEX SYSTEMS.

The role of heterogeneities, adaptation and other essential aspects of real systems.

PhD Thesis by Paula Villa Martín
for the degree of Doctor of Philosophy

Supervised by Miguel Ángel Muñoz Martínez

February 2017

Departamento de Electromagnetismo y Física de la Materia
Condensada e Instituto Carlos I de Física Teórica y Computacional
Facultad de Ciencias
Universidad de Granada

Editor: Universidad de Granada. Tesis Doctorales
Autora: Paula Villa Martín
ISBN: 978-84-9163-157-6
URI: http://hdl.handle.net/10481/45496

La doctoranda Paula Villa Martín y el director de la tesis Miguel Ángel Muñoz Martínez, Catedrático de Universidad,

Garantizamos, al firmar esta tesis doctoral, *Phase transitions and diversification in complex systems. The role of heterogeneities, adaptation and other essential aspects of real systems*, que el trabajo ha sido realizado por el doctorando bajo la dirección de los directores de la tesis y hasta donde nuestro conocimiento alcanza, en la realización del trabajo, se han respetado los derechos de otros autores a ser citados, cuando se han utilizado sus resultados o publicaciones.

Granada a 24 de Enero de 2017

Director de la Tesis:	Doctoranda:
Miguel Ángel Muñoz	Paula Villa Martín

Agradecimientos

Esta tesis ha sido fruto de un aprendizaje en el que han participado muchas personas directa e indirectamente.

En primer lugar, mi supervisor Miguel Ángel Muñoz, que me ha enseñado muchísimo, en todos los sentidos. Muchísimas gracias por tu paciencia, motivación, preocupación y buen humor durante estos años. Igualmente, quiero agradecer la dedicación y gran calidad de trabajo de mis colaboradores Juan Antonio, Paolo, Jordi y Rafa. He disfrutado y aprendido muchísimo con todos vosotros.

No menos importante han sido los buenos consejos y buen humor de Pedro, Paco, Pablo, Antonio, Joaquín Marro y Joaquín Torres. Muchas gracias. Trabajar en este departamento es un privilegio y un placer. In this regard, I want to thank David Nelson, Bryan, Thip and Severine for the warm welcome they gave me during my stay in Boston. I learned very very much with you and enjoyed the scientific discussions. I really appreciated the good environment you have at the Lab.

En un plano más personal, es imprescindible agradecer a las muchas personas que me han alegrado, apoyado y ayudado tanto estos años. Sin ellos esta tesis habría sido mucho más difícil de llevar.

Empezaré por aquellos con los que he compartido tantas horas de despacho, risas, tapas, fiestas y "preocupaciones" doctorales (por orden de llegada). En primer lugar a Jordi, que ya conocí durante la carrera. Muchísimas gracias por toda tu ayuda, tanto profesional, como personal. Desde las explicaciones más básicas de física y SOFTWARE en el primer año, hasta los papeleos pre-depósito de tesis, has estado ayudando en todo lo posible y con una sonrisa. Espero poder ser algún día tan generosa como tú. En segundo lugar a Virginia, que conocí en el famoso "gineceo" del departamento y en la inolvidable escuela de verano de Benasque. Compartir despacho y las experiencias en congresos, el Dojo, el imperial assault, los estados

absorbentes..., y mucho más, ha sido de lo mejor. Muchísimas gracias por ello y por tu ayuda durante el doctorado, sobretodo en los últimos agobios de la tesis. A Jose quiero darle las gracias, no solo por su increíble trabajo con PROTEUS, sino por su apoyo y preocupación por nosotros y su gran paciencia cuando le pedimos ayuda desesperados con el mundo tecnológico. También quiero agradecer a Nico las energías, ganas y motivación que desprende en todo lo que hace y la practicidad y calma de Pablo. Espero que se me haya pegado algo de todo ello durante estos años. Igualmente, he admirado el humor, humildad y buen hacer de Paolo. Muchas gracias por las conversaciones durante el té/café en la cocina del departamento y preocuparte de que no me pasara trabajando los viernes por la tarde. También quiero agradecer a Vanessa su alegría y los viernes ingleses.

Aunque haya pasado menos tiempo con vosotros, los doctorandos anteriores y posteriores a nosotros también han sido parte importante estos años: Dani, Juan Antonio, Jorge, Sam, Sebas, Carlos, Jesús, Ana, Jose, Serena, Carmen y Javi. ¡Espero poder volver/seguir tapeando con vosotros por Granada! En particular, querría agradecer a Jesús su ayuda en Boston soportando lo que nos cayó encima... ;D

A todos nosotros también están ligados nuestros compañeros y amigos de la universidad Álvaro, Javi, María José, Pablo (Frai ;P), Patricia, Irene, Rafa, Leo, Migue, Juanpe, German, María del Mar, Alice, Miki, Esperanza, Laura, Ben... y muchos más. He descubierto muchísimas cosas con vosotros. Muchas gracias por compartir vuestra forma de ver la vida y la sociedad, vuestros debates, y vuestra fe y acciones por un mundo mejor.

En este punto tengo también que recordar a todas las personas con las que he compartido congresos y escuelas de verano: Edgar, Uri, Edo, Sveto, Dani, Rubén, Ignacio, Ana, Salva, Luiño... Además de aprender con vosotros, he disfrutado mucho las comilonas, visitas y fiestas en Benasque, Mallorca, Barcelona, Madrid y Granada. Espero que nos volvamos a reunir en algún otro lugar.

Fuera del contexto universitario, con amigos como M Felix, Ana, Pilar, Esperanza, Carlos, Juanga, Rafa, Salva, Maite, Cristina, David ("el químico" ;P), Brayan, Davi, Jose Alberto, Jonathan, Eli, Muerte, Mariña, Jose, Cris, Fiona, Ana Celia, David, Tocayo, Ana, Manolo, Greta, y otros muchos, he pasado muy buenos momentos. Sois maravillosos. Igualmente, el aikido de Luis y los compañeros del Dojo Musubi, y los platos tan ricos del Bambi y el Bambú me han alegrado mucho estos años.

Por último (y no menos, sino más importante), quiero dar las gracias a todas las personas más cercanas a mí. A mis padres, por el cariño y los sabios consejos que me han dado en todo momento. Nuestras conversaciones siempre me calman y me dan energías para afrontarlo todo. A mis abuelos, padrinos, y resto de familia, por preguntarme interesados por mi investigación, y preocuparse por mi felicidad. Y a Fer, por ayudarme tanto y tan bien, ser tan paciente conmigo en todo (sobretodo en estos últimos momentos), y el hacer lo posible para que sea feliz.

A mis padres.

Contents

Chapter 0

Introduction

For a very long time, humans have tried to understand the seemingly capricious behavior of Nature. Since the origin of modern Science, a reductionist agenda relying on the famous words of Descartes –*"Divide each difficulty into as many parts as is feasible and necessary to resolve it"*– has been pursued. Thereby, efforts toward understanding the elements of isolated phenomena have prevailed for years, and specialized and disconnected areas of knowledge arose.

Despite the unquestionable success of Science following this strategy, numerous phenomena are still puzzling. For instance, life origins, the emergence of biodiversity, species extinctions, global climate, desertification, epidemic spreading, genetic expression, cancer success, brain functioning, social organizations or market fluctuations, are some examples. The difficulty to develop suitable models to predict or explain such phenomena emphasized the necessity of searching for other strategies. In this regard, "complexity science" has emerged as a promising research area. While reductionism strives for gathering detailed information on separated elements of some particular scale, complexity science relies on identifying the mechanisms by which emergent collective behavior, unexpected from naive analyses of the individual parts in isolation, appears from the interactions among the many constituents of lower

hierarchical levels.

Within this framework, a major and intriguing challenge arises: how can we capture the behavior of a large system while maintaining the specificity of its constituents? Usually, simple models need to renounce a proper description of either individuals, or systems. At the beginning, one might be tempted to include every possible detail of systems' elements and their interactions. However, this amount of information may obfuscate the essential features provoking the observed collective behavior.

Regarding many-body systems, statistical mechanics provides a rather useful mathematical framework for the understanding of complex systems. In particular, condensed-matter physics precisely focuses on predicting macroscopic collective behavior from the physics of its microscopic constituents, let them be atoms, molecules (of the same type or of a few different types), electrons, etc. In all cases, these are well described by the laws of physics. In problems of interest in e.g. biology, complex-system elements maybe heterogeneous and maybe not as "simple" and well-characterized as atoms. Despite this fact, valuable understanding can be obtained by adapting different techniques borrowed from standard statistical physics to these more complex scenarios. This suggests a "coarse-graining" general strategy that approximates a complex system to a more tractable one that maintains its main macroscopic behavior. Such process can reveal deep analogies in the organization of various systems that substantially differ in their elementary constituents. From a mathematical viewpoint, this idea is supported by the renormalization group theory.

The most prominent example of this type of "universality" emerges in the vicinity of phase transitions. Most many-body systems are known to exhibit macroscopic behaviors, i.e. "phases", corresponding to different microscopic organizations and different types of internal orderings. Fascinating examples of unexpected and sudden changes of such behaviors, as a consequence of the change of some external condi-

tion such as temperature, pressure, etc., are traditionally encountered in physics and chemistry. Statistical mechanics explains these phenomena as the result of some type of destabilization of the global system state. Depending on the manner in which the latter occurs we distinguish two main types of phase transitions: i) discontinuous or "first-order" transitions –characterized by abrupt changes of some of their variables and features such as phase coexistence or hysteresis cycles–; and ii) continuous or "second-order" transitions –in which variables change smoothly and scale-invariance or high susceptibilities emerge at the transition or "critical" point–. At the specific point at which these phase transitions occur, the macroscopic behavior becomes the same for systems with rather different microscopic details, for instance, the so-called critical exponents of liquid-gas transitions have been shown to coincide with those of some paramagnetic-ferromagnectic transitions. Equally, in experiments of catalytic reactions, percolation in porous media, avalanches of flowing granular matter, electro-positron collision, depinning transitions or polynuclear growth, measured critical exponents are surprisingly in accordance as well. It is important to remark that these statistical systems are studied in different ways depending on whether they obey the "detailed-balance" principle. If such principle is obeyed, the system would be in equilibrium, and it would be well-described by the Gibbs free energy. In the contrary case, the system would be out of equilibrium, and should be studied in terms of a "master equation".

The concepts of phases and phase transitions have been successfully extended to cover fields such as biology, ecology, socio-economical systems, etc. In these contexts, continuous and discontinuous transitions are also present although they are usually called "smooth" and "catastrophic" shifts, respectively. A clear example of the former is encountered in the spreading of diseases (or lack thereof). In this case, a continuous transition, between a successful or failed infection proliferation, is undergone as a function of the infection rates. Spreading would succeed for high infection rates while

it would fail for lower ones. Similar examples of smooth transitions and criticality features are ubiquitous in Nature. Continuous transitions separate for instance biodiversity versus mono-dominance in ecological systems, disagreement versus accordance in voters systems, etc. Critical behavior and scale invariance are observed in cortex activity experiments, earthquakes, bird flocks, etc. On the other hand, many systems in socio-economy and socio-ecology [148, 131], as well as ecosystems such as lakes, savannas, or oceans (with their embedded fisheries, or coral reefs) can experience, as a consequence of small changes in environmental conditions, catastrophic shifts after which recovery can be extremely difficult [180, 198, 111, 76, 34]. An important example took place in the Sahara many years ago. In this case, a gradual reduction of rains and, as a consequence, the local climate, lead to a quick collapse from a green area to the largest desert of our planet.

Regarding the previous discussion we wonder: What mechanisms make natural phenomena select a continuous or discontinuous transition? Is there some way of avoid discontinuous transitions? How are these systems altered by real mechanisms present in Nature? What are the effects of more complex mechanisms such as evolution and adaptation?

Here we try to shed light on these issues. For this we rely on standard techniques of statistical mechanics and the theory of stochastic processes, including: the theory of phase transitions both in equilibrium and away from equilibrium, mean-field approximations, renormalization group tools, as well as extensive computational analyses[1].

[1]For this purpose we have employed the super-cluster of PROTEUS that belongs to the "Instituto Carlos I de Física Teórica y Computacional" (Universidad de Granada). The huge capability of this cluster (with 13 teraflops and 1100 nuclei) has made possible to accomplish the extensive computational simulations needed in this thesis.

Outline of this thesis

In this thesis, by considering mathematical and computational models that account for the relevant aspects of some complex systems, we obtain predictions about the behavior and the phase transitions such systems exhibit. This is accomplished from two different perspectives: on the one hand, we perform technical and detailed studies of model systems of paradigmatic relevance in statistical physics, emphasizing their universal features. On the other hand, applying theories and techniques of statistical mechanics, we explore the potential of our results for real phenomena such as brain activity ecosystem dynamics and phenotypic diversification.

This work focuses on how the nature of phase transitions, whether continuous or discontinuous, is impacted by realistic, inherent, an unavoidable aspects of real out-of-equilibrium systems, such as (i) demographic and environmental fluctuations, (ii) spatial heterogeneities, and (iii) structural heterogeneities on many-body systems; paying special attention on how these ingredients may affect phase transitions. Some of the above-mentioned features can dramatically alter the type of the phase transitions that take place, changing for example from discontinuous to continuous, or the other way around. Let us briefly discuss these realistic aspects:

- (i) *The effect of demographic and environmental fluctuations.* Statistical physics tells us that some fluctuations are unavoidably present in small systems. In particular the central limit theorem quantifies the magnitude of such fluctuations by $\sqrt{N}$ (being N the size of the system). There are many situations in which fluctuations are essential to explain the actual behavior, possibly changing the deterministic (noiseless, meand-field) expectations. For instance, the capability of exploring multiple metastable states is only possible if fluctuations make the system able to escape from a given state to another. Another examples are noise-induced spatial patterns and fronts, noise-sustained waves in sub excitable

media, noise-induced ordering transitions, and noise-induced disordering phase transitions [81, 109].

In simple analyses of complex systems and their phase transitions, stochastic effects are sometimes ignored or averaged away. For example, in the studies of ecological regime-shifts deterministic approaches are customarily employed [128, 226, 145, 54]. In this thesis we analyze the effect of demographic stochasticity on such ecological complex systems subjected to a catastrophic transition.

- (ii) *Spatial heterogeneity.* Most real systems exhibit some type of spatial heterogeneity. In physics it can be attributed to solid imperfections, spatial effects which modify interactions, arrangement of adsorbates on a surface of heterogeneous catalysis, etc,. In biology or ecology it can be provoked by heterogeneous distribution of nutrients in a land, firewalls, termites mounds, etc,.

  In statistical mechanics, equilibrium arguments tell us that discontinuous transitions are precluded in low-dimensional systems presenting (quenched) spatial heterogeneity[3]. In this light, we develop a technical analysis to check whether this is the case in "non-equilibrium" physical systems. On the other hand, we study an ecological complex system presenting a discontinuous/catastrophic shift and explore the consequences of spatial heterogeneity.

- (iii) *Structural heterogeneity.* Individual components of complex systems usually interact with each other in an intricate way with interesting structural properties such as modularity, clustering, hierarchies, scale-free connectivity patterns, etc [4, 12]. Some examples include genetic networks, neural structures, food webs, social interactions, World Wide Web connections, etc. [4, 12]. Such complex networks can deeply alter expected behaviors of the system, and consequently, evidence the presence and relevance of internal non-trivial structures. We focus on the importance of complex networks on the particular case of integrative

neural dynamics (based on [1, 28, 29]) displaying discontinuous transition in the fully-connected (or mean-field) case [228].

A more detailed description of a complex biological system cannot rely solely on fluctuations and heterogeneities. According to Theodosius Dobzhansky: "Nothing in biology makes sense except in the light of evolution". It is unquestionable that biological systems, no matter what the scale is, evolve in time. Unlike disorder, fluctuations and heterogeneities, evolution acts in long time scales and no relevant effects are witnessed in communities dynamics. However, the existence of feedbacks between community and evolutionary processes are known to exist, having been empirically characterized in recent years in different types of communities (from microbes to plants and vertebrates) [171, 231, 101, 77, 211, 108, 48, 67, 45, 194, 209, 200, 201, 88, 70], and theoretically analyzed with novel and powerful mathematical tools. In this thesis, we show how evolution plays a fundamental role in systems exhibiting rapid species diversification[235]. Our results represent a first important step in the direction of a detailed study of transitions between generalist species-poor regimes, and specialist species-rich regimes.

Overview

Let us summarize the main issues treated in the different chapters of this thesis.

In **Chapter 1** basic concepts needed in this thesis are summarized. Firstly, main features of continuous and discontinuous phase transitions are presented analyzing prototypical models of statistical mechanics. Such analysis introduce the main tools that we employ throughout this work and the roles of stochasticity and diffusion in non-equilibrium systems. Then, the effect of spatial heterogeneities in equilibrium phase transitions is reviewed paving the way of its study in non-equilibrium conditions.

In **Chapter 2**, we study the importance of demographic stochasticity and diffusion in a generic system exhibiting a discontinuous transition in the mean-field approach. We investigate how the order of the transition would surprisingly depend on such mechanisms. Beside this, we also study the effects of the unavoidable presence of spatial heterogeneity in real systems. In this case, a rounding phenomenon for low dimensional systems appears. The ideas presented here can help to further understand discontinuous transitions, and contribute to the discussion about the possibility of preventing these shifts in order to minimize their disruptive ecological, economic, and societal consequences.

For a deeper understanding of some of the previous results, in **Chapter 3** we present a more technical and detailed study of the effect of spatial heterogeneity on a prototypical model exhibiting a discontinuous transition. Here we try to explain how, in analogy with what happens in problems of thermodynamic equilibrium, the existence of some form of spatial disorder implies that potentially discontinuous transitions are rounded-off, thus making the system critical (at low dimensions).

In this context, in **Chapter 4** we wonder whether a structurally (and so spatially) disordered system would also present the same smoothing effect. An extensive analysis

of all possible systems presenting this structural heterogeneity may constitute a thesis itself. As a consequence, we focus on the brain cortex, a system that is well described by models exhibiting discontinuous transitions at mean-field and which presents a complex and known network structure. Interestingly, criticality appears for small topological dimensions, in analogy to the case of spatial heterogeneity presented in **Chapter 3**. Integrative models of neural activity (which would exhibit discontinuous transitions in mean-field) are thus able to recover the features of scale invariance experimentally observed in cortical networks.

The above chapters do not consider any type of mutation or variation of its individuals due to the fact that, in those cases, evolution usually takes place in longer times than the considered ones. However, apart from the previous inherent properties, adaptation is an essential feature of real systems. What would happen if individuals rapidly evolve affecting community dynamics?

In **Chapter 5** we propose a relatively simple computational eco-evolutionary model specifically devised to describe rapid phenotypic diversification in a particular experiment of species-rich communities [235]. Despite this, the model is easily generalizable to analyze different eco-evolutionary problems within a relatively simple and unified computational framework. We show that it captures the main phenomenology observed experimentally, and it also makes non-trivial predictions. While no phase transition from poor to rich communities appear with the current simple model, in the future we will investigate what additional mechanisms may account for the emergence of such a phase transition.

Finally, thesis conclusions are presented in chapter **Chapter 6**.

What are the essential mechanisms underlying complex behavior such as cortex criticality, ecological catastrophic shifts or species diversification? How do realistic aspects such as stochasticity, diffusion or heterogeneities affect the phase transition that such systems exhibit? Is there some way to avoid catastrophic shifts? How

can cortex exhibit critical features while displaying integrative dynamics subjected to discontinuous transitions (at the mean-field level)? What are the mechanisms responsible of species diversification? Are they robust? How can such diversification be quantified? Relying on statistical mechanics techniques, we try to shed light on these questions.

Introducción

Desde hace muchos años, los humanos han intentado entender el comportamiento, aparentemente caprichoso, de la Naturaleza. Desde el origen de la Ciencia moderna, se ha seguido una estrategia reduccionista basada en las famosas palabras de Descartes ("*Divide cada dificultad en tantas partes como sea posible y necesario para resolverla*"). De este modo, un esfuerzo para entender los elementos que constituyen fenómenos aislados ha prevalecido durante años, y áreas de conocimientos especializadas y desconectadas han surgido.

A pesar del incuestionable éxito de la Ciencia al seguir esta estrategia, numerosos fenómenos naturales son aún desconcertantes y misteriosos. Algunos ejemplos son el origen de la vida, la emergencia de la biodiversidad, las extinciones de especies, el clima global, la desertificación, la propagación de enfermedades, la expresión genética, el cáncer, el funcionamiento del cerebro, las fluctuaciones del mercado... La dificultad de desarrollar modelos adecuados que predigan y expliquen estos fenómenos, enfatizaron la necesidad de buscar otras estrategias. En este contexto, la "ciencia de la complejidad" ha emergido como un área prometedora. Mientras que el reduccionismo se esfuerza por recopilar información detallada de elementos de una escala particular, la ciencia de la complejidad se basa en identificar los mecanismos por los que un comportamiento emergente colectivo –inesperado a partir de análisis sencillos de sus partes por separado– aparece de la interacción entre los muchos constituyentes del sistema a niveles jerárquicos inferiores.

Dentro de este marco teórico, un reto fascinante aparece: ¿cómo podemos capturar el comportamiento de un sistema de gran tamaño, mientras mantenemos la particularidad de sus constituyentes? Normalmente, los modelos simples tienen que renunciar a una descripción apropiada de, o sus individuos, o de los sistemas. En un primer momento, uno podría estar tentado a incluir todos los detalles posibles de los elementos del sistema y sus interacciones. Sin embargo, esta cantidad de información podría confundir sobre cuales son los aspectos fundamentales que provocan el fenómeno colectivo observado.

En cuanto a los sistemas de muchos cuerpos, la mecánica estadística proporciona un marco matemático bastante útil para entender los sistemas complejos. En particular, la física de la materia condensada se centra en predecir el comportamiento macroscópico colectivo a partir de la física de sus constituyentes microscópicos, sean estos átomos, moléculas (del mismo tipo o de pocos tipos diferentes), electrones, etc. En todos estos casos, estos están bien descritos por las leyes físicas. En problemas de interés en, por ejemplo, biología, los elementos de los sistemas complejos pueden ser heterogéneos y pueden no ser tan simples y bien caracterizados como los átomos. A pesar de este hecho, una valiosa información puede obtenerse adaptando diferentes técnicas prestadas de la física estadística estándar a estas situaciones más complejas. Esto nos sugiere una estrategia general de "grano-grueso" que aproxime los sistemas complejos por unos más fácilmente tratables que mantengan el comportamiento macroscópico principal. Tal proceso puede revelar analogías profundas en la organización de varios sistemas que difieren sustancialmente en sus constituyentes elementales. Desde un punto de vista matemático, esta idea está respaldada por la teoría del grupo de renormalización.

El ejemplo más prominente de este tipo de "universalidad" emerge en la vecindad de puntos críticos. La mayoría de los sistemas de varios cuerpos exhiben comportamientos macroscópicos, es decir "fases", correspondientes a diferentes organizaciones

microscópicas y diferentes tipos de orden interno. Ejemplos fascinantes de cambios abruptos e inesperados de estos comportamientos, como consecuencia de algún cambio de las condiciones externas como la temperatura, la presión, etc., se encuentran tradicionalmente en la física y la química. La mecánica estadística explica este fenómeno como resultado de algún tipo de desestabilización del estado global del sistema. Dependiendo de la manera en la que esto ocurre distinguimos dos tipos principales de transición, esto es, discontinua o de "primer orden" – caracterizada por cambios abruptos de algunas de sus variables y propiedades como coexistencia de fases o ciclos de histéresis– y continuas o de "segundo orden" –en las que sus variables cambian suavemente e invarianza de escala o altas susceptibilidades aparecen en el punto de transición o "crítico"–. En los valores específicos en los que estas transiciones de fase ocurren, el comportamiento macroscópico es el mismo para sistemas con detalles microscópicos diferentes, de hecho, los llamados exponentes críticos de las transiciones líquido-gas se ha visto que coinciden con las de algunos sistemas magnéticos. De igual manera, en experimentos de reacciones catalíticas, percolación en medios porosos, avalanchas de materia granulosa, colisiones electrón-positrón, o crecimiento polinuclear, los exponentes críticos medidos coinciden sorprendentemente también. Es importante remarcar que los sistemas estadísticos se estudian de manera diferente dependiendo de si obedecen el principio de "balance detallado" – el cual prohíbe cualquier intercambio de energía, partículas u otras cantidades con reservas externas– . Si tal principio se cumple, el sistema está en equilibrio, y puede ser descrito por la energía libre de Gibbs. En el caso contrario, el sistema estaría fuera del equilibrio, y debería ser estudiado en términos de la "ecuación maestra".

El concepto de fases, y transiciones de fase, ha sido extendido de manera exitosa para cubrir campos como la biología, ecología, sistemas socio-económicos, etc. En estos contextos, transiciones continuas y discontinuas están también presentes, aunque son usualmente denominadas "suaves" y "catastróficas", respectivamente. Un claro

ejemplo de la primera se encuentra en la propagación de enfermedades. En este caso, una transición continua, entre el éxito o el fracaso de la propagación, ocurre en función de la tasa de infección. La propagación será exitosa para tasas grandes de infección, mientras que fracasará para bajas tasas. Ejemplos similares de transiciones "suaves" – tales como biodiversidad frente a monodominancia en sistemas ecológicos, acuerdo frente a desacuerdo en sistemas de votantes, etc.– y propiedades propias de criticidad – como aquellas observadas en experimentos de actividad cortical, terremotos, bandadas de aves, etc. – son ubicuas en la Naturaleza. Por otro lado, muchos sistemas en socio-economía o socio-ecología, al igual que en ecosistemas como lagos, savanas u océanos (con sus bancos de peces y corales) pueden experimentar, como consecuencia de pequeños cambios en las condiciones del entorno, cambios catastróficos de los que es extremadamente difícil recuperarse. Un ejemplo importante fue observado hace seiscientos años en el Sahara. En este caso, una reducción gradual de las lluvias y, como consecuencia del cambio climático local, dio lugar a un colapso repentino, de una zona verde, al mayor desierto de nuestro planeta.

Teniendo en cuenta toda esta discusión nos preguntamos: ¿qué hace que un sistema presente una transición continua o discontinua? ¿Hay alguna forma de evitar las transiciones discontinuas? ¿Cómo son alterados estos sistemas por mecanismos realistas presentes en la naturaleza?

Aquí intentamos arrojar luz sobre estos temas. Para ello nos apoyamos en técnicas estándar de la mecánica estadística y la teoría de procesos estocásticos, incluyendo: la teoría de las transiciones de fase en equilibrio y fuera del equilibrio, aproximaciones de campo medio, herramientas del grupo de renormalización, al igual que en análisis computacionales exhaustivos [2]

[2]Para llevar a cabo este propósito se ha hecho uso del super-cluster PROTEUS que pertenece al instituto "Carlos I de Física Teórica y Computacional" de la universidad de Granada. La gran capacidad de cálculo de este cluster (con 13 teraflops y 1100 núcleos) ha hecho posible el llevar a cabo simulaciones computacionales exhaustivas necesarias para esta tesis.

Contexto de la tesis

En esta tesis, considerando modelos matemáticos y computacionales que consideren los aspectos más relevantes de diferentes sistemas, obtenemos predicciones sobre el comportamiento y las transiciones de fase que estos exhiben. Por otra parte, aplicando teorías y técnicas de la mecánica estadística, analizamos diferentes sistemas complejos tales como el córtex, savanas, o comunidades de varias especies.

Uno de los focos principales de este trabajo es el estudio del efecto de algunos mecanismos inherentes, realistas y no despreciables de los sistemas reales – tales como i) fluctuaciones demográficas, heterogeneidad ii) espacial y ii) estructural, etc.– sobre sistemas de muchos cuerpos; prestando especial atención en cómo estos ingredientes pueden afectar a las transiciones de fase. Algunas de las características mencionadas anteriormente pueden alterar drásticamente el tipo de fase que tiene lugar, cambiando por ejemplo de discontinua a continua, o a la inversa. Veamos a discutir brevemente estos aspectos realistas:

- (i) *El efecto de las fluctuaciones demográficas.* La física estadística nos dice que las fluctuaciones están presentes inevitablemente en sistemas pequeños. En particular, el teorema central del límite cuantifica tales fluctuaciones por $\sqrt{N}$ (siendo N el tamaño del sistema). Hay muchas situaciones en las que las fluctuaciones son esenciales para explicar el comportamiento de un sistema, cambiando posiblemente predicciones deterministas (sin ruido, de campo medio). Por ejemplo, la capacidad de un sistema de explorar múltiples estados metaestables es solo posible si las fluctuaciones permiten al sistema escapar de uno a otro. Otros ejemplos son frentes y patrones espaciales inducidos por ruido, ondas mantenidas por ruido en medios poco excitables, transiciones hacia estados ordenados o desordenados inducidas por el ruido [81, 109].

  En análisis simples (deterministas o de campo medio) de sistemas complejos y

sus transiciones de fase, efectos estocásticos son ignorados algunas veces. Por ejemplo, en los estudios de cambios de regímenes ecológicos, aproximaciones deterministas suelen emplearse [128, 226, 145, 54]. En esta tesis analizamos el efecto de la estocasticidad demográfica en tales sistemas ecológicos sujetos a una transición catastrófica en la aproximación de campo medio.

- (ii) *Heterogeneidad espacial.* La mayoría de sistemas reales exhiben algún tipo de heterogeneidad espacial. En física pueden ser causadas por imperfecciones en los sólidos, efectos espaciales que modifican las interacciones, agrupamiento de zonas absorbentes en superficies de catálisis heterogénea, etc. En biología o ecología pueden ser provocadas por distribuciones heterogéneas de nutrientes en el suelo, cortafuegos, termiteros, etc.

  En mecánica estadística, argumentos de equilibrio nos dicen que las transiciones de fase discontinuas están prohibidas en sistemas de baja dimensión en presencia de heterogeneidad espacial (congelada)[3]. A la luz de esto, nosotros desarrollamos un análisis técnico para comprobar si sería este el caso en sistemas físicos de no-equilibrio. Por otra parte, estudiamos un sistema complejo ecológico que presenta transiciones de fase catastróficas y exploramos las posibles consecuencias de esta heterogeneidad espacial.

- (iii) *Heterogeneidad estructural.* Componentes individuales de los sistemas complejos interaccionan normalmente con los demás de una forma intrincada con propiedades estructurales muy interesantes tales como modularidad, agrupamiento, jerarquías, patrones de conectividad libres de escala, etc. [4, 12]. Algunos ejemplos incluyen redes genéticas, estructuras neuronales, redes tróficas, interacciones sociales o conexiones en internet [4, 12]. Tales redes complejas pueden alterar los comportamientos esperados para el sistema y, consecuentemente, evidenciar la presencia y relevancia de las estructuras internas no triv-

iales. Nosotros nos centramos en la importancia de las redes complejas en el caso particular de dinámicas neuronales integrativas (basadas en [1, 28, 29]) que presentan transiciones de fase discontinuas en las redes cuyos elementos están conectados todos con todos (campo medio) [228].

Una descripción detallada de un sistema biológico complejo no puede recaer únicamente sobre fluctuaciones y heterogeneidades. De acuerdo con Theodosius Dobzhansky: "Nada en biología tiene sentido excepto a la luz de la evolución". Es incuestionable que sistemas biológicos, no importa a qué escala, evolucionan en el tiempo. Contrariamente a las fluctuaciones y heterogeneidades, la evolución actúa a largas escalas y ningún efecto relevante se observa en la dinámica de comunidades. Sin embargo, la existencia de una retroalimentación entre procesos de comunidad y evolutivos ha sido observada empíricamente en los últimos años en diferentes tipos de comunidades (desde microbios hasta plantas y vertebrados) [171, 231, 101, 77, 211, 108, 48, 67, 45, 194, 209, 200, 201, 88, 70], y analizados teóricamente con herramientas matemáticas novedosas y potentes. En esta tesis, mostramos cómo la evolución juega un papel fundamental en sistemas que exhiben diversificación [235]. Nuestros resultados representan un primer paso importante en la dirección de un estudio detallado de las transiciones entre regímenes generalistas (y con poca diversidad) y especialistas (altamente diversos).

Resumen

Vamos a resumir los principales temas tratados en esta tesis.

En el **Capítulo 1** se recopilan conceptos básicos necesarios en esta tesis. En primer lugar, se presentan las propiedades principales de las transiciones continuas y discontinuas. Más adelante, se discute el efecto de la heterogeneidad espacial en transiciones de fase en equilibrio.

En el **Capítulo 2**, estudiamos la importancia de la estocasticidad demográfica y la difusión en sistemas genéricos sujetos a una transición de fase discontinua (en aproximación de campo medio). Investigamos cómo el orden de la transición dependería sorprendentemente de tales mecanismos. Además de esto, también estudiamos la presencia inevitable de la heterogeneidad espacial en sistemas reales. En este caso, un fenómeno de "redondeo" aparece para sistemas de baja dimensión. Las ideas presentadas aquí pueden ayudar a entender mejor las transiciones de fase discontinuas, y contribuir a la discusión sobre la posibilidad de prevenirlas.

Para una mayor comprensión de algunos de estos resultados, en el **Capítulo 3** presentamos un estudio más técnico y detallado del efecto de la heterogeneidad espacial en modelos prototípicos que exhiben transiciones de fase discontinuas. Aquí intentamos explicar cómo, en analogía con lo que pasa en problemas de equilibrio, la existencia de alguna forma de desorden espacial implica un "redondeo" de la transición discontinua que hace crítico el sistema (a bajas dimensiones).

En este contexto, en el **Capítulo 4** nos preguntamos si un sistema desordenado estructuralmente (y, por tanto, espacialmente) presentaría también el mismo efecto de "suavizado". Un análisis extenso de todos los posibles sistemas que presentan heterogeneidad estructural constituiría una tesis en sí misma. De modo que nos centramos en el caso particular del córtex cerebral, un sistema bien descrito por modelos con transiciones de primer orden en campo medio y que presentan una estructura

compleja y conocida. Es interesante que en este caso, la criticidad aparezca para dimensiones topológicas pequeñas explicando la compatibilidad de modelos integrantes (con transiciones de primer orden en campo medio), y las propiedades críticas medidas experimentalmente en el córtex.

Los capítulos anteriores no consideran ningún tipo de mutación o variación de sus individuos debido al hecho de que, en dichos casos, la evolución suele ocurrir a tiempos más largos que los considerados. Sin embargo, aparte de las propiedades inherentes consideradas, la adaptación es un aspecto fundamental de los sistemas reales. ¿Qué ocurriría si los individuos evolucionaran rápidamente afectando a la dinámica de la comunidad?

En el **Capítulo 5** proponemos un modelo computacional eco-evolutivo relativamente simple con el objetivo de describir diversificación fenotípica rápida en un experimento particular de comunidades de varias especies [235]. A pesar de esto, el modelo es fácilmente generalizable para analizar problemas de eco-evolución dentro de un marco teórico computacional unificado relativamente simple. Mostramos que este modelo captura la principal fenomenología observada experimentalmente, y además consigue hacer predicciones no triviales. Aunque, a pesar de lo esperado, ninguna transición entre comunidades diversas y no diversas emerge, en el futuro investigaremos los mecanismos para los que esta transición de fase ocurra.

Finalmente, las conclusiones de la tesis son presentadas en el **capítulo 6**.

¿Cuáles son los mecanismos esenciales subyacentes a comportamientos complejos como la criticidad presente en el córtex, cambios ecológicos catastróficos o diversificación de especies? ¿Cómo afectan aspectos realistas como la estocasticidad, la difusión o la heterogeneidad a las transiciones de fase que dichos sistemas exhiben? ¿Hay alguna forma de evitar los cambios catastróficos? ¿Cómo puede el córtex cerebral exhibir propiedades críticas mientras la dinámica subyacente está sujeta a transiciones discontinuas en aproximación de campo medio?¿Cuáles son los mecanismos

responsables de la diversificación de especies? ¿Son robustos? ¿Cómo podemos cuantificar tal diversificación? Apoyados en técnicas de la mecánica estadística, tratamos de arrojar luz sobre estas cuestiones.

Chapter 1

Basic concepts of phase transitions

1.1 Introduction

Since the presocratics, the spontaneous and sudden changes in the behavior of natural systems have supposed a major and puzzling problem for philosophy and, afterwards, for Science. Statistical mechanics explains that system "phases" are characterized by specific microscopic organizations. When some changes of the external conditions occur, the current phase can destabilize and, as a consequence, the system jumps towards a more stable internal structure. A prototypical example of this phenomenon is the gas-liquid-solid transition (see figure 1-1). In this case, when high temperatures are imposed to the system, the molecules are thermally excited and freely move around the available space. On the other hand, if the temperature is reduced, clustering become a more stable solution. Thereby, the liquid phase is characterized by cohesive (but relatively free) molecules, while in the solid phase the molecules are closely packed together in a crystalline way.

This example illustrates how, for a given pressure, a temperature reduction implies a transition from a "disordered" phase to an "ordered" one, and so, a change in the degree of order or symmetry of the system. Such "order-disorder" transitions

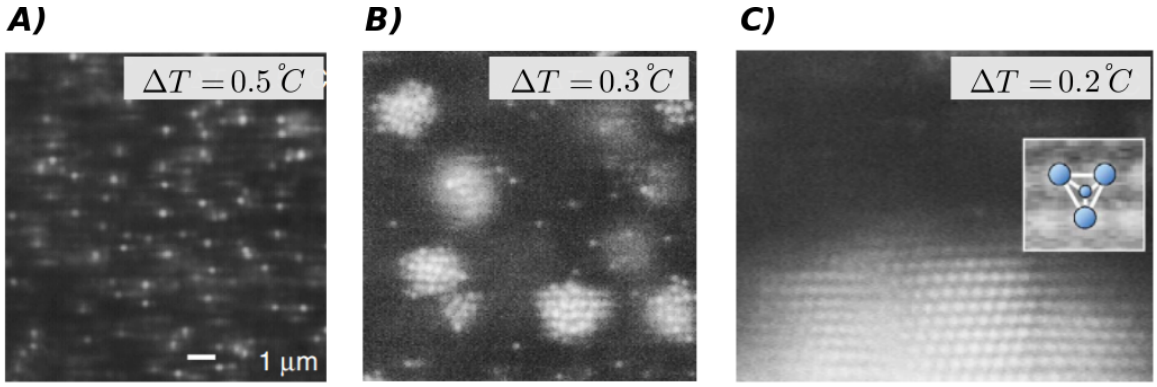

Figure 1-1: **Gas-liquid-solid transition.** Colloidal phase transitions induced by critical Casimir forces [71]: colloidal gas (A), colloidal liquid aggregates (B) and colloidal crystal (C).

are ubiquitous in physics, for instance, the ferromagnetic-paramagnetic transition is another usual example. The quantities employed to characterize phase transitions are: i) the "order" parameter (e.g. the density or the magnetization in the above examples), which quantifies the underlying order or symmetry of the system; ii) the "control" parameter (e.g. temperature), which is the cause of phase change; and iii) the "conjugate" parameter (e.g. pressure or magnetic field), which promotes the system to become ordered.

For specific values of the control and conjugate parameters, the formalism of the Statistical Mechanics of systems in thermodynamic equilibrium is able to provide the free energy potential that governs the equilibrium state [8]. However, in non-equilibrium, for which the free energy does not exist [146, 106, 161, 95], new techniques, based on the theory of stochastic process, need to be employed. Equations describing the evolution of the probability density of microscopic states often provide effective potentials – counterpart of thermodynamic potentials – that enable a satisfactory analysis of non-equilibrium phase transitions [213, 82].

In this thesis, relying on these techniques, we study simple non-equilibrium models – describing both, standard physical problems and less conventional systems in theoretical biology and ecology – and analyze the phase transition they exhibit. As the following sections expose, there exist two main types of phase transitions: i) "continuous" or second-order transitions, for which the order parameter changes smoothly as a function of the control parameter; and ii) "discontinuous" or first-order transitions, for which, contrarily, the change occurs in an abrupt manner. In this chapter, by studying prototypical non-equilibrium models, we review the main features that characterize such type of transitions and the tools to analyze them.

One of the main goals of the present work is to shed light on the effect of stochasticity, diffusion, and heterogeneities on phase transitions exhibited by non-equilibrium systems. In this regard, section 1.4 summarizes the studies about the effect of spatial heterogeneity on equilibrium phase transitions [119, 3, 19, 117] and clears a path for studying non-equilibrium cases.

1.2 Non-equilibrium continuous phase transitions

In this section we elucidate the essential aspects of systems exhibiting a second-order transition. For that purpose, the "contact process", one of the most important models exhibiting such transition, is considered [106].

The contact process is defined as a Markov process [82] on a lattice or an arbitrary network in which each site can be either empty or occupied. Occupied sites or "particles" can create other particle at rate λ at a nearest neighbor site – provided it is empty – or die at rate μ:

$$\begin{aligned} A &\xrightarrow{\lambda} 2A \ (creation), \\ A &\xrightarrow{\mu} 0 \ \ (removal). \end{aligned} \tag{1.1}$$

This process takes place on spatially-explicit systems with N sites or nodes. Equivalently, a coalescence reaction $2A \xrightarrow{\mu'} A$ can be imposed if the restriction of only one particle per site is removed. Although it is usual to employ lattice networks connecting the sites, in recent years, more complex networks have been imposed to investigate the effects of non-trivial underlying architectures on the system dynamics [4, 12]. In this light, chapter 4 inquire into the effect of hierarchical modular networks on neural dynamics.

In the following, particles creation is also referred as sites activation, and "active" and "inactive" states are equivalent to high and low density states.

1.2.1 Stochastic description

A full description of birth-death processes, such as the contact process, is achieved by the microscopic "**master equation**" [82, 213]. Considering discrete microscopic steps, the density $\rho(t) = n(t)/N$ can increase $+1/N$, decrease $-1/N$, or remain equal, and the master equation can be expressed as

$$\begin{aligned} \frac{\partial P(\rho,t)}{\partial t} &= W^+(\rho - 1/N, t)P(\rho - 1/N, t) + \\ &+ W^-(\rho + 1/N, t)P(\rho + 1/N, t) - \\ &- W^+(\rho, t)P(\rho, t) - W^-(\rho, t)P(\rho, t). \end{aligned} \tag{1.2}$$

For the contact process, the transition rates are given by:

$$\begin{aligned} creation: \quad W^+(\rho,t) &= \lambda\rho(1-\rho), \\ annihilation: \quad W^-(\rho,t) &= \mu\rho, \end{aligned} \tag{1.3}$$

and, thus, its master equation is:

$$\frac{\partial P(\rho,t)}{\partial t} = [\lambda\rho(1-\rho)]P(\rho - 1/N, t) + \mu\rho P(\rho + 1/N, t) - [\lambda\rho(1-\rho) + \mu\rho]P(\rho, t). \tag{1.4}$$

This is a good way of capturing the behavior of the system. However, solving this type of equations is usually a difficult task. For this reason it is often approximated by the called **Fokker-Planck equation** [82, 213]. Expanding P to order $1/N^2$ in space [82, 213], it is given by:

$$\begin{aligned} \frac{\partial P(\rho,t)}{\partial t} &= -\frac{\partial}{\partial \rho}\left\{\left[W^+(\rho,t)-W^-(\rho,t)\right]P(\rho,t)\right\}+ \\ &+ \frac{1}{2N}\frac{\partial^2}{\partial \rho^2}\left\{\left[W^+(\rho,t)+W^-(\rho,t)\right]P(\rho,t)\right\}. \end{aligned} \tag{1.5}$$

and, thus:

$$\begin{aligned} \frac{\partial P(\rho,t)}{\partial t} &= -\frac{\partial}{\partial \rho}\left\{\left[(\lambda-\mu)\rho-\lambda\rho^2\right]P(\rho,t)\right\}+ \\ &+ \frac{1}{2N}\frac{\partial^2}{\partial \rho^2}\left\{\left[(\lambda+\mu)\rho-\lambda\rho^2\right]P(\rho,t)\right\}. \end{aligned} \tag{1.6}$$

This equation gives the evolution of the probability density $P(\rho,t)$ and it is often a satisfactory method to obtain the effective potential that characterizes the system, as well as, the escape times as a function of the system size [82, 213].

On the other hand, when the interest resides in knowing the temporal evolution of the order parameter, the **Langevin equation** is the suitable one [82, 213]. It is well-known that there is an equivalence relation among Fokker-Planck and Langevin equations [82, 213], and so, the previous development enables for a direct derivation of the latter. For the contact process, it is given by:

$$\begin{aligned} \frac{\partial \rho}{\partial t} &= W^+ - W^- + \sqrt{\frac{W^+(\rho,t)+W^-(\rho,t)}{N}}\xi(t) = \\ &= -\mu\rho+\lambda\rho(1-\rho)+\sqrt{\frac{\lambda\rho(1-\rho)+\mu\rho}{N}}\xi(t), \end{aligned} \tag{1.7}$$

where $\xi(t)$ is a Gaussian noise. If space explicit models are considered, a term $D\nabla^2\rho$ must be included to account for effective diffusion to nearest neighbors.

This equation captures a remarkable phenomenon of the contact process, i.e. the existence of an absorbing state [146, 106, 161, 95]. Note that, for $\rho = 0$, the noise term disappears, and so, as no fluctuations exist, it is impossible to escape from it. Although the process permits the system to reach this state, it is impossible to return to the previous densities, and, as a consequence, the system is out of equilibrium by violating "detailed balance".

Note that, as the noise term disappears for $N \to \infty$, this phenomenon just occurs for finite systems. In these cases, the only stable state is the absorbing one and, although the systems remains some time in a metastable state, it eventually falls into such non-fluctuating state. In order to avoid this, spontaneous creation of particles – at low rates – can be included in such a way that $\rho = 0$ is not absorbing [146, 106]. Such process is "quasi-stationary" in the sense that the appearing stationary states are not truly stationary, and eventually decay towards zero in the original system.

1.2.2 Mean-field approximation

A simple approach to extract information of this system is the "**mean-field**" approximation, which can be interpreted as a well-mixed, fully-connected infinite system [21]. Taking $N \to \infty$ in equation 1.7, the particle density $\rho(t) = n(t)/N$ at time t is described by the following rate or mean-field equation:

$$\dot{\rho}(t) = -\mu\rho + \lambda\rho(1-\rho). \tag{1.8}$$

Stationary states

It is straightforward that the mean-field stationary solutions – for which $\dot{\rho}(t) = 0$ – are: i) $\rho_s = 0$ and ii) $\rho_s = (\lambda - \mu)/\lambda$. As negative densities make no sense, the non-trivial solution only exists for $\lambda > \mu$ and so, the first conclusion that can be

reached is that, for $\lambda = \mu$, a change of behavior or phase transition occurs. While for $\lambda < \mu$ density decays due to annihilation predominance, for $\lambda > \mu$ a positive density or "active" state is possible. Thereby, defining λ as the control parameter, the critical point is $\lambda_c = \mu$. As λ increases smoothly, $\rho_s = (\lambda - \mu)/\lambda$ does it in the same way, and a continuous transition occurs. Figure 1-2A displays the phase diagram corresponding to these stationary densities ρ_s as a function of the control parameter λ showing such continuous transition (fixing $\mu = 1$).

Besides this, it is useful to realize that the right-hand side of the equation 1.8 can be interpreted as a drift force $f(\rho)$, gradient of an effective potential $V(\rho)$ in the form $f(\rho) = -\partial V(\rho)/\partial\rho$ [205], an so, $V(\rho) = (\mu - \lambda)\rho^2/2 + \lambda\rho^3/3$. Figure 1-2B shows that the potential minimum rest in zero for $\lambda < \mu$ until λ in increased above μ. In that case, the minimum position increases continuously corroborating a continuous transition at $\lambda_c = \mu$ that separates an inactive state with $\rho = 0$ from a non-vanishing density active state $\rho > 0$.

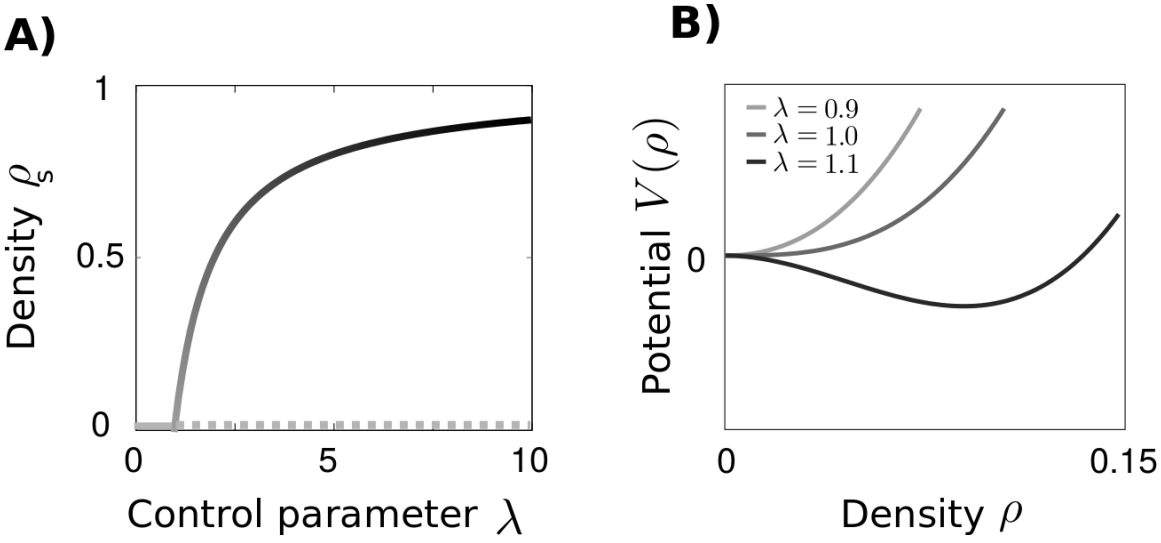

Figure 1-2: **Phase diagram (A) and effective potential (B) of the contact process** for a removal rate $\mu = 1$. In A) light and dark colors indicate low and high values of the stationary density, respectively. B) Light and dark colors indicate low and high values of the control parameter λ, respectively.

Temporal evolution

Defining $\Delta = \lambda - \mu$ as the distance to the critical point, the dynamical behavior of the contact process can be obtained from the equation 1.8:

$$\rho(t) \simeq \begin{cases} \dfrac{\Delta}{\Delta/\rho_0 - \lambda} e^{\Delta t} & (\Delta < 0), \\ (1/\rho_0 + \lambda t)^{-1} & (\Delta = 0), \\ \dfrac{\Delta}{\lambda}\left[1 + \left(1 - \dfrac{\Delta}{\lambda\rho_0}\right)\right] & (\Delta > 0). \end{cases} \tag{1.9}$$

Observe that, in the limit $t \to \infty$, the stationary solutions encountered in section 1.2.2 are recovered. Regarding temporal evolution, note that, for $\Delta < 0$, density decays exponentially towards the absorbing state $\rho_s = 0$; while, for $\Delta > 0$, the density maintains constant. Both, the exponential decay, and the constant values, depends on the initial density ρ_0, and the parameters $\Delta = \lambda - \mu$ and λ. Remarkably, the closer to the critical point ($\Delta = 0$), the slower the decay, and the smaller the density value for inactive and active states, respectively. On the other hand, an interesting behavior appears at and close to the critical point:

$$\begin{aligned} \rho(t) &\simeq t^{-1}, \\ \rho_s(\Delta) &\simeq \Delta^1, \end{aligned} \tag{1.10}$$

defining two "critical exponents": i) $\alpha_{MF} = 1$ such that $\rho(t) \simeq t^{-\alpha}$, and ii) $\beta_{MF} = 1$ such that $\rho(\Delta) \simeq \Delta^{\beta}$. Such power-law behavior is characteristic of continuous transitions and it appears for other quantities, as shown in table 1.1.

Susceptibility

The susceptibility characterizes the response of the system to external perturbations and plays an important role in continuous transitions. In the contact process, the external field corresponds to the spontaneous creation of particles within the system – at some rate λ' – and constitutes the conjugate parameter of the order parameter ρ. The mean-field equation corresponding to the presence of spontaneous creation in unoccupied sites is given by:

$$\partial_t \rho(t) = -\mu\rho + \lambda\rho(1-\rho) + \lambda'(1-\rho), \tag{1.11}$$

with a stationary solution

$$\rho_s(\Delta, \lambda') = \frac{\Delta - \lambda' \pm \sqrt{(\Delta - \lambda')^2 + 4\lambda\lambda'}}{2\lambda}. \tag{1.12}$$

Note that, for $\lambda' \neq 0$, the stationary density is not zero at the critical point and, just when $\lambda' \to 0$, its value tends to zero $\rho_s \to 0$. In order to evaluate the stationary susceptibility close to the critical point when $\lambda' = 0$, the limit $\Delta \to 0$ is taken in the previous equation 1.12 obtaining:

$$\chi_s(\Delta \to 0, \lambda' = 0) = \frac{\partial \rho_s(\Delta \to 0, \lambda' = 0)}{\partial \lambda'} \simeq \frac{\Delta}{4\lambda^2} \tag{1.13}$$

defining the critical exponent $\gamma_{MF} = 1$ such that $\chi_s \simeq \Delta^{-\gamma}$. This shows that the susceptibility also diverges as a power-law in the vicinity of the critical point.

Correlations

In equilibrium, the divergence of susceptibility is associated with the divergence of correlations, which are usually quantified by the two-point correlation function. While in equilibrium such function depends just on space, in non-equilibrium time must also be considered. The two-point correlation functions at equal time and space are, respectively, given by [106]:

$$\begin{aligned} c_{\perp}(\mathbf{r}) &\sim \mathbf{r}^{\vartheta_{\perp}} e^{-\mathbf{r}/\xi_{\perp}}, \\ c_{||}(\mathbf{t}) &\sim \mathbf{t}^{\vartheta_{||}} e^{-\mathbf{t}/\xi_{||}}, \end{aligned} \tag{1.14}$$

being $\mathbf{r} = |r' - r|$, $\mathbf{t} = |t - t'|$, $\xi_{\perp}$ the correlation length, and $\xi_{||}$ the correlation time. The latter quantities behaves as [106]:

$$\begin{aligned} \xi_{\perp} &\simeq \Delta^{-\nu_{\perp}}, \\ \xi_{||} &\simeq \Delta^{-\nu_{||}}, \end{aligned} \tag{1.15}$$

in the vicinity of the critical point. In mean-field, these exponents can be obtained from the spatially-explicit mean-field equation

$$\dot{\rho}(t) = -\mu\rho + \lambda\rho(1-\rho) + D\nabla^2\rho, \tag{1.16}$$

by introducing the ansatz $\rho(t, \mathbf{r}/t^{1/z})$ with $z = \nu_{||}/\nu_{\perp}$[106]. Thereby, $\nu_{\perp,MF} = 1/2$ and $\nu_{||,MF} = 1$.

This divergence of the correlation length implies that the fluctuations at the transition point are correlated over macroscopic distances. On the other hand, the power-law divergence of the correlation time, means that, the closer the system is to the critical point, the slower the time auto-correlation function $\langle s(t)s(t+\tau)\rangle$ decays. This phenomenon is known as "critical slowing down".

1.2.3 Beyond mean-field

It has been shown that mean-field approximations are very useful in the analysis of non-equilibrium phase transitions. However, the exponents obtained do not coincide with those of real physical systems [141, 165, 197, 21, 6].

The first step to obtain the true critical exponents relies on the "scaling theory" [141, 165, 197, 21, 6]. The above-mentioned analysis shows that many quantities diverge as power-laws at or close to the critical point. The ubiquity of such behavior led to the formulation of the scaling theory, which provides useful scaling functions to obtain good estimation of the critical exponents, and scaling laws between such exponents [141, 165, 197, 21, 6].

In order to obtain the critical exponents, several techniques such as series expansions, or renormalization group theory, can be accomplished. When analytical calculations are not possible, numerical simulations are employed.

In this section an illustrative example of the scaling theory is accomplished for the contact process, and some concepts of universality are reviewed. Finally some important concepts and strategies of numerical simulations are briefly summarized.

Scaling

Dimensional analysis of the previous equations [106] $\xi_{||}(\Delta) \simeq \Delta^{-\nu_{||}}$ and $\rho(\Delta) \simeq \Delta^{\beta}$ suggests that these quantities can be rescaled as

$$\xi_{||} \mapsto l^{-\nu_{||}}\xi_{||}, \quad \rho \mapsto l^{\beta}\rho, \tag{1.17}$$

when $\Delta \to l\Delta$. Scaling theory predicts that, for an (initially) fully activated state the scaling function is [106]:

$$\rho(t;\Delta) \simeq l^{-\beta} f(l^{-\nu_{||}}t; l\Delta). \tag{1.18}$$

Scaling functions establish scaling laws between the critical exponents. This leads to (the most cases) two independent exponents that determine all the behavior of the system [141, 165, 197, 21, 6]. Besides, these functions constitute a useful tool to determine critical exponents numerically. In this particular case, by plotting $\rho(t;\Delta)t^{\alpha}$ versus $t|\Delta|^{\nu_{||}}$ for different values of Δ, data sets must collapse as shown in figure 1-3.

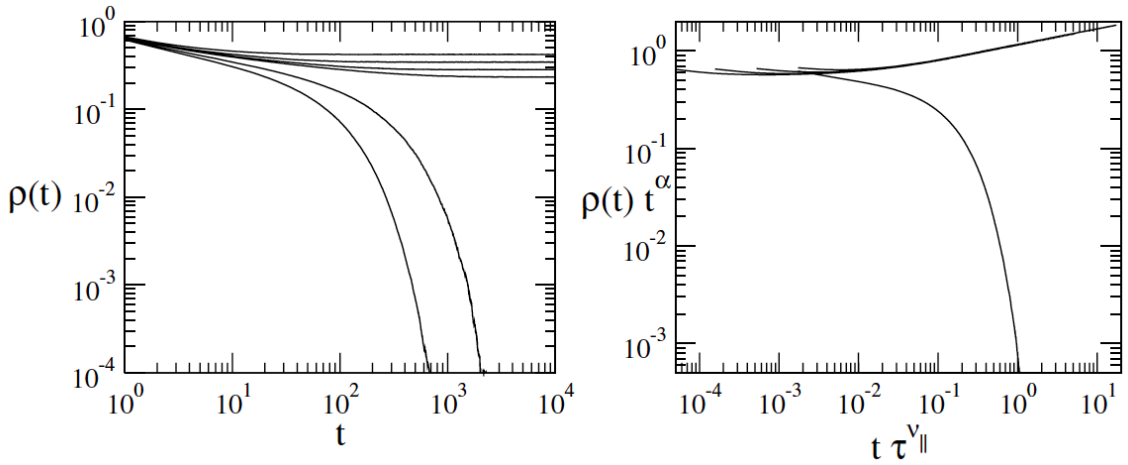

Figure 1-3: **Collapse of $\rho(t)$ for different values of Δ for the contact process [106]**.

As scaling functions and accurate values of critical exponents were obtained, it was shown that different systems shared the same critical exponents and scaling properties, defining the called "universality classes". In this light, renormalization group theory emerges has a useful tool to identify the relevant mechanisms that makes a system belong to such classes [141, 165, 197, 21, 6].

Universality

Universality originates in the macroscopically correlated fluctuations that appear at the critical point and that imply a lack of sensitivity to length transformations. Renormalization group theory, relying on such invariance under length transformations, is able to make a "coarse-graining" of the system under consideration [21, 106]. This process permits to identify the relevant features of the systems, and classify them in universality classes. This theory shows that there are just a few relevant features that determine the universality class, mainly: the dimensionality of the system, the number of components of the order parameter, the range of the microscopic interactions in the system, the conservation laws or the presence of quenched disorder [106].

The contact process belongs to one of the most important universality classes, the "directed percolation" class [122, 89, 106], which capture the main mechanisms of many different systems such as catalytic reactions, percolation in porous media, avalanches of flowing granular matter, electro-positron collision, depinning transitions or polynuclear growth.

Numerical simulations

Finite-size effects

When accomplishing numerical simulations, it is obviously impossible to account for infinite systems. It is important to realize that, when the linear system size L is comparable with the correlation length $\xi_\perp$, finite-size effects appear. This occurs specially when approaching the critical point, in which the correlation length – infinite for infinite systems – is "truncated" to $\xi_\perp \to L$. As a consequence of this, the divergences are rounded and shifted, and the phase transition disappears.

It is easy to obtain how systems quantities scale with L. Taking $\xi_\perp \to L$ and recalling $\xi_\perp \simeq \Delta^{-\nu_\perp}$ then, for example:

$$\begin{aligned} \rho_s &\simeq \Delta^{\beta} \simeq L^{-\beta/\nu_\perp}, \\ \chi_s &\simeq \Delta^{-\gamma} \simeq L^{-\gamma/\nu_\perp}. \end{aligned} \tag{1.19}$$

Another finite-size effect regards that, for finite systems, there is always a non-vanishing probability of reaching the absorbing configuration. This occurs at a characteristic time $\tau \sim L^{\nu_{||}/\nu_\perp}$ [106], and, as previously commented, can be avoided by spontaneous creation of particles [146].

Spreading and decay experiments

When studying the temporal evolution of non-equilibrium systems, initial conditions are essential. Two different situations are usually considered: i) spreading of a seed of particles in an empty system; and ii) decaying from a fully active initial state.

Regarding spreading, the principal measures considered are: i) the number of particles $N(t)$, ii) the probability of surviving without falling into the absorbing state $P_s(t)$, iii) the number of particles averaged over the surviving trials $N_s(t)$, and iv) the mean quadratic distance R_s^2 over the surviving trials. Such measures evolve in time as:

$$\begin{aligned} N(t) &\sim t^{\eta}, \\ P_s(t) &\sim t^{\delta}, \\ N_s(t) &\sim t^{\eta+\delta}, \\ R_s^2 &\sim t^{z_{spr}}. \end{aligned} \tag{1.20}$$

On the other hand, decaying experiments are usually described by the particles density:

$$\rho(t) \sim t^{-\theta}. \tag{1.21}$$

The critical exponents obtained for the contact process (and all systems belonging to the directed percolation class) are presented in table 1.1.

Relation	***Exponent***	$d=1$	$d=2$	$d=3$	Mean field
$\rho_s(\Delta) \sim \Delta^{\beta}$	β	0.276486(8)	0.5834(30)	0.813(9)	1
$\rho_s(H) \sim H^{\beta/\sigma}$	σ	2.554216(13)	2.1782(171)	2.049(26)	2
$\rho(t) \sim t^{-\alpha}$	α	0.1594664(6)	0.4505(10)	0.732(4)	1
$P_s(\Delta) \sim \Delta^{\beta'}$	$\beta' = \beta$				
$P(t) \sim t^{-\delta}$	$\delta = \alpha$				
$\chi(\Delta) \sim \Delta^{-\gamma}$	γ	2.277730(5)	1.5948(184)	1.237(23)	1
$\xi_{\perp}(\Delta) \sim \Delta^{-\nu_{\perp}}$	$\nu_{\perp}$	1.096854(4)	0.7333(75)	0.584(5)	1/2
$\xi_{\|\|}(\Delta) \sim \Delta^{-\nu_{\|\|}}$	$\nu_{\|\|}$	1.733847	1.2950(60)	1.110(10)	1
$N(t) \sim t^{\eta}$	η	0.313686(8)	0.2295(10)	0.114(4)	0
$R^2(t) \sim t^{z}$	z	1.580745(10)	1.7660(16)	1.901(5)	2

Table 1.1: Directed percolation critical exponents [106]

1.3 Non-equilibrium discontinuous phase transition

Some non-equilibrium systems with absorbing states exhibit discontinuous transitions. One of the simplest examples displaying such transition is the one-component reaction-diffusion Markov process [146, 106, 161, 95] with l-particle creation and k-particle annihilation [69] expressed by the following equations:

$$kA \to (k-n)A\,, \qquad lA \to (l+m)A\,, \tag{1.22}$$

where $k, n, l, m \in \mathbb{N}$. As in the case of the contact process, it is considered on a spatially-explicit system with N sites occupied by, at most, one particle. Models presenting these reactions exhibit a discontinuous transition for $l > k$ whenever the sites obey the latter condition or an additional reaction $iA \to jA$, with $i > j$ and $i > l$, is imposed to stabilize the system – this is easily seen from the corresponding mean-field equation –.

In this thesis we employ the simplest of these models, the often called "quadratic" contact process, which is obtained by choosing $l = 2, m = 1, k = 1, n = 1$ [228]. In this reaction-diffusion model, an individual particle can die at a fixed rate μ or diffuse to its nearest neighbors, and pairs of nearest-neighbor particles can create a single particle at some rate λ:

$$\begin{aligned} 2A &\xrightarrow{\lambda} 3A \quad (creation), \\ A0 &\xrightarrow{D} 0A \ (diffusion,) \\ A &\xrightarrow{\mu} 0 \quad (removal). \end{aligned} \tag{1.23}$$

1.3.1 Stochastic description

Following the method described in the previous section, the stochastic Langevin equation is given by:

$$\frac{\partial \rho}{\partial t} = \lambda \rho^2 (1 - \rho) - \mu \rho + \sqrt{\frac{\lambda \rho^2 (1 - \rho) + \mu \rho}{N}} \xi(t). \tag{1.24}$$

Again when $\rho = 0$, the noise disappears and, as a consequence, such low density state is absorbing.For spatially-explicit systems, effective diffusion must be included by the term $D \nabla^2 \rho$.

1.3.2 Mean-field approximation

Taking $N \to \infty$ in equation 1.24, the mean field equation corresponding to the quadratic contact process is given by:

$$\dot{\rho}(t) = -\mu \rho(t) + \lambda \rho(t)^2 (1 - \rho(t)). \tag{1.25}$$

From here, the steady-states solutions can be obtained: i) $\rho_s = 0$ and ii) $\rho_s = \frac{1}{2}(1+\sqrt{1-4\mu/\lambda})$ for $\lambda > 4\mu$. This means that, for low creation rates $\lambda < 4\mu$, particles number decays towards zero; while, for high creation rates $\lambda > 4\mu$, population can survive. The difference of this process respect to the contact process is that, when evaluating the stationary density at $\lambda = 4\mu$ – fixing $\mu = 1$ – it results to be $\rho_s = 1/2$, and so, an abrupt change of the order parameter occurs.

When evaluating the stability of these solutions it appears that, for $\lambda > 4\mu$, both $\rho_s = 0$, and the positive density solution, obey $\partial^2\rho(t)/\partial t^2 < 0$. This fact results in the appearance of metastability.

The effective potential, corresponding to the drift force $f(\rho) = -\mu\rho(t)+\lambda\rho(t)^2(1-\rho(t))$, is $V(\rho) = \mu\rho^2/2-\lambda\rho^3/3+\lambda\rho^4/4$ and is depicted in figure 1-4B. It is shown that such potential exhibits a double well corroborating the previous results. Depending on the control parameter, the truly stable state changes: while, for $\lambda = 4\mu$, $\rho_s = 0$ is stable and the active state is metastable; for other value of λ, the contrary occurs. As a consequence of this fact, the change from low-density to high-density state occurs at a different control parameter that the change from high to low densities. This phenomena is called hysteresis. On the other hand, for $\lambda = 9\mu/5$, the two phases are equally stable. Such point is known as the coexistence point, and is the transition or "Maxwell" point.

Both results lead us to expect, at this mean-field level, a discontinuous transition between an active density state $\rho > 0$ and an inactive state $\rho = 0$ at $\lambda = 4\mu$. This is due to the facilitation or Allee mechanism [204]. Thereby, low-density states are less stable that high-density phases, and stationary states of positive densities are just reached when a "critical" density is surpassed.

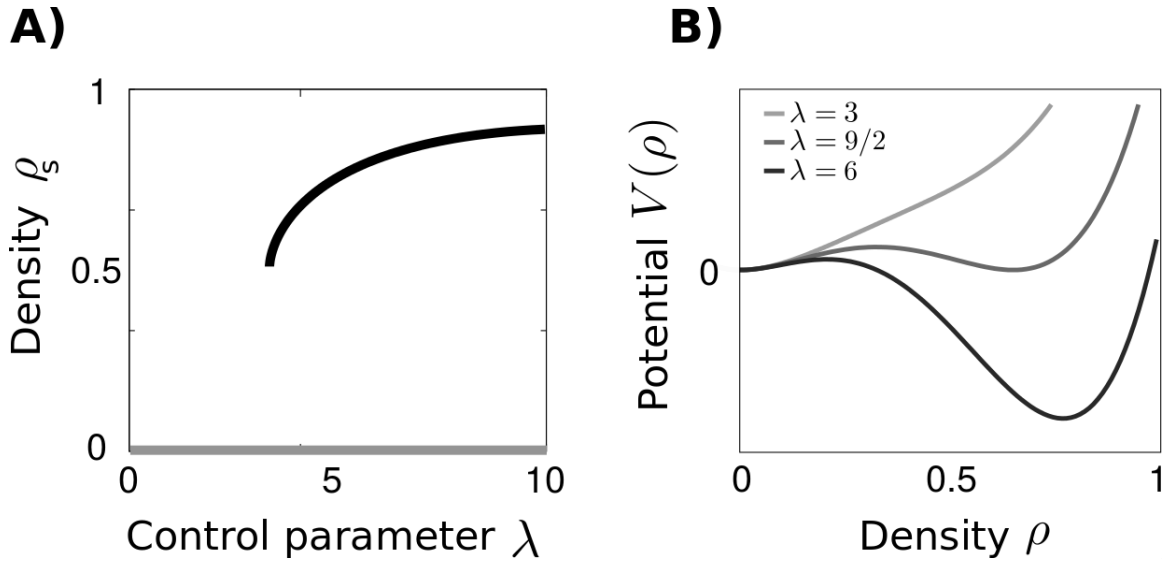

Figure 1-4: **Phase diagram (A) and effective potential (B) of the quadratic contact process** for a removal rate $\mu = 1$. In A) light and dark colors indicate low and high values of the stationary density, respectively. B) Light and dark colors indicate low and high values of the control parameter λ, respectively.

1.3.3 Beyond Mean-field

Phase transition

In chapter 2 a detailed analysis shows that deterministic predictions are not valid for low D and high demographic noise, and, instead, a continuous transitions appears. For high D and low noise, the effective potential of the stochastic system displays a well of infinite depth at $\rho = 0$, showing the absorbing behavior of such point. Contrarily, for low D and high noise, it radically changes towards an effective potential typical of an absorbing continuous transition – described in the previous section –. In figure 2-4 such effective potential can be seen.

Numerical simulations

We identify a discontinuous transition by the previous features, i.e. abrupt transition of the order parameter, phase coexistence and hysteresis. Besides the methodology described in the previous section, interesting finite-size effects are measured and interfacial experiments are performed, as we describe now.

Finite-size effects

It is important to note that, for the quadratic contact process, finite systems also falls into the absorbing configuration. This fact can difficult the measure of hysteresis in discontinuous transitions and, for this reason, spontaneous creation of particles is included – at low rates – in this case.

Besides this, a remarkable size effect in systems exhibiting discontinuous transitions is observed in the first passage time or mean survival time [151]. As it is observed in figure 1-5, for systems with size $L < L_c$, the mean passage time τ grows exponentially with L. Recalling equilibrium, this is a consequence of the Arrhenius law in which the jump probability p depends on the potential barrier ΔG – that, in turn, depends on the system size – in the form $p \propto e^{\Delta G}$. However, if the system is enlarged beyond a critical value L_c, the survival time decreases. This is due to the fact that, as the system size is greater, large regions of the alternative phase appears and can more probably invade the original phase – such invasion phenomena is known as nucleation process –. Finally, once the system surpasses a particular value L^*, several invasions – or nucleations – take place. As a consequence, the increasing of the system size does not affect the result in this case, and the mean survival time maintains constant when increasing the size.

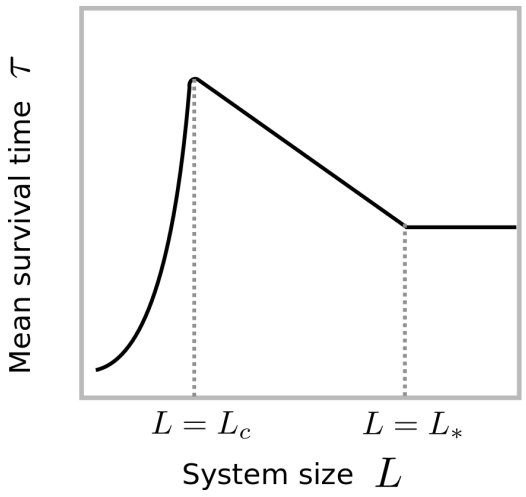

Figure 1-5: **Finite-size effect of mean survival time for the quadratic contact process** [151].

Spreading, decaying and interfacial experiments

Spreading and decaying experiment are also employed in the study of discontinuous transitions. As an abrupt jump occurs at this case, the exponents at the transition point are all zero, for instance, $\rho(t) \simeq t^0$.

Apart from this, interfacial experiments are very useful when characterizing discontinuous transitions. There exists a coexistence point, at which both phases are equally stable; it corresponds to the transition or Maxwell point λ_M. This means that, while for $\lambda > \lambda_M$ (or $\lambda < \lambda_M$) the active (or inactive) phase invades the other, for $\lambda = \lambda_M$, the interface velocity between both phases is zero. In non-equilibrium systems, this point can be obtained by interfacial experiments in which two halves of the system are occupied by different states. The control parameter at which the front velocity is zero corresponds to the transition point.

1.4 Spatial heterogeneities in equilibrium phase transitions

One of the focal points of this thesis is to discern the effect of spatial heterogeneities on phase transitions. Here, a brief summary of what is know about quenched (spatial) disorder effects on equilibrium phase transitions is presented.

1.4.1 Continuous transitions

Quenched spatial disorder has a dramatic effect on both the statics and the dynamics of phase transitions [105, 94, 120]. A time-honored argument by Imry and Ma explains in a simple and parsimonious way why symmetries cannot be spontaneously broken in low-dimensional systems in the presence of quenched random fields [119]. In a nutshell, the argument is as follows. Suppose a discrete symmetry (e.g., Z_2 or up-down) was actually spontaneously broken in a d-dimensional system and imagine a region of linear size L with a majority of random fields opposing the broken-symmetry state. As a direct consequence of the central limit theorem, by reversing the state of such a region the bulk-free energy would decrease proportionally to $L^{d/2}$, but this inversion would also lead to an inter-facial energy cost proportional to L^{d-1}. Comparing these two opposing contributions for large region sizes, it follows that for $d \leq 2$ the first dominates, making the broken-symmetry state unstable. If the distinct phases are related by a continuous symmetry, soft modes reduce the effect of the boundary conditions to L^{d-2} and the marginal dimension is $d = 4$ [3]. Thus, the energetics of low-dimensional systems is controlled by the random field, which is symmetric, thus preventing symmetries from being spontaneously broken and continuous phase transitions from existing. Instead, in higher dimensional systems, the situation is reversed, symmetries can be spontaneously broken, and phase transitions exist.

The Imry-Ma argument *i)* holds for equilibrium systems (where the free energy is well defined), *ii)* is backed by more rigorous renormalization group calculations, which prove that no symmetry breaking occurs even at the marginal case $d = 2$ (where rough interfaces could potentially break the argument above [3]), *iii)* has been verified in countless examples both experimentally and numerically, and (iv) has been extended to quantum phase transitions [92, 219].

1.4.2 Discontinuous transitions

Let us now shift the discussion to first-order phase transitions, for which system properties such as the magnetization, energy, density, etc., change abruptly as a control parameter crosses a threshold value at which two distinct phases coexist. As shown by Aizenman and Wehr, first-order phase transitions in low-dimensional equilibrium systems are rounded (made less sharp) by disorder, and, even more remarkably, the rounding may result into a critical point; i.e., first-order/discontinuous phase transitions become second-order/continuous ones upon introducing (random-field) disorder [3]. A similar conclusion applies to the case of random interactions [3, 19, 117]; indeed, a random distribution of interactions (e.g., bonds) locally favors one of the two phases, and thus, it has the same effects as random fields. Different Monte Carlo results support this conclusion; furthermore they suggest that the disorder-induced continuous transition exhibits critical exponents which are consistent with those of the corresponding pure model. An argument explaining these findings was put forward by Kardar *et al.* [141].

In close analogy with the argument above for the absence of symmetry-breaking, in the case of phase coexistence as well, regions (or "islands") of arbitrary size of one of the phases appear in a stable way within the other. Therefore, islands exist within islands in any of the two phases in a nested way, leading always to hybrid

states. Hence, two distinct phases cannot possibly coexist and first-order transitions are precluded in disordered low-dimensional equilibrium systems.

Although these equilibrium expectations may not be obeyed in non-equilibrium conditions, they can cut a path to understand the behavior in such situations.

1.5 Summary

In this chapter, continuous and discontinuous transitions have been characterized, and the role of spatial heterogeneity on such transitions has been explicitly discussed.

On the one hand, relying on the contact process, we described second-order phase transitions. Such a transition presents smooth changes of the control parameter, and a critical point at which several quantities diverge as power-laws. Besides, we have introduced the main techniques to study the systems presenting such transitions, specifically, the mean-field approach, stochastic processes techniques, renormalization group, and numerical simulations.

On the other hand, as light modification of the previous process, the quadratic contact process, has provided us with a simple model to study first-order transitions. In this case, the presence of a discontinuous change of the control parameter, phase coexistence, and hysteresis characterize the transition. Besides this, finite-size analyses and interfacial experiments have been introduced as a useful tool in the description of such transition.

Finally, a brief review of the effect of spatial heterogeneities on equilibrium transitions has highlighted that, in low-dimensional equilibrium systems, continuous transitions are precluded and discontinuous transitions become continuous. In this light, chapter 2 and 3 analyze if this is the case in non-equilibrium systems.

The presented concepts regarding standard physical problems have been successfully applied to other systems in biology, ecology, socio-economic systems, etc. Such

systems are much more complex than physical or chemical ones in the sense that they are usually constituted by elements which are not well described by simple rules – contrarily to atoms or molecules – and that usually differ between them. However, simplification of these systems in terms of statistical mechanics models, has revealed to be a extremely useful strategy to understand and anticipate its behavior. In this regard, the concepts presented in this chapter are applied, not only in physical problems, but also in complex biological and ecological systems in the following chapters.

Chapter 2

Eluding discontinuous transitions. *The relevance of stochasticity, diffusion and heterogeneity*

Transitions between regimes with radically different properties are ubiquitous in the nature. Such transitions can occur either smoothly or in an abrupt and catastrophic fashion. Important examples of the latter can be found in ecology, climate sciences, and economics, to name a few, where regime shifts have catastrophic consequences that are mostly irreversible (e.g. desertification, coral-reef collapses, market crashes). Predicting and preventing these abrupt transitions remains a challenging and important task.

In this chapter, we study spatially-explicit stochastic systems that are susceptible a priori to exhibiting discontinuous transitions. Our goal is to scrutinize how intrinsic stochasticity influences these systems; in particular, to explore whether stochasticity in combination with other realistic mechanisms such as limited diffusion and spatial (quenched) heterogeneity may alter the nature of phase transitions.

By using a combination of computational and analytical techniques, together with known results from the statistical mechanics of phase transitions, we show that these realistic ingredients can potentially round-up abrupt discontinuities, giving rise to more predictable, progressive, and easy-to-reverse transitions. As a possible application of our novel understanding, we speculate that basic and widespread aspects of natural systems could be potentially exploited to prevent abrupt regime shifts and their undesired consequences.

2.1 Introduction

2.1.1 First-order transitions in nature

Discontinuous transitions are an ubiquitous and important phenomena in nature [181, 185]. For instance, socio-economic and socio-ecological systems [148, 131], as well as ecosystems such as lakes, savannas, or oceans (with their embedded fisheries, or coral reefs) can experience, as a consequence of small changes in environmental conditions, sudden collapses after which recovery can be extremely difficult [180, 198, 111, 76, 34]. As a consequence of this irresistibility, they are often called "catastrophic shifts".

Abrupt transitions from vegetation-covered states to desertic ones in semiarid regions constitute an illustrative example [128, 216, 103, 183, 184, 127, 178, 191]. The latter habitats are characterized by positive feedback loops between vegetation and water: the presence of water fosters plant growth that, in turn, fosters water accumulation in plant-covered regions by, for instance, reducing evaporation rates. The fate of the ecosystem is determined by the overall precipitation rate, with a green or a deserted stable state for high and low rates, respectively. Interestingly, there is an intermediate bistable precipitation regime compatible with either a barren or a vegetated landscape. Thus, as a response to some small environmental change, or

if the feedback loop is incidentally interrupted, there can be a regime shift, implying a collapse of the vegetation cover and the mostly-irreversible emergence of a deserted landscape [181, 128, 216, 103, 199].

This mechanism, in which population growth (or, more generally, "activity" generation) is reinforced by a positive feedback, constitutes the basic ingredient for multistability and for possible catastrophic regime shifts –also called tipping points or "critical transitions". Similar "facilitation" mechanisms appear in a vast variety of examples in population ecology (Allee effect)[204], neuroscience (synaptic facilitation) [234], systems biology [164] and, in general, in climate, biological, and social sciences [181, 192, 193].

Opposite to abrupt shifts, many other systems in nature and society exhibit much smoother transitions between active and quiescent states, with a more-easily-reversed progressive deterioration. Examples of the latter appear in epidemic spreading, fixation of alleles in population genetics, computer virus propagation, and autocatalytic chemical reactions, to name a few [159, 163, 106, 110, 161].

2.1.2 Previous studies

Predicting and anticipating catastrophic regime shifts and distinguishing them from their smoother counterparts constitutes a timely subject with a vast number of important applications, including the prevention of biodiversity collapse or radical climate changes as the result of anthropogenic pressures [182, 52, 51, 130, 164]. Indeed, early warning indicators of regime shifts (such as increasingly slower return rates from perturbation and rising variance) have been proposed and some of them have been empirically tested [34, 52, 51, 184], even if their degree of robustness and reliability is still under debate [22, 23]. Most of these approaches rely on understanding derived from simple deterministic equations in which spatial dependence is averaged

out [182, 52, 51, 130, 164]. Recently, spatially explicit versions of these deterministic approaches have also been considered in the literature [135]. In particular, ingredients such as spatial heterogeneity and mobility (e.g. diffusion) have been incorporated into those models, leading to interesting consequences and a much richer phenomenology that includes patchiness and pattern formation [51, 53, 54, 35, 17, 160, 75, 65, 72, 97]. Moreover, it has been suggested that emerging spatio-temporal patterns could be potentially employed as early indicators of tipping points, or that transitions in these improved models can become more gradual [127, 178, 191, 173, 144, 145].

2.1.3 Importance of stochasticity

However, common to most previous studies is the fact that stochastic effects such as demographic or intrinsic noise –an unavoidable feature of real systems– are typically left out of the picture (see, however, e.g. [128, 226, 145, 54]). Stochasticity or noise is known to play a fundamental role in complex problems with many degrees of freedom, inducing non-trivial effects such as noise-induced transitions, stochastic resonance, and stochastic amplification of fluctuations [81, 109]. In particular, demographic noise can have dramatic effects in spatially-explicit low-dimensional systems, profoundly influencing the features of the expected transitions [21]. Thus, although external or environmental noise could also play an important role [179, 215], here we focus on analyzing explicitly the effects that demographic or internal noise may have on abrupt shifts.

Spatially-explicit stochastic differential equations (such as "Langevin" equations) constitute the most appropriate mathematical formalism to study the role of stochasticity on phase transitions [112]. Alternatively, individual-based models could be also employed (see e.g. [54, 128] and refs. therein), but Langevin equations can be usually derived from these individual-based approaches by using standard techniques [82].

Furthermore, Langevin equations provide a much more generic and robust framework, highlighting universal features and therefore transcending the specificities of particular systems [112]. Thus, beyond the theory of dynamical systems, the language and tools of statistical mechanics prove to be best suited for shedding light upon stochastic problems with many degrees of freedom. Within this framework, simple bifurcations exhibited by deterministic (or "mean-field" [21]) systems are just fingerprints of true phase transitions. Catastrophic shifts stand for first-order or discontinuous (i.e., abrupt) transitions showing bistability and hysteresis [20], while smooth bifurcations correspond to continuous or second-order phase transitions, in which the system reaches scale-invariant (fractal) organization with diverging characteristic lengths and times, and other remarkable and distinct features [21].

2.2 Mathematical model

Mathematically, smooth regime shifts into quiescent states are usually described and understood in terms of simple deterministic equations such as the logistic equation, $\partial_t \rho(t) = a\rho(t) - b\rho^2(t)$. In the latter, ∂_t stands for time derivative, $\rho \geq 0$ is the relevant variable (e.g. population density) that we call henceforth "activity", a is the growth rate, and $b > 0$ fixes the maximal activity density (e.g. carrying capacity) [159]. This equation describes a smooth (transcritical) transition between an active and a quiescent state as a is varied beyond a critical value (see figure 2-1A and 1C). This equation can be easily modified to include a generic facilitation term, representing the positive-feedback mechanisms discussed in the previous section. In its simplest form, facilitation alters linearly the growth rate a, enhancing it in the presence of activity: $a \to a + \alpha\rho$, with $\alpha > 0$. This variation generates an effecttive quadratic term $-\alpha\rho^2$, which is fully equivalent to leaving the growth term unaltered and replacing $b \to b - \alpha$ in the logistic equation. Thus, the coefficient of the resulting quadratic term – which,

for simplicity, we continue to call b– can potentially change its sign, and the new equation takes the form:

$$\partial_t \rho(t) = a\rho(t) - b\rho^2(t) - c\rho^3(t), \qquad b < 0 \tag{2.1}$$

A new higher-order (cubic) term has been added to enforce a finite carrying capacity (i.e., to prevent the population density to diverge when $b < 0$). equation (2.1) is the simplest equation employed to study catastrophic shifts at a deterministic level [159, 181, 185, 192, 193] (see figure 2-1). This equation admits two alternative stable solutions (bistability) as well as an abrupt, discontinuous (i.e., fold) bifurcation (see figure 2-1B and 1D) [159, 36, 163].

As the figure illustrates, the right-hand side of equation (2.1) can be interpreted as the gradient of a potential [205], and the sign of the parameter b controls the nature of the transition at the deterministic level: continuous for $b > 0$ or abrupt for $b < 0$. This observation is essential for the discussion that follows.

Aiming at capturing the relevant phenomenology of catastrophic shifts in a parsimonious yet complete way, we extend the equation above to include explicit spatial dependence and demographic or intrinsic stochasticity

$$\begin{aligned} \partial_t \rho(\mathbf{x}, t) &= a\rho(\mathbf{x}, t) - b\rho^2(\mathbf{x}, t) - c\rho^3(\mathbf{x}, t) \\ &+ D\nabla^2 \rho(\mathbf{x}, t) + \eta(\mathbf{x}, t), \qquad b < 0 \end{aligned} \tag{2.2}$$

where $\rho(\mathbf{x}, t)$ quantifies the activity at position $\mathbf{x}$ and time t.

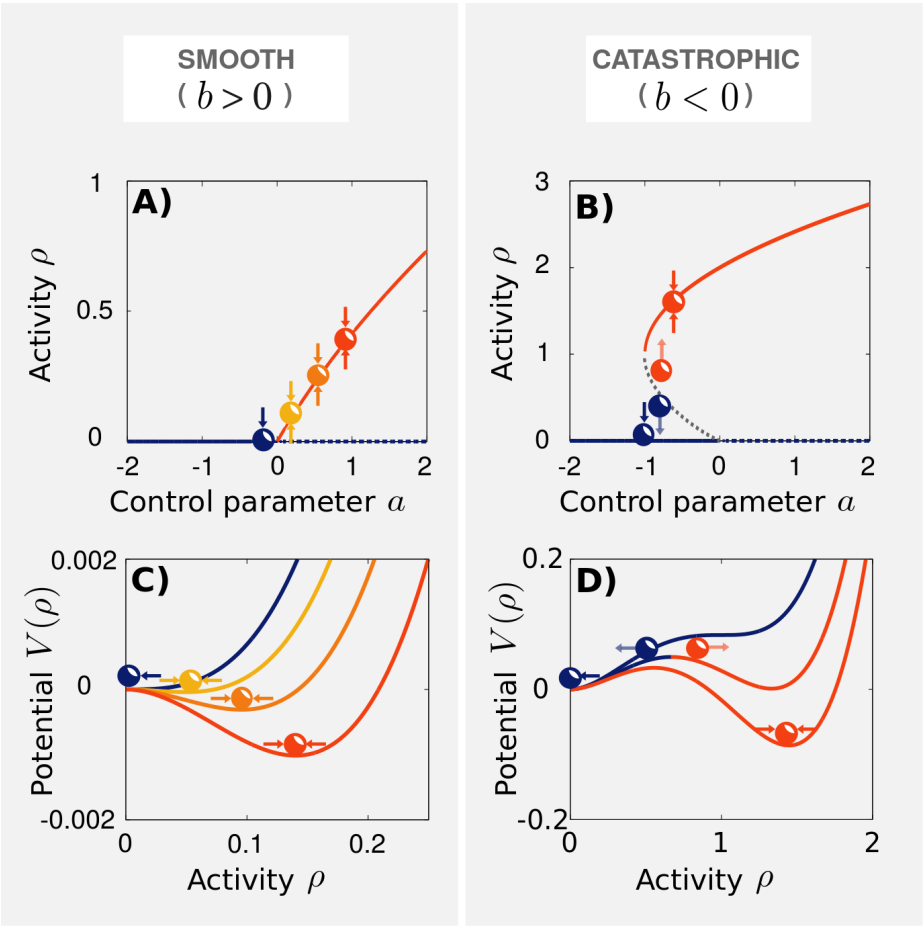

Figure 2-1: **Bifurcation diagrams and deterministic potential $V(\rho)$ for continuous (panel A) and abrupt (panel B) transitions.** (Top) Lines represent the steady-state solutions of $\dot{\rho}(t) = a\rho(t) - b\rho^2(t) - c\rho^3(t)$ as a is varied, with b either positive (left) or negative (right), displaying continuous and abrupt transitions, respectively. Four particular values of a are highlighted with spheres (blue for quiescent states and increasingly more reddish for active ones). (Bottom) Effective potential $V(\rho) = -(\frac{a}{2}\rho^2 - \frac{b}{3}\rho^3 - \frac{c}{4}\rho^4)$ –from which the deterministic forces above are derived– plotted as a function of the activity, ρ, for the same values of a highlighted above. In panel **C**, $b > 0$ and the transition is smooth and continuous (transcritical bifurcation), while in panel **D**, $b < 0$ and there is an abrupt jump in the location of the potential absolute minimum, $a^* = -b^2/4c$, as the control parameter a is varied corresponding to a discontinuous transition (fold bifurcation). In summary, the sign of b in equation (2.1) controls the nature of the transition at the deterministic or "fluctuation-less" level.

This equation, similar to the one employed to describe the strong Allee effect [204], consists of three different contributions:

- A local deterministic force (with $b < 0$), which coincides at each location $\mathbf{x}$ with the r.h.s. in equation (1).

- Diffusion, represented by the Laplacian term $D\nabla^2\rho(\mathbf{x}, t)$, with proportionality constant $D > 0$; this term accounts for dispersal of activity to neighboring locations.

- Demographic stochasticity, encoded in the Gaussian (white) noise $\eta(\mathbf{x}, t)$ with zero mean and variance proportional to $\sigma^2\rho(\mathbf{x}, t)$; this multiplicative noise ensures that demographic fluctuations do not exist in the bulk of regions deprived of activity.

equation (2.2), with $b < 0$, could *a priori* –i.e., thinking in a deterministic or "mean-field" way [21]– be expected to capture the behavior of catastrophic shifts in spatially-extended systems. However, as a result of the presence of noise, its emerging phenomenology might not be straightforwardly inferable from the mean-field reasoning. Therefore, we first need to provide an overview of the actual properties of systems described by equation (2.2) with $b < 0$ under standard circumstances. Afterward, we shall scrutinize how these results might be altered once other ingredients such as large demographic noise, limited diffusion, and/or environmental disorder are introduced. Here, we resort to extensive computational analyses as well as renormalization group calculations to discuss aspects of equation (2.2) that are relevant to our discussion. For other (fundamental) aspects of this equation, such as existence and uniqueness of solutions as well as more formal analytical approaches including small-noise calculations we refer the reader to the existing vast mathematical literature [49, 44, 13, 38, 31, 32, 39, 151, 68].

2.3 Computational results

Integrating numerically equation (2.2) is not a trivial task owing to the presence of multiplicative noise. However, as described in appendix A, there exists to this end an exact integration scheme [64] that has already been successfully employed to study spatially-explicit problems in ecology [25]. As a note of caution, let us remark that determining numerically the nature of a phase transition in an extended system can be a difficult enterprise; the literature is plagued with claims of discontinuous transitions in systems with quiescent states [57] that eventually were proven to be continuous ones once sufficiently large sizes, times, and enough statistics were collected [106]. Thus, in order to avoid any ambiguity in our conclusions, we performed very extensive large-scale computer simulations and different types of numerical experiments. We considered discrete square lattices of size up to 1024×1024 with either periodic or open boundary conditions, averaged over up to 10^6 realizations, for each of the different types of computational experiments we performed: *i) decay experiments* from an initial homogeneously active state, *ii) spreading experiments* from an initially localized seed of activity in an otherwise quiescent state, and *iii) interfacial experiments* in which the evolution of an initially half-empty/half-occupied lattice –with a planar interface in between– is investigated.

In *decay experiments* the system is initialized with a homogeneously active state, $\rho(\mathbf{x}, t = 0) = 1$, and the evolution of $\rho(t)$ is monitored, averaging over all sites and over many different realizations. In *spreading experiments*, we follow the dynamics of an initially localized seed of 100 active sites forming a 10×10 squared box at the center of an otherwise empty lattice, measuring how the averaged total (integrated) activity changes as a function of time. In *Interfacial experiments:* an initially half-empty/half-occupied lattice is considered, and the dynamics of the interface separating the two halves is analyzed (see figure 2-2). In first-order transitions this interface moves on

average in one direction or the other depending on the value of the control parameter, and remains stable right at the Maxwell point. Instead, in second-order continuous transitions the interface is quickly erased rather than moving as a whole.

Catastrophic shifts can appear in 2D noisy systems

A summary of the main features shown by a two-dimensional system described by equation (2.2) with typical parameter values is presented in figure 2-2. In particular, figure 2-2A shows the averaged activity in the steady states as a function of the control parameter a revealing the existence of two alternative homogeneous stable solutions: an active one with $\rho > 0$ and a quiescent one with $\rho = 0$, with an intermediate regime of bistability, and all the characteristic signs of a discontinuous transition. In particular, as illustrated in the inset of figure 2-2A, which steady state is reached may depend upon initial conditions revealing the existence of bistability and hysteresis, i.e., trademarks of first-order phase transitions.

Regarding probabilistic aspects, which are essential here, let us remark that small systems –even in the active phase– may fall into the quiescent state owing to rare demographic fluctuations; however, the averaged time for this to happen grows exponentially with system size in the active phase [82], and it is much larger than computational times for the sizes we have considered. On the other hand, different "routes to extinction" –all of them of stochastic nature– exist in the regime of bistability (these have been studied computationally in chapter 3 and analytically in [151] for a discrete version of our model) confirming the discontinuous nature of the transition.

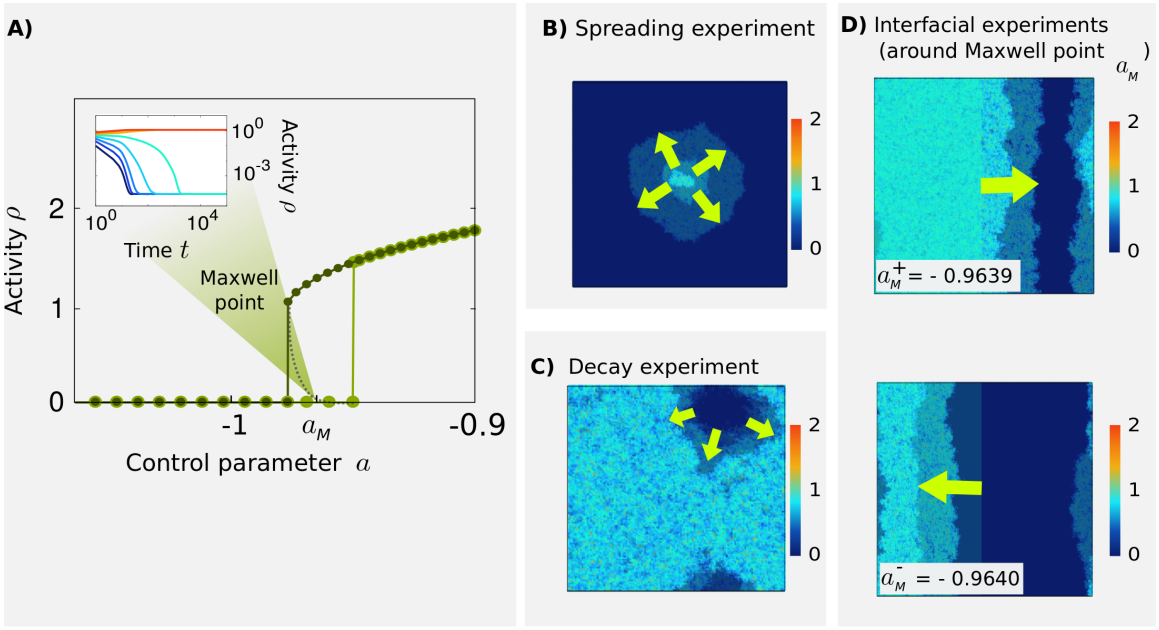

Figure 2-2: **Computational results for equation (2.2) in a two dimensional lattice, showing an abrupt regime shift**. Parameter values are: $D = c = 1$ and $\sigma^2 = 1$, and $b = -2$. Panel **A**: Steady-state averaged activity as a function of the tunable parameter a (different colors correspond to different type of initial conditions: light green for small initial activities and dark green for large initial activities). There are two distinct stable solutions: one with an associated large stationary activity (which disappears around $a \approx -0.98$) and a trivial or quiescent one with $\rho = 0$ (which becomes unstable at some point near $a \approx -0.95$). These two alternative steady states are separated by a line of unstable solutions (dashed grey). In the interval between the two limits of stability, two alternative stable states compete. The existence of bistability is confirmed by results in the inset, showing that the steady state depends upon initial conditions ($a = -0.9640$). Panel **B** illustrates how an initially localized seed of activity expands throughout the system (spreading experiment) near the threshold of instability of the quiescent phase. Similarly, panel **C** illustrates the decay of an initially homogeneous state towards the quiescent state (decay experiment). Panel **D**: In interfacial experiments, half of the system is initially occupied and half is empty; either the active phase invades the quiescent one (top panel) or viceversa (bottom panel); these two regimes are separated by a Maxwell point at which the interface does not move on average. In panels **B** to **D**, arrows indicate the direction of system's advance with time.

As a visual illustration, figure 2-2B and figure 2-2C show examples of how an "island" of one of the phases may propagate, invading a "sea" of the other, when the latter phase is close to the threshold of instability. We have found no evidence of the

existence of an intermediate critical behavior with a non-trivial power-law exponent –as would correspond to a continuous transition– in any of the numerical (spreading or decay) experiments we have performed.

Finally, we have also conducted interfacial experiments to determine the relative stability of both phases. If the system described by equation (2.2) shows a catastrophic shift, there should be a value of a for which the interface separating two perfect halves of the system –each half in one of the two coexisting states– does not move on average; this is the so-called Maxwell point [17]. As shown in figure 2-2D, there indeed exists a Maxwell point for the system described by equation (2.2).

Hence, all this evidence allows us to safely conclude that equation (2.2) experiences a true discontinuous, first-order phase transition in two dimensions, in agreement with deterministic expectations. This conclusion is quite robust against changes in parameter values but, as detailed in what follows, it may eventually break down in the presence of certain additional mechanisms, giving rise to very different scenarios.

Factors preventing catastrophic shifts in 2D noisy systems

The role of *enhanced* (demographic) noise

The noise amplitude, σ^2, is a measure of the level of demographic stochasticity present in the system. This factor is, thus, a straightforward indicator of how far the actual stochastic system is from its deterministic counterpart. To explore the consequences of high stochasticity, we have carried out the same type of computational experiments described above, but now enhancing the noise amplitude (from $\sigma^2 = 1$ above to $\sigma^2 = 4$) while keeping fixed the remaining parameters. As illustrated in figure 2-3A the situation is very different from the one in the previous section. In particular, now there is a continuous phase transition at a specific value of the control parameter, a_c. At this point, the relevant quantities in spreading and decay experiments exhibit

power-law (scale-free) behavior, characteristic of continuous transitions (see inset). Moreover, the associated critical exponents coincide within-numerical-precision with the expected values in standard continuous transitions into quiescent states, i.e., those characteristic of the well-known directed percolation (DP) universality class (see section 1.2) [106, 110, 161, 157]. For completeness, we have also verified that there is no bistability and, as a consequence, a Maxwell point cannot possibly be identified. Further computational experiments confirmed that, for any parametrization, it is possible to find a threshold for the noise amplitude that alters the character of the transition, therefore leading to the same conclusions. This provides strong evidence that equation (2.2) exhibits a continuous (more specifically, a DP) phase transition if demographic stochasticity is large enough. This conclusion is in contrast with the deterministic expectation and thus manifests that strong demographic fluctuations play an essential role in these low-dimensional spatially explicit systems.

The role of *limited* diffusion

Similarly, we have scrutinized the effect of reducing the diffusion constant, D, in equation (2.2), while keeping fixed all other parameters. Limited diffusion is very widespread in ecological systems. For example, under certain conditions, plants may restrict their range of seed dispersal as an evolutionary strategy to enhance survival [150]. When limited diffusion occurs, one could expect spatial effects to be enhanced and thus departures from mean-field behavior are more likely to occur; at the opposite extreme of very large diffusion (e.g. long-ranged seed dispersal) results are expected to be much closer to the deterministic limit. Indeed, for small D (e.g. $D = 0.1$ in figure 2-3B) computational evidence reveals the existence of a continuous transition in the DP class, in contrast to the catastrophic shift reported above for $D = 1$.

As an explicit illustration of the probabilistic nature of the discussed phenomena, the inset of figure 2-3B includes results for the surviving probability as a function

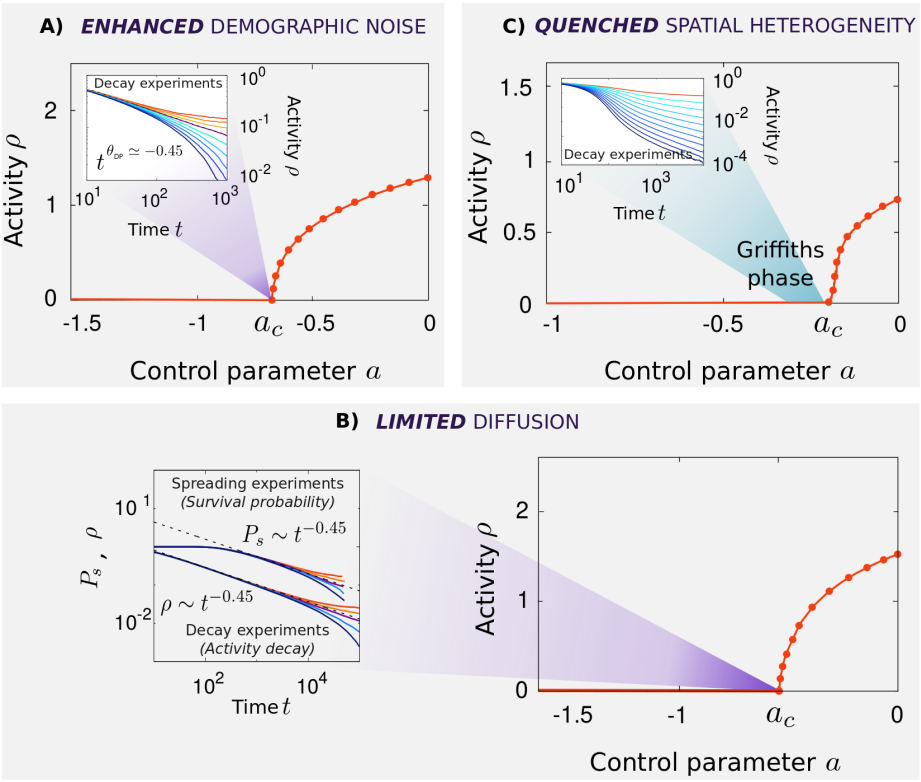

Figure 2-3: **Realistic ingredients can alter the nature of potentially catastrophic shifts in two-dimensional environments.** Using the same parametrization as in figure 2-2, we study separately the effects induced in equation (2.2) by **A**) enhanced demographic noise ($\sigma^2 = 4$, $D = 1$), **B**) limited diffusion ($D = 0.1$, $\sigma^2 = 1$), and **C**) spatial heterogeneity ($b \to b(\mathbf{x})$). In all three cases, the transition becomes continuous, with no sign of bistability nor discontinuous jumps. In **A** and **B**, power-law behavior is observed (see insets) for all the computed time-dependent (decay and /or spreading) quantities right at the critical point ($a_c \approx -0.708$ in **A** and $a_c \approx -0.5236$ in **B**. Moreover, the corresponding exponent values (both of them close to 0.45) coincide with the expected values for the directed percolation class (see section 1.2). Curves in the insets correspond to values of a between -0.702 and -0.718 in **A**, and between -0.5234 and -0.5238 in **B**, both in equal intervals. In **C**, alongside the continuous transition, there appears a broad region within the quiescent phase, called a "Griffiths phase", characterized by an extremely slow decay of activity, i.e., by power-laws with continuously varying exponents, as illustrated in the inset (values of a between -0.250 and -0.300 in equal intervals).

of time $P_s(t)$ in spreading experiments, showing a smooth continuous change in its asymptotic behavior and a DP-like power-law decay at criticality. Similarly to the enhanced stochasticity case, there always can be found a threshold for D below which

equation (2.2) exhibits a continuous transition (see section 2.4).

The role of (quenched) spatial heterogeneity

A relevant ingredient which is unavoidably present in real systems is spatial heterogeneity. Here, we focus on cases where disorder does not change with time (i.e., quenched disorder). Local differences in environmental conditions can generate regions that are more prompt to collapse and others that are more resilient, giving rise to patchy and irregular activity patterns.

To study explicitly the consequences of heterogeneity in a system described by equation (2.2), we assume b, to be position-dependent, i.e., $b \to b(\mathbf{x})$. The value of $b(\mathbf{x})$ at each location $\mathbf{x}$ is randomly extracted from a uniform distribution in the interval $(-2, 0)$, essentially ensuring a different $b < 0$ at each location. Results of extensive computer simulations, summarized in figure 2-3C, show that any amount of spatial heterogeneity induces a smooth transition. In this transition, the collapse from the active phase to the quiescent one occurs in a rather gradual way, with a progressive deterioration of the less favorable regions. Furthermore –and differently for the two previous cases– spatial disorder induces a broad region around the transition point in which power-law scaling is generically observed. In particular, the averaged activity decays in a very slow (power-law) fashion as a function of time towards the quiescent state, not just at the critical point (as usually happens) but rather for a whole range of values of the control parameter a. This region, with generic scale-free behavior, is usually dubbed "Griffiths phase" and stems from the fact that unfavorable zones are emptied first and then, progressively, more and more resilient zones collapse in a step-by-step fashion [220]. In chapter 3 a detailed and technical analysis in this respect is accomplished.

The role of spatial dimensionality

All the results above have been obtained for two-dimensional systems. However, some of the reported noise-induced effects might depend profoundly on the system dimensionality. Thus, we now discuss the one-dimensional and three-dimensional cases.

For one-dimensional systems, fluctuation effects are expected to be extremely severe [21]. Indeed, existing analytical arguments predict that stochasticity completely washes away discontinuous transitions into absorbing states, converting them into continuous ones [106]. Thus, catastrophic shifts into quiescent states cannot possibly occur in one-dimensional systems [106, 226]. We have verified computationally this prediction: our simulations show clearly a continuous phase transition in all one-dimensional cases.

In three-dimensional systems, the combined effect of amplified demographic noise and limited diffusion still affect the nature of the transition, even if to a lesser extent (as shown by our analytical calculations; see below). On the other hand, and contrarily to the two-dimensional case, spatial random heterogeneity combined with demographic stochasticity, do not suffice to destroy abrupt regime shifts in three-dimensional systems: alternative stable states and abrupt shifts can survive the introduction of spatial disorder. see chapter 3. In consequence, catastrophic shifts can occur more easily in three-dimensional systems than in their two-dimensional counterparts.

In summary, the smaller the spatial dimension the more likely fluctuations play a fundamental role, potentially breaking deterministic predictions, preventing catastrophic shifts and generating much more gradual and smooth transitions.

2.4 Analytical results

In addition to the strong numerical evidence presented so far, we now provide analytical understanding on why the transition may become continuous under the above-discussed circumstances; in particular, for low diffusion as well as for the large noise case. To this end, we rely again on statistical mechanics and use renormalization group theory [21, 106].

In fluctuating spatially-extended systems, crucial information about large-scale features –including the nature of possible phase transitions– cannot be derived from the associated deterministic potential (figure 2-1). The reason is that the true (or "renormalized") effective potential includes fluctuation effects, which are lacking in such deterministic or "bare" potential [227, 21]. Therefore, in order to rationalize the previous numerical conclusions, we need to think in terms of the (true) "renormalized" potential, $V_R(\rho)$. In particular, fluctuations have the net effect of shifting the effective parameter values characterizing the potential, from their original deterministic or "bare" values to their "renormalized" or "dressed" variants.

Renormalization group techniques were devised to compute analytically $V_R(\rho)$ as the scale of description is enlarged [227, 106]. To illustrate how this works, we have computationally measured the probability distribution for the local activity, $\mathrm{Prob}(\rho_m)$, in the stationary steady state, where ρ_m is the activity averaged in square boxes of progressively larger linear size, m (i.e., at coarser and coarser scales). In this way, it is possible to measure the renormalized coarse-grained effective potential as $-\log(\mathrm{Prob}(\rho_m))$ [227, 21]. The most likely value of the activity at each coarse-grained scale lies at the minimum of the corresponding potential.

As an example, results for the limited diffusion case ($D = 0.1$, $\sigma^2 = 1$) are shown in figure 2-4 for different values of the control parameter. For "fine-grain" scales such as $m = 1$, the effective potential is expected to coincide with the deterministic one [21].

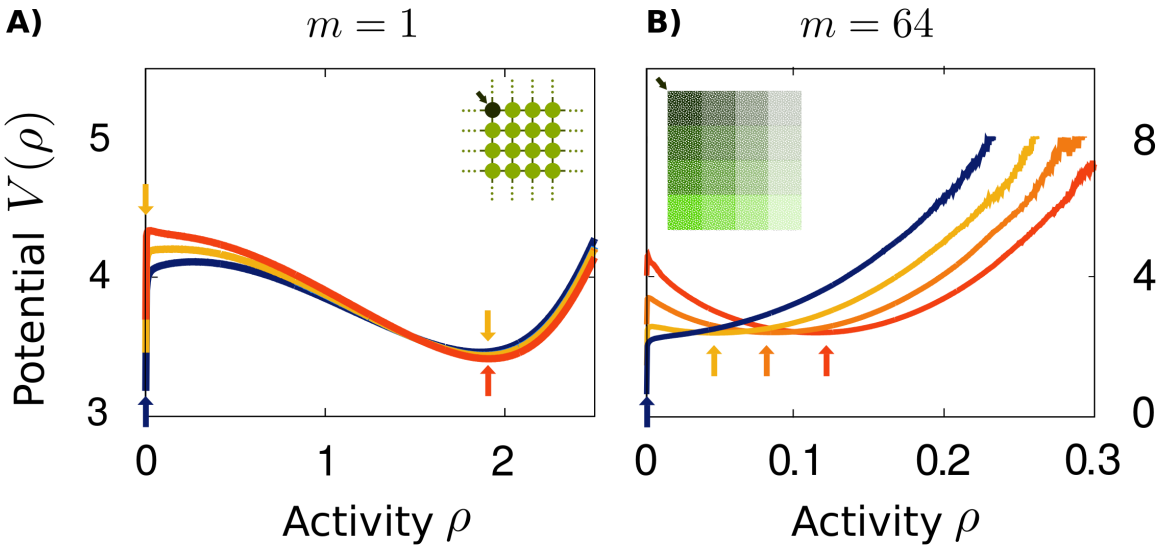

Figure 2-4: **The effective potential at coarse-grained scales**. Effective potential for the averaged activity ρ measured in cells of linear size m, in a square lattice of size $N = 256 \times 256$ (segmentation of the system into boxes schematically illustrated in the insets). The potential is defined, for each value of m as $-\log(\text{Prob}(\rho_m))$, where $\text{Prob}(\rho_m)$ is the steady state probability distribution of the activity ρ averaged in boxes of linear size m with **A**) $m = 1$ and **B**) $m = 64$. Colors represent different values of a, namely $a = 0.15, 0.11, 0.07$ and $a = 0.521, 0.522, 0.523, 0.524$, respectively (other parameters: $b = -2, c = 1, \sigma^2 = 1, D = 0.1$). As the coarse-graining scale m is increased the shape of the effective potential changes, from that typical of discontinuous transitions (for $m = 1$) to the one characteristic of continuous ones (at larger coarse-graining scales, e.g. $m = 64$. This is tantamount to saying that the "renormalized" value of b changes sign, from $b < 0$ to $b > 0$ and that even if the deterministic potential exhibits a discontinuous transition, the renormalized one does not.

Indeed, it exhibits a discontinuous transition as its global minimum jumps abruptly from 0 to a non-vanishing value in a discontinuous way. However, as the level of coarse-graining is increased, a dramatic change of behavior is observed. For instance, for boxes of size $m = 64$, it can be already seen that the effective potential experiences a continuous transition from 0 to arbitrarily small activity values. This illustrates the change in the nature of the phase transition –occurring for small diffusion constants or for large demographic noise amplitudes– once fluctuations and spatial effects are taken into account.

Renormalization group calculation

These results can be understood using renormalization group ideas. Here we employ standard procedures to perform an analytical renormalization group calculation (*a la* Wilson [227]). This allows us to compute (up to first order in a perturbative expansion) how every parameter appearing in the potential changes or "flows" upon coarse-graining.

Renormalization group techniques [227, 21] have been applied to equations such as equation (1.8) and equation (2.2). In particular, equation (1.8) –sometimes called Reggeon field theory or Gribov process– captures the relevant features of continuous transitions into absorbing or quiescent phases, defining the so-called directed percolation (DP) class [122, 89, 106]. For a clear and concise presentation of how renormalization group techniques can be applied to equation (1.8) we refer the reader to [110]. The calculation consists of a perturbative expansion around the critical dimension, $d_c = 4$, above which standard deterministic (mean-field results) hold.

Here, we just follow the calculation in [110] and briefly describe the modifications required to deal with equation (2.2) rather than with equation (1.8). All the basic ingredients of the perturbative theory remain unchanged (see figure 2-5 and [110]),

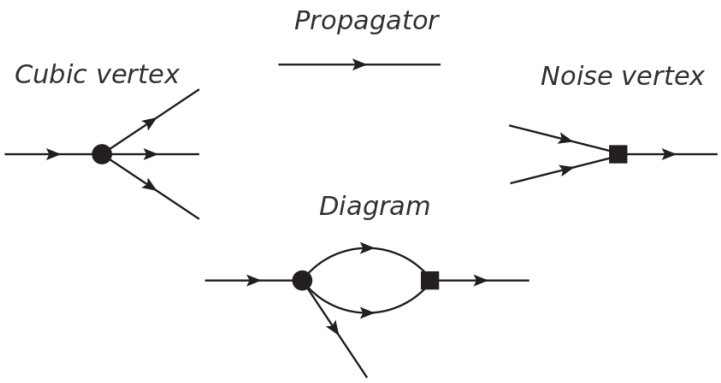

Figure 2-5: **Basic elements of a perturbative (diagrammatic) expansion.** Propagator, vertices and novel Feynman diagram contributing to lowest-order perturbative correction to b. For more details and proper definitions see e.g. [110].

but the sign of b needs to be inverted and an additional cubic non-linearity, $-c\rho^3$ (which has an associated new "vertex" as shown in figure 2-5) needs to be included.

Naive dimensional analysis tells us that the new cubic term is irrelevant around four spatial dimensions (at which the perturbative expansion is performed); however, if b is negative, then c is needed to stabilize the theory and, thus, it is a so-called dangerously-irrelevant operator, which needs to be explicitly taken into consideration to obtain stable results.

The renormalization procedure consists in first rescaling coordinates and fields: $\mathbf{x} \to \Lambda\mathbf{x}$, $t \to \Lambda^z t$, and $\rho \to \Lambda^\chi \rho$ (where Λ is an infinitesimal dilatation in momentum space, which can be expressed a $\Lambda = \exp(l)$) and then, eliminating short-range fluctuations, i.e., integrating out the moments in the shell $\Omega \leq |\mathbf{k}| \leq \Omega\Lambda$, where Ω is the original cut-off in momentum space (i.e., the inverse of the underlying lattice space). By doing this one can readily obtain a renormalized effective theory at a coarser scale, i.e., it is feasible to compute effective values for all parameters appearing in equation (1.8) as a function of the coarse-graining parameter l [227, 110, 122, 89].

Here we consider only the lowest-order correction in a series expansion in the parameter c. The new leading correction to $b(l)$ within this approximation stems from the combined effect of the noise vertex σ^2 and the cubic non-linearity c (as schematically represented by the the corresponding Feynman diagram showed in 2-5) and yields: $3c\sigma^2 l S_d/(4(2\pi)^d(\Omega^2 D + a))$, where S_d is the surface of a d-dimensional hypersphere. Incorporating this additional correction to the standard DP renormalization group flow equations and fixing the spatial dimension to $d = 2$, we obtain the flow diagram shown in figure 2-6.

Renormalization group results

Figure 2-6 clearly illustrates how, starting with a negative value of b, the flow keeps it negative for large values of D. Meanwhile, for small D's, the renormalized value crosses the line $b = 0$, thus becoming positive and remaining so. As soon as b becomes positive, the standard DP theory is recovered, the term c becomes irrelevant and, therefore, it starts flowing to 0 at larger coarse-graining scales. As c approaches 0, the renormalization group becomes identical to that of the standard directed percolation class, and in particular, b reaches the DP fixed point. This is in perfect agreement with our numerical observations, which reported a transmutation in the nature of the transition only in the low-diffusion limit.

Similarly, keeping D, the same phenomenon can be observed by increasing the (demographic) noise variance σ^2. Let us remark that a "tricritical" point –at which the renormalized b vanishes– should also appear at some value of D (located at $D \approx 0.9$ in figure 2-6). This point separates continuous from discontinuous transitions and can be also investigated in detail using renormalization group techniques [162].

This renormalization group calculation can also be used to illustrate that the system's dimensionality plays an important role in these results. Observe that,

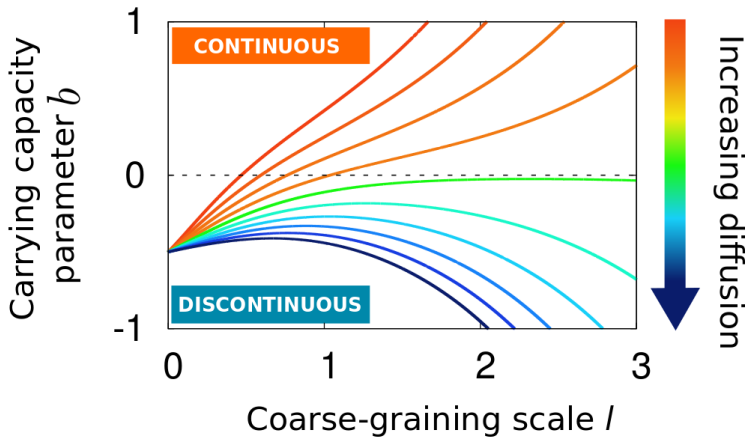

Figure 2-6: **Renormalized value of the carrying- capacity-related parameter b as a function of the coarse-graining scale l.** As l increases and coarser levels of description are achieved, an initially negative b can invert its sign for sufficiently small values of the diffusion constant D. This change of sign induces a change in the order of the transition, from discontinuous (at small scales or deterministic level) to continuous (at sufficiently large scales). On the contrary, for large values of the diffusion constant D, b remains always negative and the transition abrupt. Parameter values $a = 1$, $c = 0.5$, $\sigma^2 = 1$, initial value $b = -0.5$, and diffusion constants (from bottom to top) from $D = 2.0$ to $D = 0.2$ in equal intervals. A very similar plot can be obtained as a function of σ^2: large noise amplitude values induce a change in the sign of b and thus, the nature of the phase transition.

as $S_d/(2\pi)^d$ increases with decreasing dimensionality, the effect becomes more pronounced for low-dimensional systems: the lower the dimension the larger the value of D at which the transition changes nature. Thus, discontinuous transitions and catastrophic shifts are predicted to be much easily found in three-dimensional than in two-dimensional systems, in agreement with our numerical findings.

In summary, renormalization/coarse-graining techniques –both computationally and analytically implemented– allowed us to confirm the numerical results above, and understand how a discontinuous transition can mutate into a continuous one once fluctuations are taken into account and sufficiently large scales are considered.

2.5 Conclusions. *Eluding catastrophic shifts*

Catastrophic shifts occur when –as a consequence environmental or external changes– a system crosses abruptly from one phase to a radically different competing one, from which recovery may be exceedingly difficult due to hysteresis effects. Such abrupt regime shifts can affect the system at multiple levels, entailing for instance important ecological and/or socio-economic consequences to name a few. Classical examples include studies of insect outbreaks [140], shallow lakes, savannas, socio-ecological systems and markets [181, 185, 148, 131]. Therefore, there is an increasing interest in finding early-warning signals that may help to predict when one of these tipping points is about to occur. Most studies and predictions concerning catastrophic shifts and their early-warning indicators have been based on deterministic equations where demographic stochasticity –a natural and unavoidable ingredient of real systems– is left out of the picture. Statistical mechanics tells us that intrinsic noise can play a fundamental role in the behavior of complex systems with many degrees of freedom, generating non-trivial effects such as stochastic resonance and noise-induced transitions among many others [81]. Therefore, it is important to go beyond deterministic

approaches in order to develop robust and reliable predictors of the occurrence of catastrophic shifts.

In this work, we have introduced and analyzed the simplest possible stochastic theory of catastrophic shifts in spatially extended systems, namely equation (2.2). A simplistic deterministic analysis of this equation would average out the noise and would lead –in general– to the prediction of alternative stable states and an abrupt transition between them (see equation (2.1)). Here, we have studied instead the full stochastic model, including demographic noise, by using a combination of computational and analytical tools, and have explored the effects of stochasticity. First, we have verified that for low or moderate levels of demographic noise two-dimensional systems may truly exhibit a bona fide first-order transition, with bistability and hysteresis. Thus, catastrophic shifts can actually appear in noisy systems. However, we also show that adding any of the following ingredients, *i)* enhanced demographic variability, *ii)* limited dispersal/diffusivity, and/or *iii)* spatial (quenched) heterogeneity, suffices to alter the nature of the phase transition, giving rise to a second-order (continuous) one.

Most of our results have been obtained for two-dimensional systems, which have obvious applications to ecological problems such as desertification processes, or vegetation dynamics in savannas. However, some of the reported noise-induced effects depend profoundly on the system dimension. For example, in one spatial dimension, relevant for the study of, e.g. the oceanic water column, or rivers, fluctuation effects prohibit the very existence of discontinuous transitions, as has already been suggested in the literature [106]. In three spatial dimensions the smoothing effects of limited diffusion and amplified demographic noise are still present even if to a lesser extent (see analytical results), and –contrarily to the two-dimensional case– discontinuous transitions can survive to the introduction of spatial (quenched) heterogeneity. Thus, as a rule of thumb, the smaller the spatial dimension the more likely fluctuations play

an important role, potentially breaking deterministic predictions and smooth abrupt transitions. However, fluctuation effects need to be carefully analyzed in each spatial dimension to reach robust conclusions.

In this work we have put the focus onto demographic or intrinsic noise, but environmental or external sources of noise can also potentially be an important actor of this picture [179, 215, 214]. Preliminary studies suggest that this type of variability could also alter the order of phase transitions [215] but more detailed analyses of this, as well as of the interplay between demographic and environmental noise, would be highly desirable.

This study offers obvious opportunities for ecosystem management. All the relevant features present in equation (2.2) and its variations have straightforward counterparts in natural systems. Thus, identifying these mechanisms in specific problems may provide a reliable indicator as to when a transition is expected and of whether it is expected to be abrupt or smooth. Moreover, the conclusions here can potentially help prevent catastrophic transitions from occurring by forcing their transformation into continuous ones. Most of the current ecosystem management strategies focus on stopping or slowing down the ongoing change before the shift occurs. For instance, the declaration of a species as protected aims to prevent species extinction. In the system's phase diagram, this is equivalent to preventing the control parameter a (e.g. poaching pressure) from reaching its transition value. Unfortunately, this goal is not always possible to achieve, e.g. when the control parameter is linked to natural resource availability, climatological factors, or hardly-unavoidable human activities. In these cases, our study offers alternative strategies with which the catastrophic effects of those shifts can be reduced (that is, the discontinuous shift transformed into a continuous one), allowing the transition to be more predictable and even eventually reverted. Continuous transitions show a single stable state changing progressively with environmental conditions; therefore, they are easier to handle, foresee, and undo.

Some examples of ecosystem engineering that could potentially take the system in that direction include introducing or enhancing spatial disorder (e.g. grazing, watering, or burning selected zones in the vegetation example), forcing a reduction of effective diffusion (e.g. preventing seed dispersal by herbivores), or artificially enhancing demographic variability. Similarly, these ideas may be potentially useful in the design of practical programs for ecosystem restoration, and management policies to avoid the collapse of natural resources. For instance, using any of the mechanisms we present here to smooth an abrupt transition to extinction, could potentially open the door to the existence of low-density states of the focal species, which were not possible in the discontinuous case. These low-density states could be ideally used as early-warning indicators and therefore help prevent such extinctions. On the other hand, introducing these mechanisms may enlarge the absorbing phase (i.e. shift the transition point a_c towards less negative values). Therefore, the system may become more vulnerable, as the same pressure will drive the population extinct. Thus, the suitability of these mechanisms for ecosystem management depends on this important trade-off between predictability and vulnerability, which needs to be carefully evaluated.

In summary, we have proposed a general framework under which specific studies of potential catastrophic shifts should be set in order to obtain more reliable and informative predictions. Given the growing concerns about the impact of anthropogenic pressures on climate and biodiversity, we hope that this novel framework will help to understand better and open new research roads to explore possible strategies to mitigate the radical and harmful effects of sudden undesirable regime shifts.

Chapter 3

Spatial heterogeneity.

From first to second order

In chapter 2 we observe that spatial heterogeneity, on diffusive stochastic systems, can change discontinuous transitions to much smoother and easily-reversible continuous ones. Aimed at shedding some light on this issue, we present a detailed and technical study in this respect.

In this chapter we consider a prototypical microscopic model usually employed in the study of discontinuous transitions, the "quadratic contact process" described in section 1.3. As a first step, we verify that the pure version of the model exhibits a first-order transition separating an active phase from an absorbing one. Then we introduce disorder in the form of a site-dependent transition rates and investigate its effects.

Based on Imry-Ma-Aizenman-Wehr-Berker equilibrium arguments, we show how phase coexistence and first-order phase transitions become continuous in non-equilibrium low-dimensional systems in the presence of quenched disorder. We also study the universal features of the disorder-induced criticality and find them to be compatible with the universality class of the quenched-disordered directed percolation.

3.1 Introduction

In contrast with the equilibrium case described in section 1.4, recent work by Barghathi and Vojta [11], shows that second-order phase transitions may survive to the introduction of random fields even in one-dimensional cases [147, 168] in genuine non-equilibrium systems with absorbing states for which there is not such a thing as free energy [146, 106, 161, 95]. Therefore, *the Imry-Ma argument does not apply to these non-equilibrium systems owing to the presence of absorbing states, and, in consequence, states of broken symmetry can exist in the presence of random fields.*

Thus, the question arises as to whether shifting to the non-equilibrium realm entails the shattering of a fundamental cornerstone of equilibrium statistical mechanics as it happens for continuous phase transitions (see table 3.1 for a synthetic summary); do first-order phase transitions, and, hence, phase coexistence, exist in low-dimensional non-equilibrium disordered systems?

System with Random Fields $d \leq 2$	2^{nd} **order** **(spontaneous sym. breaking)**	1^{st} **order** **(phase coexistence)**
Equilibrium	NO [119]	NO [119, 3, 19, 117]
Non-equilibrium **(abs. states)**	YES [11]	?

Table 3.1: **Random fields in low-dimensional disordered systems.** Summary of the effects of quenched random fields on the existence of continuous/second-order transitions (with spontaneously symmetry breaking), and discontinuous/first-order (with associated phase coexistence) phase transitions in $d \leq 2$ systems. Both, the equilibrium and non-equilibrium cases are considered, the latter including the possibility of one or more absorbing states.

Two alternative scenarios might be expected *a priori* for the impure/disordered model:

1. the Imry-Ma argument breaks down in this non-equilibrium case and a *first order phase transition* is observed, or

2. the Imry-Ma prediction holds even if the system is a non-equilibrium one, and a disorder-induced *second-order phase transition* emerges.

If the latter were true, we could then ask what universality class such a continuous transition belongs to. A priori, it could share universality class with other already-known critical phase transitions in disordered systems with absorbing states [114, 30, 221, 222, 220] or, instead, belong to a new universality class defined by this disorder-induced criticality.

If no novel universal behavior emerges, then it is expected for the model to behave as a standard two-dimensional contact process (or directed percolation) with quenched disorder with the following main features [114, 221, 222, 220]:

- there should be a critical point separating the active from the absorbing phase,

- at criticality, a logarithmic or *activated* type of scaling (rather than algebraic) should be observed. For instance, for quantities related to activity spreading such as the survival probability, averaged number of particles, and radius from a localized initial seed, we expect $P_s(t) \sim [\ln(t/t_0)]^{-\bar{\delta}}$, $N(t) \sim [\ln(t/t_0)]^{\bar{\theta}}$, and $R(t) \sim [\ln(t/t_0)]^{1/\Psi}$, respectively; t_0 is some crossover time, and $\bar{\delta}$, $\bar{\theta}$, and Ψ should take the values already reported in the literature [222].

- there should be a sub-region of the absorbing phase, right below the critical point, exhibiting generic algebraic scaling with continuously varying exponents, i.e. a Griffiths phase [93]. Griffiths phases stem from the existence of rare

regions where the disorder takes values significantly different from its average [220].

These features follow from a strong-disorder renormalization group approach for the disordered contact process, which concludes that this anomalous critical behavior can be related to the random transverse-field Ising model for sufficiently strong disorder [114], and have been confirmed in computational studies which suggested that this behavior is universal regardless of disorder strength [222, 220, 115].

3.2 Microscopic model

Pure version

As mentioned in section 1.3, the simplest non-equilibrium model with absorbing states exhibiting a first-order/discontinuous transition is the "quadratic" contact process. Among the many possible ways in which this particle system can be implemented [73, 230, 228], we employ the model proposed in Ref. [228], which was numerically studied in two-dimensions and verified to exhibit a first-order phase transition separating an active from an absorbing phase [228].

We consider a two-dimensional square lattice and define a binary occupation variable $s = 0, 1$ (empty/occupied) at each site. We consider some initial conditions and perform a sequential updating following the standard procedure [146, 106, 161, 95]: *i)* an active site is randomly selected (from a list including all active ones); *ii)* with probability p_d (death) the particle is annihilated, otherwise, with complementary probability $1 - p_d$ a nearest neighbor site is chosen; *iii)* if this latter is empty, the selected particle diffuses to it, and otherwise an offspring particle is created at a randomly chosen neighboring site with probability p_b (birth) provided it was empty; otherwise nothing happens. We keep $p_b = 0.5$ fixed and use p_d as the control parameter.

Spatially disordered version

In the disordered version of the model, each lattice site has a random uncorrelated (death) probability. In particular, we take $p_d(\mathbf{x}) = p_d r$ where p_d is a constant and r is a homogeneously-distributed random number $r \in [0, 2]$ (and, thus, the mean value is p_d). Spatial disorder is refreshed for each run, to ensure that averages are independent of any specific realization of the disorder.

3.3 Computational results

Characterizing a discontinuous transition

In the first place, we study the pure model presented above to ensure the presence of a first-order transition. As customarily done, we perform two types of experiments [146, 106, 161, 95], considering as initial condition either a homogeneous state, i.e., a fully occupied lattice of linear size L, or a localized seed, consisting in this case of a few, at least a couple, neighboring particles in an otherwise empty lattice.

Homogeneous initial conditions– Figure 3-1 shows results of computer simulations for the temporal decay of the particle density from $\rho(t = 0) = 1$. The upper panel shows an abrupt change of behavior at a threshold value $p_{d_{thr}} \approx 0.0747$; activity survives indefinitely for $p_d < p_{d_{thr}}$ (at least up to the considered maximum time) and the particle density converges to relatively large steady state values ($\rho \approx 0.6$), while activity dies off exponentially for any $p_d > p_{d_{thr}}$. This behavior is compatible with a first order phase transition, but the location of the threshold value has to be considered as a rough estimate.

To better locate the transition point, we study the mean survival time (MST) as a function of system size. Figure 3-1b shows a non-standard non-monotonous dependence of the MST as a function of size $N = L^2$. As we see, there are two regimes:

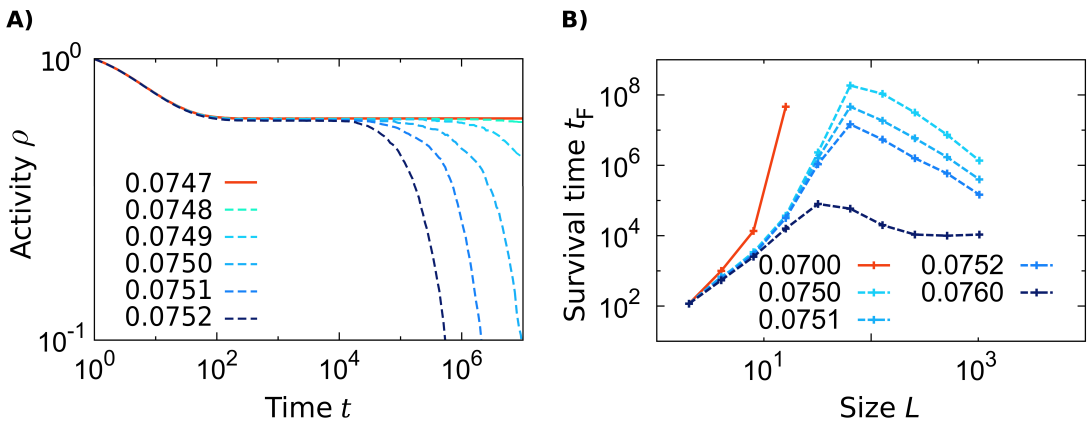

Figure 3-1: **Decay from a homogeneous initial condition in the pure model** . (a) Time evolution of the total averaged particle density for $N = L^2 = 256^2$; a first order phase transition can be observed near $p_{d_{thr}} \approx 0.0747$. (b) Mean survival time, t_F, required to reach an arbitrarily small density value here fixed to 0.01 (results are robust against variations of this choice) as a function of system size. Up to 10^3 realizations have been used to average these results. From this finite size analysis, the threshold point can be bounded to lie in the interval $[0.070, 0.075]$.

i) for $L < L_c$ there is an exponential increase of the MST with system size; *ii)* for $L_c < L$, and quite counter-intuitively, the MST decreases with increasing system size. This behavior can be rationalized following recent work where a particle system very similar to ours is studied by employing a semiclassical approach [151] (see also Ref. [212]). Following this study, the first regime corresponds to the standard Arrhenius law, i.e., the fact that a quasi-stationary state with a finite particle density experiences a large fluctuation extinguishing the activity in a characteristic time which grows exponentially with system size [82]. On the other hand, there is a "critical system size" above which the most likely route to "extinction" consists on the formation of a critical nucleus that then expands in a ballistic way, destabilizing the quasi-stationary state. Obviously, the larger the system size the most likely that a critical nucleus is spontaneously formed by fluctuations. Finally, for sufficiently large system sizes there is a last "multi-droplet" regime in which many nuclei are formed and the MST ceases

to depend on system size, reaching and asymptotic value [151]. This picture fits perfectly well with our numerical findings.

From this analysis, we conclude that, with the present computational resolution, we can just give a rough estimation for the location of the transition point $0.070 < p_{d_{thr}} < 0.075$.

To show further evidence of the discontinuous nature of the phase transition, figure 3-2 illustrates the system bistability around the transition point: depending on the density of the initial configuration, a homogeneous steady state may converge either to a stationary state of large density (active) or to the absorbing state. A separatrix marks the distinction between the two different basins of attraction. Let us remark that systems exhibiting a first-order transition are bistable only at exactly the transition point but for finite system sizes the coexistence region has some non-vanishing thickness. The existence of bistability makes a strong case for the discontinuous character of the transition.

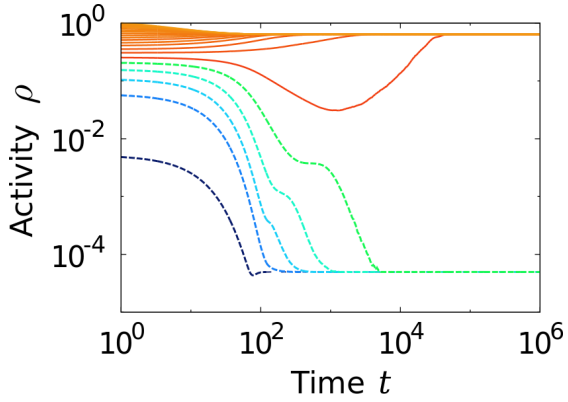

Figure 3-2: **Bistability at the transition point of the pure model**. Log-log plot of the averaged particle density as a function of time for different initial conditions in the neighborhood of the transition point (results here are for $p_d = 0.07315$). Depending on the initial density, the system stabilizes in the active or in the absorbing phase. The selected initial densities are equi-spaced in the interval $[0.005, 1]$ with constant increments 0.05; system size $N = 256^2$ and averages performed over up to 10^6 realizations.

Spreading experiments from a localized seed– We consider a few (at least 2) neighboring particles at the center of an otherwise empty lattice, and monitor how activity spreads from that seed. Each simulation run ends whenever the absorbing state is reached or when activity first touches the boundary of the system. We monitor the averaged squared radius from the origin $R^2(t)$, the averaged number of particles over surviving trials, $N_s(t)$, and the survival probability, $P_s(t)$ [146]. Figure 3-3 shows log-log plots of these three quantities as a function of time. In all cases, we find a threshold value $p_{d_{thr}} \approx 0.073$ that marks a change of tendency, signaling the frontier between the absorbing and active phases. In the active phase ($p_d < p_{d_{thr}}$) and for large values of t, both $N_s(t)$ and R^2 grow approximately as t^2 (as expected for ballistic expansion), while $P_s(t)$ converges to a constant (i.e. some runs do survive indefinitely). On the other hand, in the absorbing phase all three quantities curve downwards indicating exponential extinction.

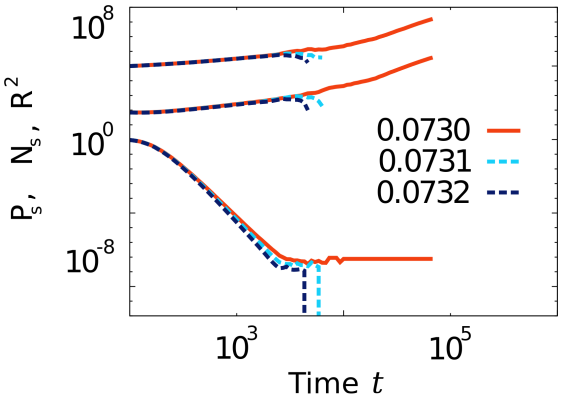

Figure 3-3: **Spreading experiments for the pure model**. Double-logarithmic plot of the (from bottom to top), (i) the survival probability $P_s(t)$, (ii) the averaged number of particles $N_s(t)$ (averaged over surviving runs), and (iii) the averaged squared radius (averaged over of all runs), as a function of time, for $N = 1024^2$ using up to 4×10^{10} experiments. Curves for $R^2(t)$ have been shifted upwards for clarity. In spite of the large number of runs used to average, curves are still noisy. This is due to the fact that, being very close to the transition point, a large fluctuation is needed for the system to "jump" to the active phase from the vicinity of the absorbing one and only a few runs reach large times.

Thus, the pure model exhibits a discontinuous transition at some value of $p_{d_{thr}} \approx 0.073$, which separates a phase of high activity from an absorbing one. Observe, that the estimation of the transition point is compatible with the interval obtained above.

The appearance of a continuous transition

We now analyse whether the discontinuous transition is maintained in presence of quenched disorder. To that purpose we perform the previous experiments in the disordered model version.

Homogeneous initial conditions– We have computed time series for *i)* the mean particle density averaged over all runs and *ii)* the mean particle density for surviving runs (i.e. those which have not reached the absorbing state). Figure 3-4 shows time evolution after up to 2×10^4 realizations. Results are strikingly different from those of the pure-model.

For values below threshold, $p_d < p_{d_c} \approx 0.077$, the particle density converges to a constant value for asymptotically large times, while for $p_{d_c} > 0.077$ curves decay as power laws (a much more precise estimation of the critical point will be computed below). The generic algebraic decay is observed for a wide range of p_d; however, the transient before the power-law regime increases with p_d, which makes it difficult to determine the exact boundaries of the mentioned range. The presence of generic algebraic scaling in an extended region is the trademark of Griffiths phases.

Plotting the activity over the surviving trials [Fig. 3-4b], we observe that the evolution is non-monotonous in the absorbing (Griffiths) phase: the curves decrease up to a minimum value and then increase. This stems from the fact that realizations with large rare active regions remain active for longer times than those with smaller ones; as realizations with only relatively small rare-regions progressively die out, those with larger and larger rare-regions are filtered through and, thus, the overall average

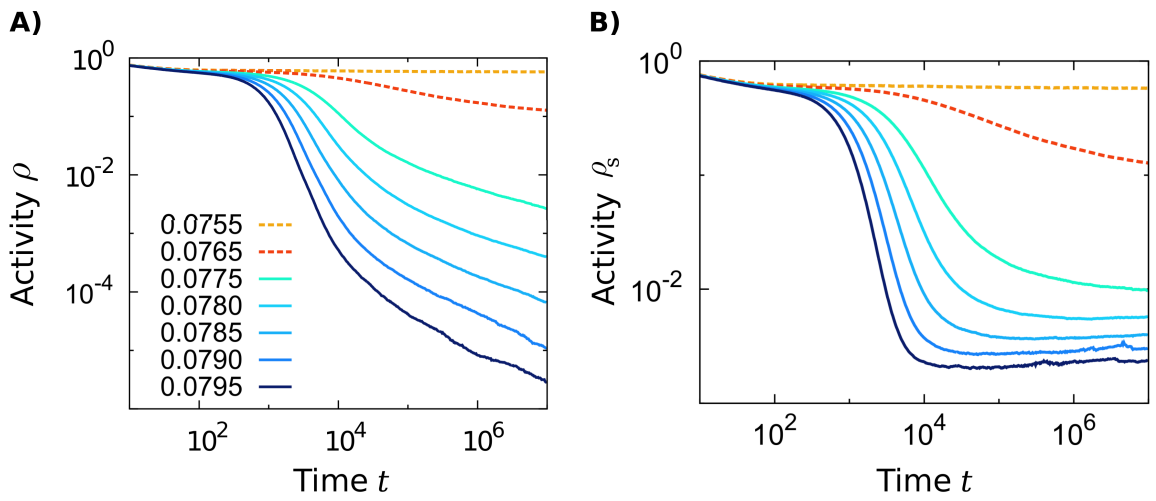

Figure 3-4: **Density decay from a homogeneous initial conditions in the disordered model.** (a) Particle density averaged over all trials in a lattice of size 256^2 and up to 2×10^4 realizations (curves in the active phase are plotted with dashed lines). Observe the presence of a broad region with generic power-law behavior, i.e. a Griffiths phase which starts roughly at $p_d = 0.0775$. (b) As (a) but averaging only over surviving trials. Note the non-monotonic behavior in the Griffiths phase (see main text for details).

density grows as a function of time, being limited only by system size.

In addition, we observe that, contrarily to the pure case, there is no bistability around the transition point (figure 3-5). Indeed, very near to the transition point ($p_d = 0.07650$), all curves regardless of their initial value converge to a unique well-defined stationary density close to zero, as appropriate for a continuous transition to an absorbing state.

Spreading experiments from a localized seed– Figure 3-6 shows results for three spreading observables as a function of time; for all of them, we clearly observe generic asymptotic power laws with continuously varying exponents.

These spreading quantities also allow us to scrutinize the behavior at the critical point. As discussed in the Introduction, in a disordered system as the one under study, we expect logarithmic (activated scaling) at criticality. Indeed, Figure 7 shows results for the usual spreading quantities represented in a double logarithmic plot

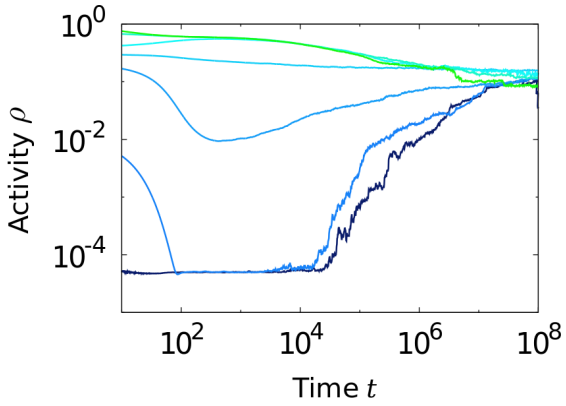

Figure 3-5: **Absence of bistability in the disordered model.** Double-logarithmic plot of the averaged particle density as a function of time for $p_d = 0.0765$, with $N = 256^2$, and up to 10^6 realizations. Initial densities are $\rho_0 = 0.00006, 0.01, 0.2, 0.3, 0.4, 0.7, 1$. Regardless of the initial condition, the system stabilizes to a constant small value of the density, as expected for a second-order phase transition.

of the different quantities as a function of $ln(t/t_0)$. The value of t_0 is in principle unknown and constitutes a significant error source [222]. We fix it as the value of t such that it gives the best straight lines at the transition point for all three quantities [222]). Right at the critical point ($p_c \approx 0.07652$ to be obtained with more accuracy below) a straight asymptotic behavior indicates that results are compatible with logarithmic (i.e. activated) type of scaling. The best estimates for the (pseudo)-exponents listed in the previous section are: $\bar{\delta} \approx 1.90$, $\bar{\theta} \approx 2.09$, and $\Psi \approx 0.43$, which are compatible with the values reported in the literature for the universality class of directed percolation with quenched disorder (i.e. $\bar{\delta} = 1.9(2)$, $\bar{\theta} = 2.05(20)$, $\Psi = 0.51(6)$).

Similarly, following the work of Vojta and collaborators [222], we represent in Fig. 8 one of the spreading quantities as a function of another one, e.g. $N(t)$ as a function of $P_s(t)$ to eliminate the free variable t_0 from the plot. This type of plot allows for the identification of power-law dependencies rather than logarithmic ones, i.e. $N(t) \sim P_s(t)^{-\bar{\theta}/\bar{\delta}}$. If the second-order phase transition belongs to the

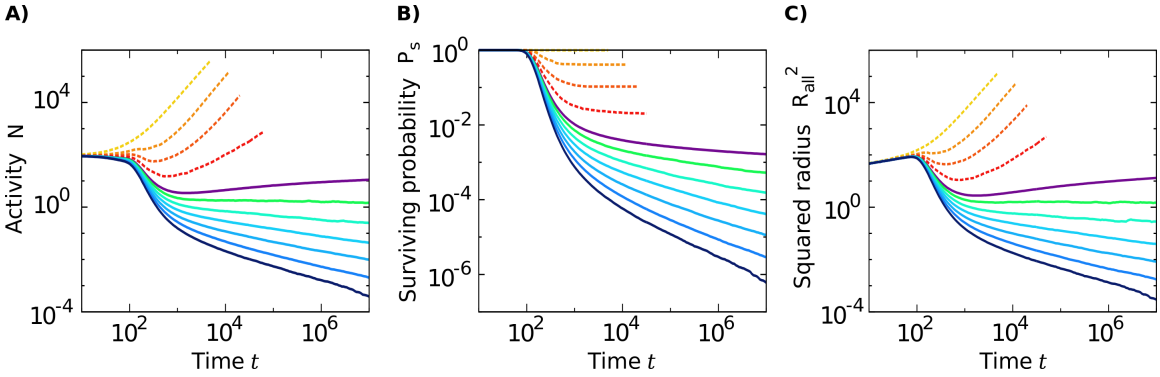

Figure 3-6: **Spreading experiments in the disordered model**. Double logarithmic plot of the three usual spreading quantities showing the presence of generic power-laws with continuously varying exponents all along the Griffiths phase ($p_d \lesssim 0.07652$). Parameter values (from top to bottom) $0.06, 0.07, 0.073, 0.075, 0.07652, 0.077, 0.0775, 0.078, 0.0785, 0.079, 0.0795$ (curves in the active phase are plotted with dashed lines), up to 5×10^7 realizations.

universality class of the directed percolation with quenched disorder, we should have $N(t) \sim P_s(t)^{-1.08(15)}$, using as a reference the values in the literature [222]. Indeed, as shown in Figure 8 we obtain $N(t) \sim P_s(t)^{-1.10(2)}$, in very good agreement with the expected value [222], and this is the method by which the critical point location, $p_d \approx 0.07652$, is obtained with best accuracy.

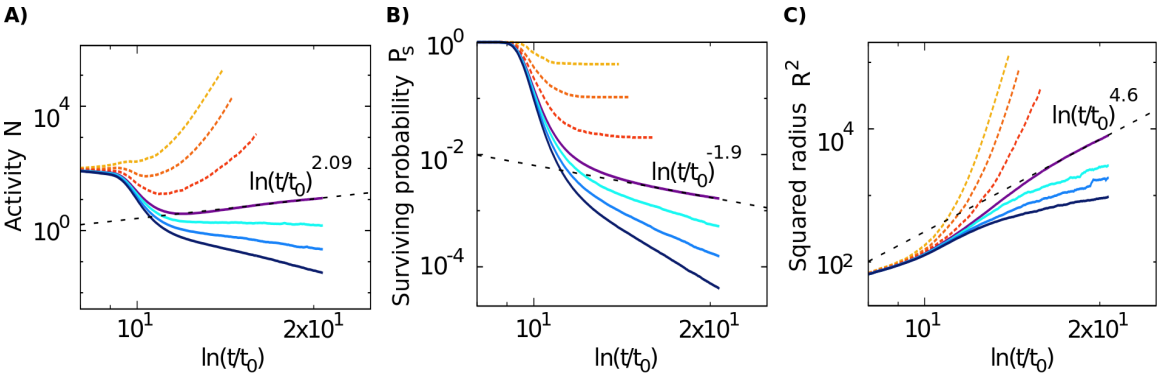

Figure 3-7: **Spreading experiments in the disordered model**. Double logarithmic plot of the three usual spreading quantities as a function of $\ln(t/t_0)$ for different parameter values (from top to bottom $0.07, 0.073, 0.075, 0.07652, 0.077,\ 0.0775, 0.078$ (curves in the active phase are plotted with dashed lines). Same network sizes as in the homogeneous case and up to 10^6 realizations. By conveniently choosing $t_0 = 0.01$ (see main text) we observe straight lines at the critical point, $p_d \approx 0.07652$. From their corresponding slopes we measure the associated (pseudo)-exponents: $\bar{\theta} \approx 2.09$, $\bar{\delta} \approx 1,9$, and $2/\Psi \approx 4.6$ (slopes marked by dashed lines). These values have a large uncertainty, as changes in the value of t_0 severely affect them. Estimating these exponents with larger precision is computationally very demanding.

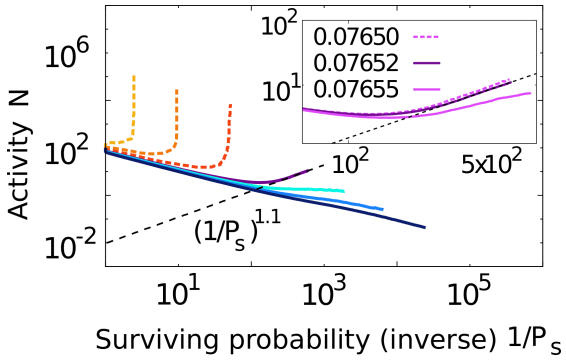

Figure 3-8: **Double logarithmic plot of $N(t)$ as a function of $1/P_s(t)$ for spreading experiments at criticality in the disordered model [220].** Our best estimate for the slope of at the critical point (separatrix of the curves, see main panel) is compatible with the value reported in the literature $N(t) \sim P_s(t)^{-\bar{\theta}/\bar{\delta} \approx -1.08}$ corresponding to the universality class of the directed percolation with quenched disorder. The inset shows a zoom around the critical point. Lattice size $N = 1024^2$; averages up to 5×10^7 realizations, and same parameters as in Figure 7.

3.4 Conclusions. *"Non equilibrium Imry-Ma argument"*

In contrast with the pure model, in the disordered case we have found a Griffiths phase and a second-order phase transition with an activated type of scaling. Therefore, in this non-equilibrium system with one absorbing state the situation remains much as in equilibrium situations: disorder annihilates discontinuous transitions and induces criticality.

Results are rather similar to those reported for the standard contact process with quenched disorder. Indeed, results are fully compatible (up to numerical precision) with the standard strong-disorder fixed point of the universality class of the directed percolation with quenched disorder [114, 220, 222]. We believe that our results are robust upon considering other types of (weaker) disorders [115]. Thus, two different models with significantly different pure versions –i.e. one with a first-order and one with a second-order transition– become very similar once quenched disorder is introduced. Both exhibit Griffiths phases and activated scaling at the transition point.

From a more general perspective, deciding whether novel universal behavior emerges in disorder-induced criticality is still an open problem in statistical mechanics. For illustration, let us point out that recent work suggests that disorder-induced second-order phase transitions in an Ising-like system with up-down symmetry does *not* coincide with Ising transition [18]. Similarly, in Ref. [115] a novel type of critical behavior is found for disorder-induced criticality. In the case studied here, the disorder-induced criticality does not seem to lead to novel behavior (up to numerical precision); indeed, all evidences suggest that it behavior coincides with the universality class of the directed percolation with quenched disorder.

After a careful inspection of the literature in search of discontinuous transitions in disordered non-equilibrium low-dimensional systems, we found a very recent work in which the authors study the popular (two-dimensional) Ziff-Gulari-Barshad (ZGB)

model for catalytic oxidation of carbon monoxide [233] in the presence of catalytic impurities (a fraction of inert sites) [27]. The pure ZGB model is known to exhibit, among many other relevant features, a discontinuous transition into an absorbing state. However, after introducing quenched disorder, no matter how small its proportion, the discontinuous transition is replaced by a continuous one [27], similarly to our findings here.

In conclusion, we conjecture that first-order phase transitions cannot appear in low-dimensional disordered systems with an absorbing state. In other words, the Imry-Ma-Aizenman-Wehr-Berker argument for equilibrium systems can be extended to non-equilibrium situations including absorbing states. The underlying reason for this is that, even if the absorbing phase is fluctuation-less and hence is free from the destabilizing effects the Imry-Ma argument relies on, the other phase is active and subject to fluctuation effects. Therefore, intrinsic fluctuations destabilize it as predicted by the Imry-Ma-Aizenman-Wehr-Berker argument, precluding phase coexistence.

Remarkably, in the case studied by Barghathi and Vojta, in which the Imry-Ma argument is violated in favor of a second-order phase transition, the two broken-symmetry states are absorbing ones: once the symmetry is broken in any of the two possible ways, the system becomes completely frozen, i.e., free from fluctuation effects, and, consequently, the Imry-Ma argument breaks down. Thus, the only possibility to have first-order phase transitions in low-dimensional disordered systems would be to have (in its pure version counterpart) a discontinuous phase transition between two different fluctuation-less states, and we are not aware of any such transition. Therefore, we conclude that quenched disorder forbids discontinuous phase transitions in low-dimensional non-equilibrium systems with absorbing states.

Chapter 4

Structural heterogeneity.

Rounding of abrupt transitions in cortex networks

In chapter 3 we conjectured that dynamical models of activity propagation characterized by discontinuous phase transitions, at the mean-field level, exhibit a rounding phenomenon in finite dimensional disordered systems, eventually leading to continuous phase transitions at dimension $d \leq 2$. Such behavior has been envisaged as the non-equilibrium analogue of the well-know Imry-Ma criterion, which states that (in the presence of quenched disorder) first-order phase transitions are prohibited in equilibrium systems at $d \leq 2$ [119, 3, 19].

Analogously to quenched disorder in lattices, structural disorder is integral to any non-trivially connected system and may thus be responsible for the rounding of discontinuous phase transitions in such systems [158]. In this light, we investigate how topological disorder can potentially alter the order of phase transitions exhibited by the prototypical quadratic contact process. In analogy with the Imry-Ma criterion, a

priori, this effect should be expected to occur in networks with topological dimension d less than 2 (chapter 3).

Due to the great variety of complex networks present in nature, an extensive analysis of all of them would be difficult. In this chapter we focus on a system that is well described by the previous model and extremely affected by its structure, the brain cortex. We present an extensive numerical study of the quadratic contact process, which would describe activity propagation in brain networks through the integration of different neighboring spiking potentials (mimicking basic neural interactions). The requirement of signal integration may lead to discontinuous phase transitions , thus preventing the emergence of critical points in such systems. Here we show that criticality in the brain is instead robust, as a consequence of the hierarchical organization of the higher layers of cortical networks.

4.1 Introduction

4.1.1 Criticality in brain cortex and "single-node" models

Experimental evidence of critical or quasi-critical behavior in brain networks was gathered over the past decade [15, 16, 170, 14, 166, 100, 43]. The discovery of scale-invariant avalanches of neural activity led to the conjecture that the brain might operate close to a critical point [15, 16]. It was argued that critical behavior might bear functional advantages; for instance, the divergence at criticality of quantities such as susceptibilities and correlation lengths could entail the ability of brain networks to coordinate system-wide activities and efficiently respond to a broad range of stimuli. A vast number of studies have since flowered, focusing on the numerical simulation of simple dynamical models that could recover phenomenologically the hallmarks of criticality observed in experiments [125, 124, 176, 224, 225]. In particular, it was noted

that effective highly-simplified models of activity propagation –such as the contact process and the quiescent-excited-refractory-quiescent model– could provide valuable information on large-scale brain properties [96]. In these ideal models, an active "unit" or node –be it a neuron at a microscopic scale or a coarse-grained active region at a larger mesoscopic scale– can propagate its activity to neighboring units and/or become deactivated. Such simple dynamics –where activity propagation involves a single active node– lead generically to continuous phase transitions, with a critical point separating an active from a quiescent phase [146, 137, 161, 106]. Moreover, relatively simple modifications of these models implementing standard mechanisms of self-organized criticality lead to robust critical or quasi-critical behavior without the need of parameter fine tuning [136, 154, 24].

4.1.2 Discontinuous transitions and integrative neural models

A closer look at real neural dynamics suggests that neural activity propagation may follow more complicated rules. In particular, individual neurons usually require to integrate up to hundreds of post-synaptic potentials before spiking themselves, as typically captured by integrate-and-fire models [1, 28, 29].

At mesoscopic scales, such requirement may be less stringent; however it is reasonable to consider that a few neighboring active units might be required to generate further activity: i.e. the dynamics follow a schematic rule of the type: $n\mathrm{A} \rightarrow (n+m)\mathrm{A}$, with $n > 1$ and m of the order of a few units, where each A stands for an active location or site [146, 137, 161, 106].

Such types of (n, m)-processes are well known in reaction-diffusion systems [146, 137, 161, 106], and they are often used in the modeling of neural dynamics. In particular, it is known that they lead to broad phases of sustained activity [125] and enhanced dynamic ranges [129, 86]. However, these processes are also well-

known to lead to pattern formation (Turing patterns) and to discontinuous phase transitions between active and quiescent phases, with associated phase coexistence [228] and lacking critical points, in seeming contradiction with the observation of scale-invariant behavior in brain dynamics. In other words, the requirement of more than one source of activity to generate further activity leads to discontinuous phase transitions, separating two highly different active and quiescent phases, with no sign of criticality nor scale-invariance in between [146, 137, 161, 106].

A goal in this chapter is to reconcile the need for signal integration at the neuron scale, supposedly leading to discontinuous transitions, with the empirical observation of critical-like features, characteristic of continuous phase transitions. As we hope to convincingly argue, the key to this puzzling ambiguity lies in the topology of the underlying network of neural connections, which we will prove responsible for the generic rounding of discontinuous transitions.

4.2 The model

Dynamics

In what follows, we provide extensive numerical tests of the above conjecture, showing how the topological dimension of a disordered network can tune the nature of the dynamical phase transition, ultimately forcing $n\mathrm{A} \to (n+m)\mathrm{A}$ dynamics to exhibit continuous transitions for $d \leq 2$. To this end, we consider the prototypical quadratic contact process, in which we choose $n = 2$ and $m = 1$, whose Monte Carlo implementation is as follows: each of the N nodes of the network is endowed with a binary state variable $\sigma = 0, 1$, inactive or active, and $\rho(t)$ is the density of active nodes at time t; i) at each time step an active node R_1 is selected and time is increased by $[N\rho(t)]^{-1}$; ii) with *death* probability p_d, R_1 is deactivated, while with complementary probability

$1 - p_{\mathrm{d}}$, a neighboring node R_2 is considered and one of the following actions is taken; iiia) if R_2 is inactive, activity diffuses to R_2, leaving R_1; iiib) if R_2 is active, a new neighbor R_3 of R_1 is considered and, if inactive, it is activated with *birth* probability p_{b}. From a neurophysiological perspective, p_{d} encodes the exhaustion mechanism that accounts for spontaneous deactivation of neurons and neural regions, which proves essential in maintaining sustained activity bounded [125]. The integrated activation is tuned by p_{b}.

Notice that different choices of $n, m > 1$, which might account for enhanced realism in the physiological description of brain networks at the mesoscale, would not affect the behavior. A more detailed theoretical description of this system –taking explicitly into account the underlying network topology– would be provided by a quenched-mean-field approach [158].

Structure

In spite of the huge complexity that would be required to represent the detailed structure of the brain down to the single-neuron level, an effective coarse-grained description of neural contact patterns can be provided by a network –the connectome– whose nodes represent groups of neurons, such as cortical columns, and whose links represent the groups of fibers connecting them [124].

Studies employing different neuroimaging techniques have revealed that the Human Connectome, the current mapping of human brain connections, is organized in a hierarchical and modular fashion, in which local regions are clustered into large-scale moduli, which in turn form higher level structures and so on [196, 152, 126, 195, 99, 232]. The resulting hierarchical modular network (HMN) can be visualized as built-up from moduli of large internal neural connectivity, enclosed into higher-level sparser moduli, in a nested hierarchical fashion.

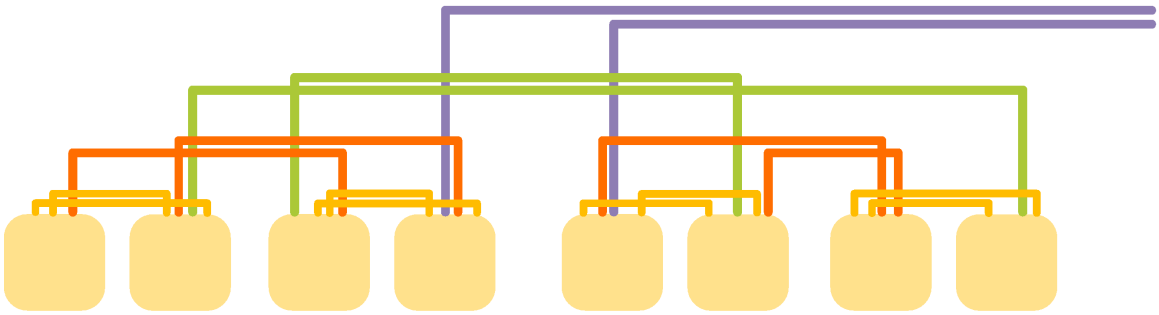

Figure 4-1: Sketch of the HMN construction method. Given a positive integer s, consider 2^s basal fully connected moduli of size M. At the lowest hierarchical level, moduli are linked pairwise into super-moduli by establishing a fixed number α of random unweighted and undirected links between the elements of each modulus ($\alpha = 2$ in figure). Newly formed blocks are then iteratively linked pairwise with the same α for a total of s iterations, until the network becomes connected. The resulting network has size $N = 2^s M$.

HMNs have been recently found to play a crucial role in neural dynamics. In particular, simple models of activity propagation were recently found to display Griffiths phases when running on top of HMNs [156], corroborating the experimental observation of extended critical regions in the human at its resting state [202]. Similarly, they were argued to extend the region of apparent criticality in self-organized models of neural activity and they were used to explain the ability of the brain to sustain activity over extended time windows [125, 124, 176, 224, 225, 156].

Here we shall use a simple structural model to build-up synthetic HMNs as follows: local densely connected moduli are used as building blocks; they are recursively grouped by establishing additional inter-moduli links in a level-dependent way, as exemplified in Figure 4-1. Further details of the construction methods can be found in Reference [156]. A crucial feature of HMNs is represented by their finite topological dimension d. The topological dimension of a network can be defined as follows: starting from a single node, the number of neighbors N_z reachable after z steps is computed for increasing z until the entire network is covered [158]. The network is finite dimensional with dimension d if $\langle N_z \rangle \sim z^d$, generalizing the familiar behavior of

regular lattices. The topological dimension of a HMN can be tuned easily, by changing the average number α of links between pairs of modules at each hierarchical level (see Fig. 4-1 and [156]). Although brain moduli and columns may be densely connected, at larger mesoscopic and macroscopic scales the hierarchical contact patterns become very sparse. At such scales, the effective network becomes finite dimensional [80, 156].

As a substrate on which the above dynamics run, we considered different HMNs, characterized by different topological dimensions d. In the rest of the chapter we will show results for HMN extracted from two ensembles $\mathcal{N}_-$ and $\mathcal{N}_+$, each with a fixed average dimension $d_{-,+}$ below and above the threshold value $d = 2$. In particular, we show results for $d_- \approx 1.6$ and $d_+ \approx 2.8$ (networks with such properties are obtained by choosing $\alpha = 1$ and $\alpha = 4$ respectively, in the HMN building-up process; see Figure 4-1).

4.3 Results

We ran Monte Carlo simulations of the above process on such networks. Figure 4-2 shows the steady state value of the average activity density, as a function of the control parameter p_{d}, respectively below and above dimension $d = 2$, in spreading simulations starting both from localized active seeds ($\rho_0 \approx 0$) and from the homogeneously active state ($\rho_0 = 1$). While the discontinuity encountered above $d = 2$ is in agreement with the mean-field behavior for this type of dynamics, below $d = 2$ the dynamical phase transition is evidently continuous, confirming the conjecture of a low-dimensional rounding.

To provide further evidence of the radical difference in the transition nature, Figure 4-3 shows the time evolution of the average activity density ρ upon changing the initial activity ρ_0, for both cases in Figure 4-2, each at the estimated threshold

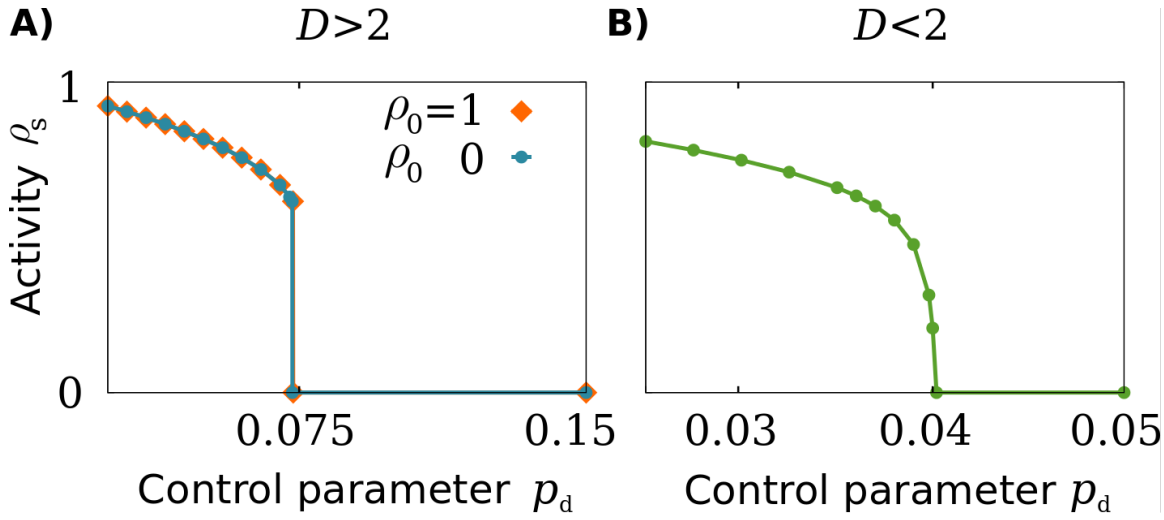

Figure 4-2: Phase diagrams for topological dimension d above and below $d = 2$ respectively. In high dimension, the phenomenology of a discontinuous phase transition is recovered, in agreement with the mean-field prediction for the quadratic contact process. Below $d = 2$, the transition becomes continuous. A feeble appearance of hysteretic behavior is recorded in the $d > 2$ case, where different colors correspond to different initial conditions and spinodal points marking the transition are located at $p_{\mathrm{d_{thr}}} \approx 0.0732(1)$ and $p_{\mathrm{d_{thr}}} \approx 0.0734(1)$ for $\rho_0 = 0$ and $\rho_0 = 1$ respectively (not distinguishable in figure). Such dependence disappears for $d < 2$, in accordance with the the hypothesis of a continuous phase transition, the critical point being located at $p_{\mathrm{d_{thr}}} \approx 0.0402(1)$ Simulations are run on HMNs of size $N = 2^{17} = 131072$, partitioned into $s = 13$ hierarchical levels.

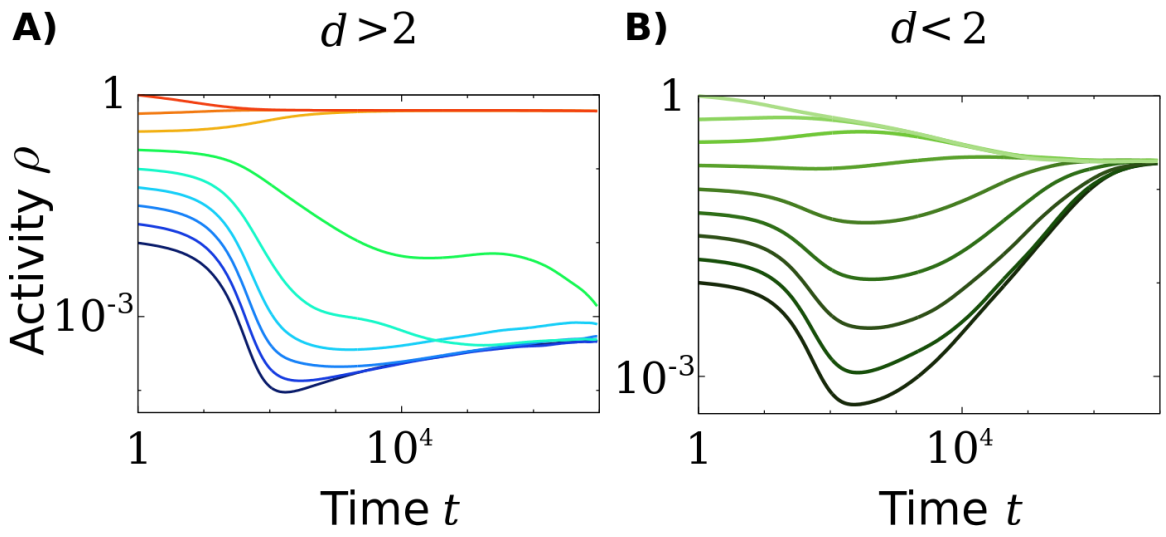

Figure 4-3: Time evolution of the activity density ρ for different initial values ρ_0 (different colors), for dimension above and below $d = 2$ respectively. In both cases, the control parameter p_{d} is chosen at the threshold value. For high dimension, bistable behavior is recovered, as in standard first-order transitions, whereas no sign of bistability is encountered below $d = 2$. Notice however that both configuration converge very slowly to their expected behavior. In particular, in the $d > 2$ (discontinuous) case, large enough initial conditions lead to very long transients, which could be misinterpreted as continuous behavior for short simulation times. Such traits of quasi-critical states become stronger as $d = 2$ is approached from above, and corroborate the picture of a rounding phenomenon.

p_{d}. Above $d = 2$ clear signs of bistability emerge, signaling coexistence phenomena, which typically characterize discontinuous phase transitions. Below $d = 2$, however, the steady state does not depend on the initial condition anymore, as expected for a continuous transition, in which correlations become system-wide and coexistence is prohibited. In order to gain a deeper understanding of the rounding phenomenon, we can analyze the nature of the inactive (absorbing) phase in both cases.

To this end, let us consider simulations starting from a homogeneous $\rho_0 = 1$ state. Time evolution of ρ is shown in Figure 4-4, for different values of p_{d} in the inactive phase. As usual, above $d = 2$ results for p_{d} point to an abrupt change in behavior at the dynamic threshold $p_{\mathrm{d_{thr}}}$, below which activity dies off exponentially fast as soon

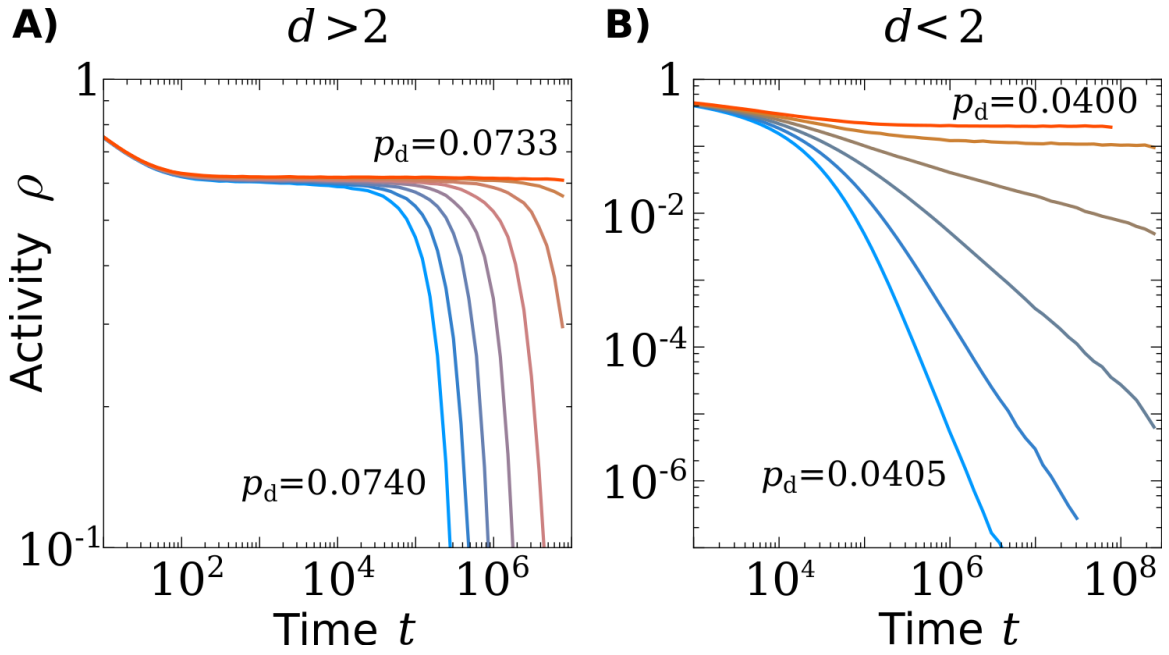

Figure 4-4: Time evolution of the activity density ρ for different values of the control parameter p_{d} (different colors) below the dynamic threshold, for dimension above and below $d = 2$ respectively. For high dimension, the transition between the inactive and the active state is abrupt, with no signs of criticality. Below $d = 2$, a Griffiths phase emerges for $p_{\mathrm{d}} > p_{\mathrm{d_{thr}}}$, characterized by generic power-law relaxation and critical-like behavior.

as a large enough fluctuation breaks the coexistence of active and inactive islands. At $p_{\mathrm{d_{thr}}}$, such coexistence becomes stable in the large-N limit and the phenomenology of a discontinuous phase transition is recovered. For dimensions below $d = 2$, instead, the system displays a Griffiths phase[220, 218]: the average activity density decays as power laws with continuously varying exponents as a function of the control parameter p_{d}. A critical point, characterized by activated scaling logarithmic time decay ($p_{\mathrm{d_{thr}}} \approx 0.0402(1)$ in Fig.4-4) separates the Griffiths phase from the active phase, marking the recovery of critical behavior at low dimension. Griffiths phases are a manifestation of rare-region effects: islands of localized activity are able to remain active for long times. Their relevance for both complex networks [158] and brain networks [156] has been recently discussed in the literature. Activity propagation models without signal integration yield such behavior in HMNs as they naturally lead to continuous phase transitions regardless of dimensionality constraints [156]. Remarkably, the quadratic contact process dynamics at low dimensions recovers here those fingerprints of criticality, in spite of being typically associated with discontinuous transitions at mean field. Interestingly, upon approaching the threshold dimension from above, $d \to 2^+$, the discontinuous nature of the transition is rounded: although coexistence is genuinely recovered at very large times, activity is able to self-sustain even in the absorbing state for times potentially longer than any observation window.

4.4 Conclusions. *Rounded large-scales transitions in neural dynamics*

A recent study showed that the quadratic contact process adopted here as a paradigm for first-order phase transitions may show tricritical behavior in certain families of ordered fractal lattices of dimension $1 < d < 2$ [229]. Such a finding implies that for each family of ordered fractals, there exist a "critical" dimension $1 < d_c < 2$, below which the transition is continuous, recovering the known behavior of one dimensional chains, and above which the transition becomes discontinuous, anticipating the behavior of pure two-dimensional lattices. In our study we have introduced disorder in the topology and shown that finite-dimensional disordered hierarchical modular networks of relevance in neuroscience *always* display continuous phase transitions for $d < 2$. In fact even square lattices ($d = 2$) exhibit this behavior provided that disorder is introduced, specifically in the form of quenched impurities (chapters 2 and 3). Such results corroborate the conjecture that, due to disorder, non-equilibrium systems with absorbing states do not sustain first-order dynamical phase transitions for *any* $d \leq 2$. We provided further evidence for this claim, proving its validity for HMNs, and we focused on the relevance that such result may have for neuroscience. Brain activity is known to exhibit critical-like behavior, which would suggest its ability to sit constantly in the vicinity of a continuous transition. We have shown that even if realistic dynamic models lead to first-order phase transitions in the mean-field approximation, in low-dimensional disordered systems such transitions are rounded. A natural question arises whether the brain actually is a low-dimensional network, provided that each single neuron may have up to thousands of neighbors. The solution to this apparent contradiction comes from the hierarchical organization of brain connections. At the lowest scales, neurons are grouped in well connected moduli which act as small worlds of diverging topological dimension. At such scales, integrate-and-fire dynamics

naturally trigger coexistence and local discontinuous activations of moduli. At the largest scales, however, inter-moduli connectivity is very sparse in order to maintain the volume of white-fiber matter bounded [124], allowing only for weak small-world effects [80]. Such connectivity patterns become finite dimensional, and discontinuous phase transitions are prohibited. Notice that the $d = 2$ bound should not be read strictly in real systems. We found that significant traits of quasi-critical behavior appear even above $d = 2$, suggesting a gradual rounding phenomenon. Such systems will theoretically show discontinuous transitions for large enough times, yet they are able to sustain anomalous activity for typical time windows of experimental observations. More detailed and realistic models of neural dynamics could be provided. While the behavior presented here is conserved for different choices of the parameters (n, m), realistic models supposedly include ingredients such as refractory times, explicit time integration, inhibition and dependence on synapse directedness. While such details are of primary importance in correctly describing physiological aspects of brain activity, we believe that our simple approach has the advantage of focusing on the large-scale topology of the Human Connectome [196, 99], in order to provide insight about its large-scale behavior. An understanding of low-level synaptic activity requires realistic neuron models and remains a formidable task.

In conclusion, we have studied the properties of a family of dynamic models of relevance in the description of neural activity in the presence of signal integration. Although signal integration may be responsible for the emergence of first-order phase transitions in generic networks, we have shown that phase transitions are rounded in finite dimensional hierarchical networks, eventually turning continuous for $d \leq 2$. Such finding is relevant in explaining the observation of critical behavior in the brain at large scales, in spite of the high degree of signal integration required to fire neuron activity at small scale.

Chapter 5

Co-evolutionary systems.

Rapid phenotypic diversification in ecological systems

There is no denying that, besides the mechanisms studied in previous chapters, adaptation and evolution are essential aspects of living systems. Usually, the times needed to observe them is extremely long compared to communities dynamics, however, recent experiments lead us to believe that, in some systems, rapid evolutionary changes can feed back into ecological interactions. A recent long-term field experiment has explicitly shown that communities of competing plant species can experience very fast phenotypic diversification, and that this gives rise to enhanced complementarity in resource exploitation and to enlarged ecosystem-level productivity.

In this chapter, we build on progress made in recent years in the integration of eco-evolutionary dynamics, and present a computational approach aimed at describing these empirical findings in detail. In particular we model a community of organisms of different but similar species evolving in time through mechanisms of birth, competition,

sexual reproduction, descent with modification, and death. Based on simple rules, this model provides a rationalization for the emergence of rapid phenotypic diversification in species-rich communities. Furthermore, it also leads to non-trivial predictions about long-term phenotypic change and ecological interactions.

Our results illustrate that the presence of highly specialized, non-competing species leads to very stable communities and reveals that phenotypically equivalent species occupying the same niche may emerge and coexist for very long times. Thus, the framework presented here provides a simple approach (complementing existing theories, but specifically devised to account for the specificities of the recent empirical findings for plant communities) to explain the collective emergence of diversification at a community level, and paves the way to further scrutinize the intimate entanglement of ecological and evolutionary processes, especially in species-rich communities.

Although, contrarily to expected, no phase transition between poor and rich species diversity (generalist and specialists regimes, respectively) appears, we will investigate the conditions under which this occurs in future work.

5.1 Introduction

Community ecology studies how the relationships among species and their environments affect biological diversity and its distribution, usually neglecting phenotypic, genetic and evolutionary changes [143, 174, 207]. In contrast, evolutionary biology focuses on genetic shifts, variation, differentiation, and selection, but –even if ecological interactions are well-recognized to profoundly affect evolution [74]– community processes are often neglected. Despite this apparent dichotomy, laboratory analyses of microbial communities and microcosms [171, 231, 101, 77, 211, 108, 48, 67, 45, 194] as well as long-term field experiments with plant communities [209, 200] and vertebrates [201, 88] provide evidence that species can rapidly (co)evolve and that eco-

and evolutionary processes can be deeply intertwined even over relatively short (i.e. observable by individual researchers) timescales [70].

Over the last two decades or so, the need to consider feedbacks between ecological and evolutionary processes has led many authors to develop a framework to merge together the two fields [190, 134, 59, 60, 133, 206, 58, 62, 63, 188, 138, 37, 78, 56, 40, 123, 90, 55, 189, 102, 61, 210]. In particular, the development of quantitative trait models [79] and the theories of adaptive dynamics [84, 83] and adaptive diversification [59, 60, 133, 58, 62, 63, 40], reviewed in [79, 61], has largely contributed to the rationalization of eco-evolutionary dynamics, shedding light onto non-trivial phenomena such as sympatric speciation and evolutionary branching [61].

On the empirical side, the recent work by Zuppinger-Dingley *et al.* on long-term field experiments of vegetation dynamics appears to confirm many of the theoretical and observational predictions [235]. This study provided strong evidence for the emergence of *rapid collective evolutionary changes*, resulting from the selection for complementary character displacement and niche diversification, reducing the overall level of competition and significantly increasing the ecosystem productivity within a relatively short time. This result is not only important for understanding rapid collective evolution, but also for designing more efficient agricultural and preservation strategies. More specifically, in the experimental setup of Zuppinger-Dingley and colleagues, 12 plant species of different functional groups were grown for 8 years under field conditions either as monocultures or as part of biodiverse communities. Collecting plants (seedlings and cutlings) from these fields, propagating them in the laboratory, and assembling their offspring in new communities, it was possible to quantify the differences between laboratory mixtures consisting of plants with a history of isolation (i.e. from monocultures) and plants from biodiverse fields. While the former maintained essentially their original phenotypes, the latter turned out to experience significant complementary trait shifts –e.g. in plant height, leaf thickness,

etc.– which are strongly suggestive of a selection for phenotypic and niche differentiation [210] (see figure 5-1 therein). Furthermore, there were strong *net biodiversity effects* [139], meaning that the relative increase in total biomass production in laboratory mixtures with respect to laboratory monocultures was greater for plants from biodiverse plots than for plants coming from monocultures. These empirical results underscore the need for simple theoretical methodologies, in the spirit of the above-mentioned synthetic approaches [190, 203, 60, 62, 63, 79, 90, 61, 50]. These approaches should explain the community and evolutionary dynamics of complex and structured communities such as the ones analyzed in [235].

The phenotypic differentiation observed in the experiments of Zuppinger-Dingley et al. might be partially rationalized within the framework of relatively simple deterministic approaches to eco-evolution such as adaptive dynamics (see e.g. [190, 203, 60, 62, 63, 79, 90, 61]). In this context, diversification is the natural outcome of an adaptive/evolutionary process that increases fitness by decreasing competition through trait divergence.

However, it is not obvious what would be the combined effects in this simplistic version of adaptive dynamics of introducing elements such as sexual reproduction, space, and multi-species interactions that could play an important role in shaping empirical observations. Moreover, questions such as whether phenotypic differentiation occurs both above and below the species level (i.e., within species or just between them), the possibility of long term coexistence of phenotypically equivalent species in the presence of strong competition (i.e., emergent neutrality), or the expected number of generations needed to observe significant evolutionary change remain unanswered and require a more detailed and specific modeling approach, within the framework of adaptive dynamics.

Our aim in this chapter is to contribute to the understanding of eco-evolutionary dynamics, emphasizing collective co-evolutionary aspects rather than focusing on in-

dividual species or pairs of them. For this purpose, we developed a simple computational framework –similar to existing approaches– specifically devised at understanding the emerging phenomenology of the experiments of Zuppinger-Dingley *et al.* In particular, we propose an individual-based model, with spatial structure, stochasticity, sexual reproduction, mutation, multidimensional trait-dependent competition and, importantly, more than-two-species communities (in particular, possibly owing to analytical difficulties, relatively limited work has been published about more than three-species communities, which is crucial to achieve a realistic integration of ecological and evolutionary dynamics for natural communities; see however [186, 26, 121]). Furthermore, our method is flexible enough as to be easily generalizable to other specific situations beyond plant communities and can rationalize the circumstances under which phenotypic diversification and niche specialization may emerge using simple, straightforward rules.

5.2 Co-evolutionary model

Model essentials

We construct a simple model which relies on both *niche* based approaches [142, 42, 41] and *neutral* theories [116, 175, 223, 7]. The former prioritize trait differences and asymmetric competition, underscoring that coexisting species must differ in their eco-evolutionary trade-offs, i.e., in the way they exploit diverse limiting resources, respond to environmental changes, etc., with each trade-off or "niche" choice implying superiority under some conditions and inferiority under others [143, 207, 42, 41]. Conversely, neutral theory ignores such asymmetric interactions by making the radical assumption of species equivalence, and focuses on the effects of demographic processes such as birth, death and migration.

Here, we adopt the view shared by various authors [208, 91, 98, 90] that niche-based and neutral theories are complementary extreme views. In what follows, we present a simple model that requires of both neutral and niche-based elements. In particular, our model incorporates trade-off-based features such as the existence of heritable phenotypic traits that characterize each single individual. However, the impact of these traits on individual fitness is controlled by a model parameter, that can be tuned to make the process more or less dependent on competition, in the limit even mimicking neutral (or "symmetric") theories [116, 175].

The traits of each single individual are determined by quantitative phenotypic values that can be regarded as the investment in specific functional organs. For instance, the traits could represent the proportion of biomass devoted to exploit soil nutrients (roots), light (leaves and stems), and to attract pollinators and capture pollen (flowers; see figure 5-1). We then assume a hard limit –constant across generations– to the amount of resources that can be devoted to generate the phenotype, i.e. it is impossible to increase all phenotypic values simultaneously. Thus each individual is constrained to make specific trade-offs in the way it exploits resources. Because similar values in the trade-off space entail comparable exploitation of the same resource (e.g., water, light or pollinators) similar individuals experience higher levels of competition, which translates into a lower fitness. This can be regarded as a frequency dependent selection mechanism providing an adaptive advantage to exceptional individuals, able to exploit available resources. Therefore, the ecological processes of competition, reproduction, and selection lead to evolutionary shifts in the distribution of phenotypic traits which feed back into community processes, giving rise to integrated eco-evolutionary dynamics.

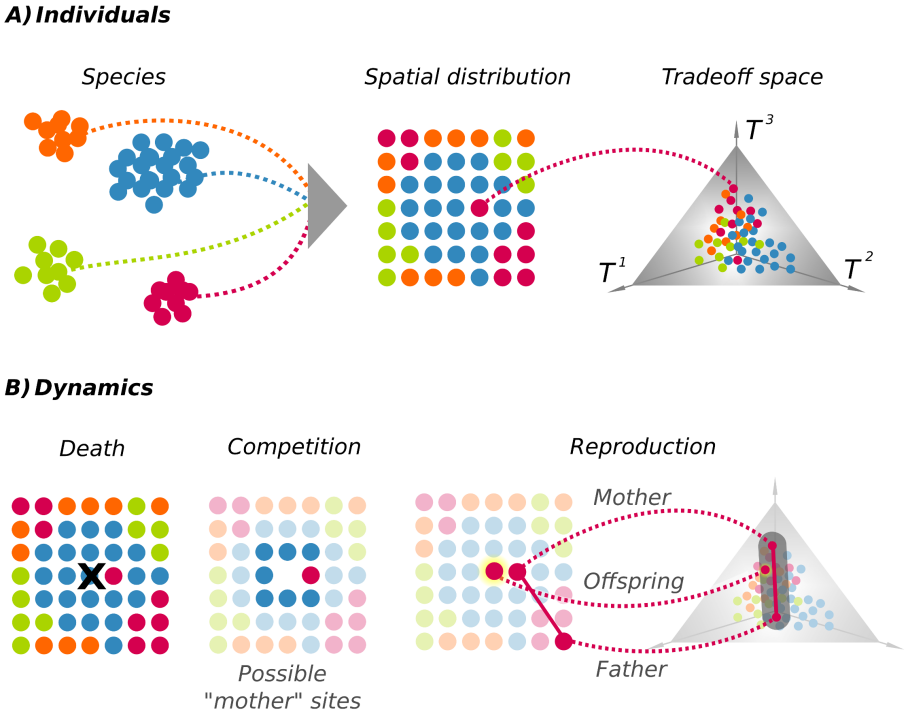

Figure 5-1: **Sketch of the model. (A)** Individuals of different species (different colors) compete for available resources in a physical space (two-dimensional square lattice), which is assumed to be saturated at all times. Each individual is equipped with a set of phenotypic traits that corresponds to a single point in the trade-off space. This is represented here (as a specific example) as an equilateral triangle (a "simplex" in mathematical terms) corresponding to the case of 3 coordinates which add up to 1 (e.g., fraction of the total biomass devoted to roots, leaves/stems and flowers, respectively [210]). For instance, a point close to vertex T^1 exploits better the limiting resource 1 (e.g. soil nutrients) than another one near vertex T^2, but is less efficient at exploiting resource 2 (e.g. light) than this latter one (see section 5.3). **(B)** Individuals die after one timestep, giving rise to empty sites; each of these is occupied by an offspring from a "mother" within its local neighborhood (consisting of 8 sites in the sketch for clarity, although we considered also a second shell of neighbors in the simulations, i.e. a kernel of 24 sites). The mother is randomly selected from the plants occupying this neighborhood in the previous generation, with a probability that decreases with the level of similarity/competition with its neighbors (see section 5.3). The implanted seed is assumed to have been fertilized by a conspecific "father" from any arbitrary random location, selected also with a competition-level dependent probability. The offspring inherits its phenotype from both parents; its traits can lie at any point (in the shaded region of the figure) nearby the the parental ones, allowing for some variation. For a given number of initial species S, two key parameters control the final outcome of the dynamics: β, characterizing the overall level of competition, and μ, representing the variability of inherited traits. We fix most of the parameters in the model (lattice site, individuals within the competition/reproduction kernel, etc.) and study the dependence on S, β and μ.

Model construction

The basic components of the model are as follows (further details are deferred to the following section). We consider a community of individuals of S different species, that are determined initially by mating barriers (i.e. a species is defined as a set of individuals that can produce fertile offspring [47]). Each individual occupies a position in physical space (represented as a saturated square lattice) and is characterized by the label of the species to which it belongs and a set of intrinsic parameters (i.e. trait values), specifying its coordinates in the "trade-off space" as sketched in figure 5-1 (see also [177, 210]). All positions within the trade-off space are assumed to be equally favorable *a priori*. In what follows, we make a perfect identification between the trade-offs of a given individual and its phenotypic traits, which also determine the "niche" occupied by each individual. In principle, each individual, regardless of its species, can occupy any posititon in the trade-off space. Positions near the center of the trade-off space (figure 5-1) correspond to phenotypes with similar use of the different resources (i.e., "generalists"), while individuals near the corners specialize in the exploitation of a given resource ("specialists").

Individuals are subjected to the processes of birth, competition for resources, reproduction, descent with modification, and death. Individuals are assumed to undergo sexual reproduction, as in the experiments of [235] (implementations with asexual reproduction are discussed later); they are considered to be semelparous, so that after one simulation time step (i.e, a reproductive cycle) they all die and are replaced by a new generation. Importantly, demographic processes are strongly dependent on phenotypic values. In particular, the main niche-based hypothesis is that individual organisms with a better "performance" are more likely to reproduce than poorly performing ones. To quantify the notion of "performance", we rely on classical concepts such as limiting similarity, competitive exclusion principle and niche overlap

hypothesis [149, 167], which posit that in order to avoid competition, similar species must differ in their phenotypes. More specifically, our model assumes that the performance of a given individual increases with its trait "complementarity" to its spatial neighbors [167], as quantified by its averaged distance to them in trade-off space (see section 5.3); i.e. the larger the phenotypic similarity among neighbors, the stronger the competition, and the worse their performance. Although the performance of a given individual depends on its complementarity with its neighbors, the model is symmetric among species and phenotypes; performance is blind to species labels and does not depend on the specific location in the trade-off space.

The reproduction probability or performance of any given individual is mediated by a parameter β which characterizes the global level of competitive stress in the environment (see section 5.3). In the limit of no competition, $\beta = 0$, the dynamics become blind to phenotypic values and can be regarded as fully neutral, while in the opposite limit of extremely competitive environments, $\beta \to \infty$, niche effects are maximal and a relatively small enhancement of trait complementarity induces a huge competitive advantage. Finally, a mother selected as described in the competition process is assumed to be fertilized by a conspecific "father" in the population (interspecies hybridization is not considered here) which is also selected with the same reproduction probability function based on its performance. The offspring inherits its traits from both parents, with admixture and some degree of variation μ (see figure 5-1 and the following section). This process is iterated for all lattice sites and for an arbitrarily large number of reproductive cycles, resulting in a redistribution of species both in physical and in trade-off space. Species can possibly go extinct as a consequence of the dynamics. In this version of the model, speciation is not considered, though it could be easily implemented by establishing a dependence of mating on phenotypic similarity, making reproduction between sufficiently different individuals impossible [55].

Model details

In this model, each individual plant, i, is fully characterized by (see also figure 5-1): *(i)* a label identifying its species, *(ii)* its coordinates in the physical space, and *(iii)* a set of real numbers specifying its phenotypic traits. Some details to take into account in this respect are:

- *i) Species.* A fixed number of species, labeled from 1 to S, is taken. While the emergence of new species is not considered here, some of them may become extinct along the course of evolution.

- *ii) Physical space.* We consider a two-dimensional homogeneous physical space described by a $L \times L$ square lattice, assumed to be saturated at all times, in which the neighborhood of each individuals is determined by the closest K sites (in our simulations, we took $L = 64$ and $K = 24$).

- *iii) Phenotypic traits and trade-off space.* As energy and resources are limited, each individual plant needs to make specific choices/trade-offs on how to allocate different functions. The way we implement the "trade-off space" is inspired in the field of multi-constraint (non-parametric) optimization that it is called Pareto optimal front/surface [153]; it includes the set of possible solutions such that none of the functions can be improved without degrading some other. Thus, the phenotype of any individual can be represented as a trade-off equilibrium, a point in this space and encapsulated in a set of real numbers $\mathbf{T} = (T^1, T^2, ..., T^n)$ (all of them in the interval $[0, 1]$), such that $\sum_{k=1}^{n} T^k = 1$ where n is the number of trade-offs (see figure 5-1 and [210]). All positions within the trade-off space are equivalent a priori, although this requirement can be relaxed.

The dynamics that determine each individual relies on competition, reproduction, and mutation. These processes would be characterized by the following considerations:

- *Competition for resources.* It is based on the concept of trait "complementarity" between two individuals i and j. It would be quantified as their distance in the trade-off space: $c_{ij} = \sum_{k=1}^{n} |T^k(i) - T^k(j)|/n$, which does not depend on species labels. The averaged complementarity, (or simply "complementarity") over all the neighbors j of individual i is $C_i = \sum_{j \in n.n.(i)} c_{ij}/K$.

- *Reproduction.* Each timestep, every individual is removed from the population; the resulting vacant site i is replaced by an offspring of a potential mother plant j which is selected from the list of K local neighbors of the vacant site with a given probability $P_{\text{mother}}(j)$. This probability controls the dynamical process; we assume it to increase as the mother's trait complementarity C_j increases (i.e. as its effective competitive stress diminishes): $P_{\text{mother}}(j) = e^{\beta C_j} / \sum_{j' \in n.n.(i)} e^{\beta C_{j'}}$, where the sum runs over the set of K neighbors of i; $e^{\beta C_j}$ is the "performance" of individual j and β is a tunable "competition parameter" controlling the overall level of competitive stress in the community. Once the mother has been selected, the father is randomly chosen from all its conspecific individuals l in the community, with a probability proportional to their performance, $e^{\beta C_l}$. In other words, individuals with lower competition pressure are more likely to sire descendants both as females and as males.

- *Inheritance, admixture and variation of phenotypes.* The traits of each single offspring are a stochastic interpolation of those of both parents with the possibility of variation: $T^k_{\text{new}} = \eta T^k_{\text{mother}} + (1-\eta) T^k_{\text{father}} + \xi^k$, for $k = 1, ..., n$, where η is a random variable (uniformly distributed in $[0, 1]$) allowing for different levels of admixture for each offspring, and ξ_k are (Gaussian) zero-mean random variables

with standard deviation μ, a key parameter that characterizes the variability of inherited traits. To preserve the overall constraints $T^k \in [0,1]$ and $\sum_k T^k = 1$, mutations are generated as $\xi^k = (r^k - r^{k+1})$, where $\{r^1 = r^{n+1}, ..., r^n\}$ are independent Gaussian random variables with zero-mean and standard deviation $\mu/\sqrt{2}$; in the rare case that $T^k_{\text{new}} < 0$ (resp. > 1), we set it to 0 (resp. to 1) and added the truncated difference to another random trait.

5.3 Methods and measures

Simulations are started with individuals of S different species (e.g. $S = 16$) randomly distributed in space. Initially, the traits of all individuals are sampled from a common Gaussian distribution centered around the center of the simplex. Note that, as shown in section 5.5, results do not depend on the particular choice of initial conditions. Time evolution of this initialized system is quantified by different measures of biodiversity described in this section. In this model, time can be implemented either as discrete/synchronous updating or continuous/sequential updating without significantly altering the results.

Species distances

We define two different distances in our framework:

- *Interspecies distance*, the distance between the centroids of two different species s and s' in the trade-off space $d_{s,s'} = \sum_k |B^k(s) - B^k(s')|/n$, averaged over all surviving species.

- *Intraspecific distance*, the average distance in trade-off space between all pairs of individuals of a given species s, $d_s = \sum_{i,j \in s} c_{ij}/n_s(n_s - 1)$ averaged over all surviving species.

Here, the centroid of species s is given by $\mathbf{B}(s) = \{B^1(s), ..., B^n(s)\}$, with $B^k(s) = \sum_i T^k(i)/n_s$ for each trait k, where i runs over the n_s individuals of species s.

Complementarity

We distinguish three different measures regarding averaged complementarities (see the sketches in figure 5-2):

- *Local complementarity (LC).* It is defined as the mean phenotypic distance between an individual and its spatial neighbors, $\mathrm{LC} = \sum_i (\sum_{j \in n.n.(i)} c_{ij}/K)/N$ (N is the total number of individuals and K is the number of local neighbors.)

- *Global complementarity (GC).* The complementarity averaged over all pairs of individuals regardless of their relative positions in physical space, $\mathrm{GC} = \sum_{i,j \neq i} c_{ij}/(N(N-1))$. Similarly $\mathrm{GC}_{\mathrm{inter}}$ is the averaged complementarity between individuals of different species and $\mathrm{GC}_{\mathrm{intra}}$ is the averaged complementarity between conspecific individuals. In the case of monocultures, $\mathrm{GC}_{\mathrm{inter}}(S = 1)$ is measured from two different/independent realizations.

- *Relative complementarity (RC).* A measure of the averaged difference in the level of competition between randomly sampled conspecific and non-conspecific individuals, $\mathrm{RC} = \mathrm{GC}_{\mathrm{inter}} - \mathrm{GC}_{\mathrm{intra}}$.

While local measurements capture the effect of spatial correlations, global ones are useful to characterize the evolution of the whole community in trade-off space. In analogy with the experimental setup of Zuppinger-Dingley *et al.* [235], we performed computer simulations using both monocultures and mixtures. For the case of monocultures, $\mathrm{GC}_{\mathrm{inter}}$ was estimated taking individuals coming from two independent realizations of the simulations. Zuppinger et al. gathered seeds from surrounding populations and grew them together in their experimental set-up. This removed any

cumulative, trans-generational effect of spatial correlations. In this way, GC measurements (figure 5-2 B) constitute better proxies (as compared to LC) to contrast our results with global community (biodiversity) effects in [235].

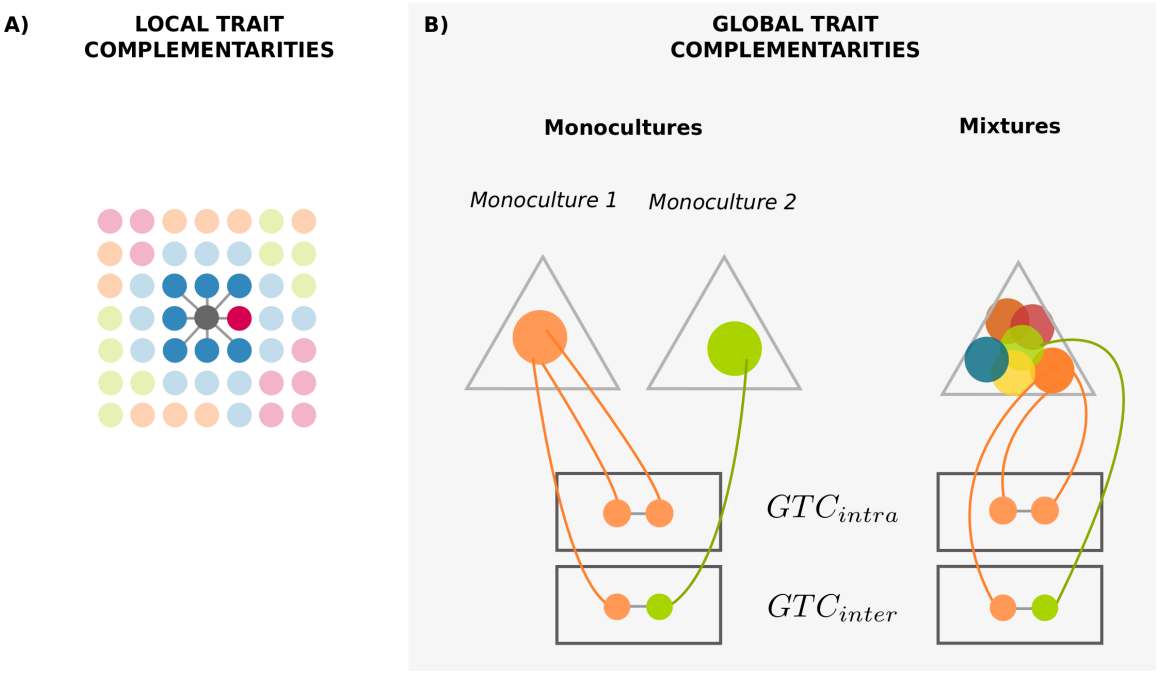

Figure 5-2: **Complementarity measurements:**
A) Local complementarity (i.e. mean phenotypic distance between spatially close neighbors) reveals the effect of spatial correlations; B) Intraspecific and interspecific global complementarities (i.e. mean phenotypic distance between individuals of the same and of different species, respectively, regardless of their spatial location). In all cases, we performed computer simulations using monocultures and mixtures.

Moran index

The Moran's index [155] quantifies the likelihood of an individual to be surrounded by individuals of the same species. When Moran's index is negative, individuals are less likely to be close to their co-specifics than what would be expected by pure chance, while positive values indicate spatial clustering of species. Mathematically, given a species s we compute its Moran's index I_s as

$$I_s = \frac{\sum_{i \in s} \sum_{j \in n.n.(i)} (X_s^i - \bar{X}_s)(X_s^j - \bar{X}_s)}{K \sum_{i \in s} (X_s^i - \bar{X}_s)^2}, \tag{5.1}$$

where K is the number of local neighbors (kernel size), and X_s^i is a variable such that $X_s^i = 1$ when the specie of i is equal to s and $X_s^i = 0$ if it is different, with $\bar{X}_s$ the density of individuals of species s. Finally, we obtain the total index averaging over species, $I = \sum_{i=1}^{S} I_s/S$. As a result, positive, zero, and negative values of I correspond to positive spatial correlation, random, and anti-correlation of species, respectively.

5.4 Results

Statistical patterns emerging from the eco-evolutionary dynamics described above are analyzed as a function of the number of generations and as a function of the number of species S, for different values of the two free parameters: the overall level of competition β and the variability of inherited traits μ. Results are illustrated in figure 5-3 showing *(i)* phenotypic diagrams (top row) specifying the position of each single individual and its species in the trade-off space for different parameter values and evolutionary times *(ii)*; values of complementarity for all individuals (central row) in the trade-off space, and *(iii)* the spatial distribution of individuals and species (bottom row). Finally, several biodiversity indexes are reported in figure 5-4.

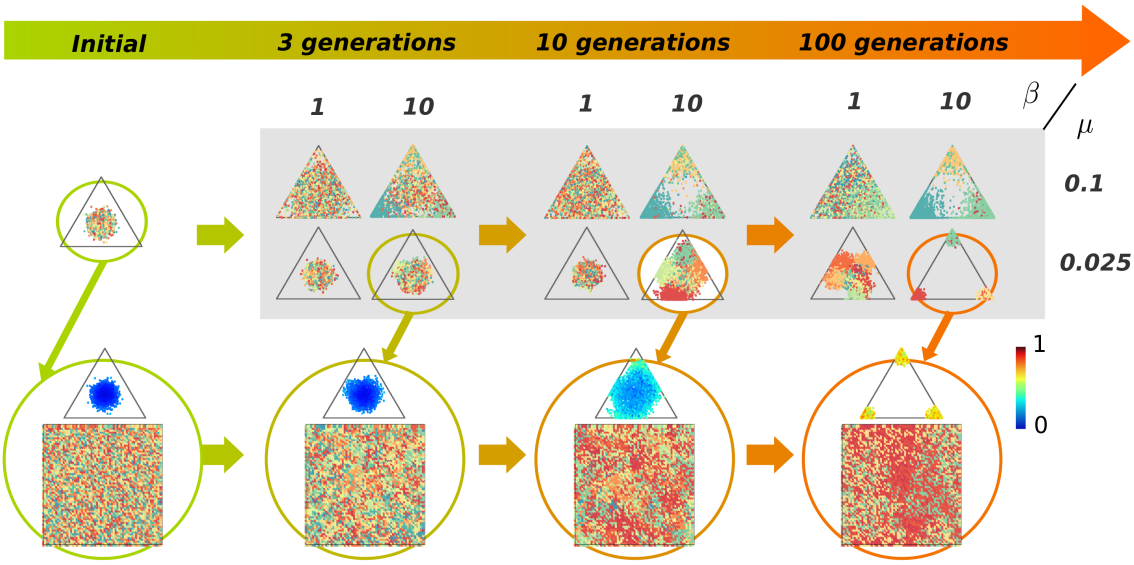

Figure 5-3: **Illustration of the emergence of rapid phenotypic diversification** for a computational system of size 64×64 and 16 species (labeled with different colors). **(Top). Phenotypic diagrams** measured at different evolution stages (1, 3, 10 and 100 generations, respectively) for different values of the two parameters: level of competition β (1 for the case of low competition and 10 for strong competition) and variation in inherited traits μ (0.1 for large variation and 0.025 for small variation). In all cases, phenotypic differentiation among species is evident even after only 10 generations. In the long term (100 generations) species diversification and specialization is most evident for small μ and large β; in this last case, different species (colors) can coexist for large times in the same region/corner of trade-off space. **(Central). Complementarity diagrams** representing the values of averaged local complementarity for all individuals of any species for small μ (0.025) and large β (10). Individuals with small complementarity (i.e. under strong competition with neighbors) disappear in the evolutionary process, while communities with high degrees of local complementarity are rapidly selected. **(Bottom). Spatial distribution of species** for different number of generations. As a result of the eco-evolutionary dynamics, anti-correlated patterns –in which neighboring plants tend to be different– emerge (note that colors represent species assignment and do not reflect phenotypic values)

.

Species differentiation

As illustrated in figure 5-3 (shaded area), different distributions of individuals in the trade-off space appear depending on the specific values of β and μ. Visual inspection reveals the emergence of rapid phenotypic differentiation, i.e. segregation of colors in trade-off space after a few (e.g. 10) reproductive cycles. The segregation is much more pronounced for relatively small variability (e.g. $\mu = 0.025$) and large competitive stress (e.g. $\beta = 10$). This is quantified (see figure 5-4A) by the average interspecies distance, whose specific shape depends on parameter values. As shown in figure 5-4B, the fastest growth is obtained for $S = 2$, but the curves converge to a constant value (mostly independent of S) after a sufficiently large number of generations. Moreover, as shown in the central row of figure 5-3 the complementarity –averaged over all individuals in the community (see section 5.3)– also grows during the course of evolution (i.e. colors shift from blue to yellowish). Observe in figure 5-3. that, for asymptotically large evolutionary times, there is a tendency for all species to cluster around the corners of the trade-off space, suggesting that the optimal solution to the problem of minimizing the competition with neighbors corresponds to communities with highly specialized species. This specialization does not occur in monocultures ($S = 1$), as sexual mating pulls the species together and avoids significant phenotypic segregation.

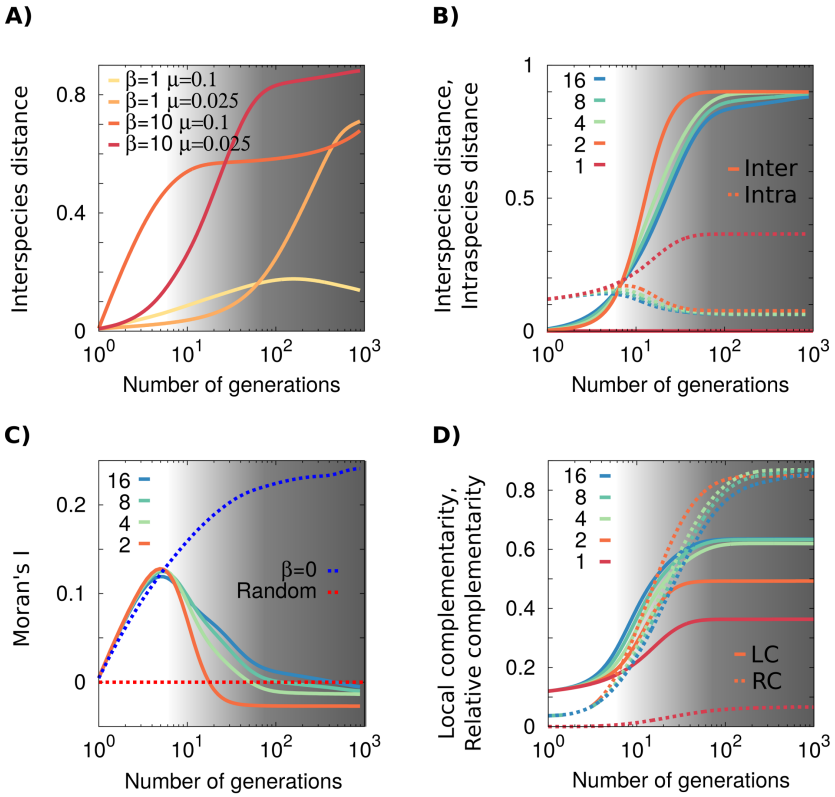

Figure 5-4: **Measurements of different biodiversity indexes. (A) Phenotypic distances among species** grow systematically during the eco-evolutionary process, reflecting a clear tendency towards species differentiation (same sets of parameter values as in figure 5-3, $S = 16$). Differentiation is faster for relatively small values of trait variability μ and large values of the competitive stress β. **(B) Phenotypic differentiation among and within species**. While interspecies distances grow in time for all values of S and converge to similar values on the long term, intraspecific phenotypic variability is much larger on the long term for monocultures than for biodiverse mixtures. **(C) Phenotypic similarity among close neighbors.** Moran's index (I) for $\beta = 10$ and different values of S as well as for $\beta = 0$ and for a random distribution (i.e. in the absence of spatial interactions). Figure clearly indicates the avoidance of close cohabitation ($I < 0$) in competitive systems ($\beta > 0$). **(D) Averaged local and relative complementarity** in the community increase with time and reach larger values for more biodiverse communities. In all plots, parameters are $L = 64$ and, unless it is specified, $\beta = 10$ and $\mu = 0.025$; curves are averaged over at least 10^3 runs; shaded light grey areas stand for times during which extinction tends to occur causing S to decrease (see below for details), while in dark grey ones the system tend to stabilize at a given final number of species.

Emergence of local anti-correlations

The high level of phenotypic specialization observed after large evolutionary times for large competition stress and small variability, might seem in contradiction with the overall tendency to niche differentiation. In other words, most of the trade-off space becomes empty in this case, while individuals aggregate at the (highly populated) corners. The answer to this apparent conundrum is that similarly specialized individuals have a statistical tendency to avoid being spatial neighbors. Indeed, as qualitatively illustrated in the lowest right panel of figure 5-3, extreme specialization is accompanied by a tendency to diminish spatial clustering, i.e. to create spatial anti-correlations within each species. This tendency –which stems from intraspecific competition and opposes to the demographic tendency of similar individual to cluster in space– is quantitatively reflected by negative values of Moran's index I (see figure 5-4C and section 5.3). Note also that I and thus the spacial distribution of species, is radically different in the presence and in the absence of competition (i.e. for $\beta \neq 0$ and $\beta = 0$, respectively) as can be seen in figure 5-4C. In the absence of competition, species are distributed randomly forming aggregated spatial clusters without competition-induced local anti-correlations.

Intraspecific diversity

This quantity is defined as the mean "complementarity" among all pairs of conspecific individuals in the community, and illustrates the level of phenotypic diversity within species. As shown in figure 5-4B, the intraspecific diversity is much larger for monocultures. In monocultures, neighbors are obviously conspecific and the only available mechanism to reduce overall competition is to increase intraspecific diversity. Therefore, as a general result, monocultures tend to enhance their intraspecific phenotypic distances, while biodiverse communities tend to enhance phenotypic differentiation

among species but result in more similar conspecifics.

Local complementarity

Figure 5-4D shows the evolution of the mean complementarity of individuals respect to its spatial neighbors. This averaged *local* complementarity (LC) controls the dynamics and the actual reduction in the level of competition for a given spatial distribution, and is much larger for mixtures than for monocultures (it grows monotonously with S and saturates at a maximal value).

Global complementarity

Similarly, we can measure "*global*" complementarity (GC), i.e. the average phenotypic distance among all individuals in the experiment, regardless of their spatial coordinates, after a given number of generations. Additionally, we measured $\mathrm{GC}_{\mathrm{intra}}$ (resp. $\mathrm{GC}_{\mathrm{inter}}$) which is GC averaged only over individuals of the same (resp. different) species (see section 5.3). In figure 5-4D we present results for the *relative* complementarity $\mathrm{RC} = \mathrm{GC}_{\mathrm{inter}} - \mathrm{GC}_{\mathrm{intra}}$, which is a measure of the averaged difference in the level of competition between randomly sampled non-conspecific and conspecific individuals, respectively. Observe that the RC is larger for mixtures than for monocultures, $\mathrm{RC}(S > 1) > \mathrm{RC}(S = 1)$, and that it grows faster in time for smaller values of S (e.g. $S = 2$), but reaches almost equal constant values after a sufficiently large number of generations.

Complementing the results presented in figure 5-4, figure 5-5 shows measurements for LC and $\mathrm{GC}_{\mathrm{intra/inter}}$ for different initial number of species S after 10 and 1000 generations. We observe that, even though complementarities become almost independent of S at $t = 1000$ (due to the extinction of some species), transient measurements at $t = 10$ clearly show that communities with fewer species exhibit higher values of GC

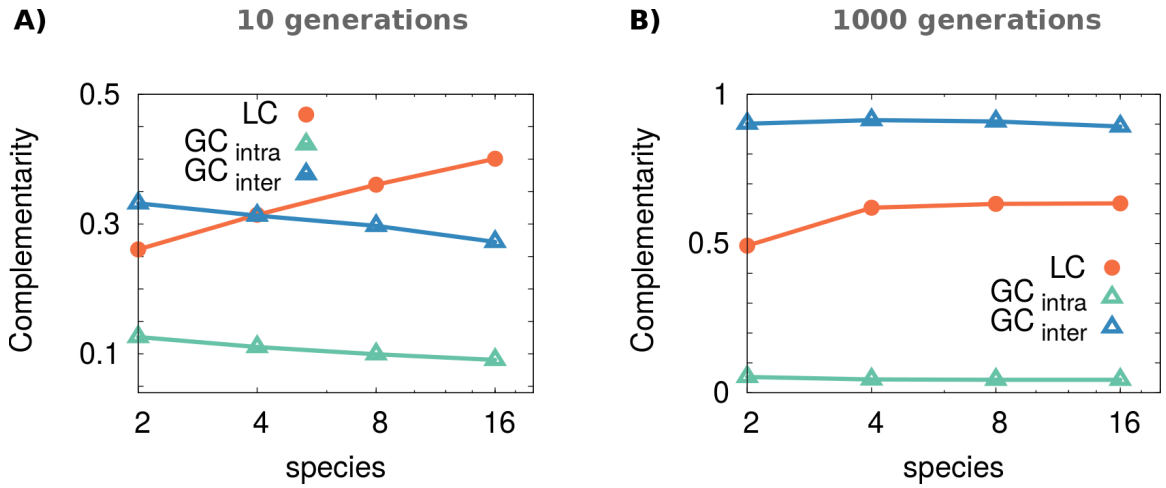

Figure 5-5: **Local and global complementarities after A)** 10 **and B)** 1000 **reproductive cycles**, plotted as a function of the initial number of species S in the community. Parameter values: system size $L = 64$, competition $\beta = 10$ and variability $\mu = 0.025$.

and, consequently, reach the stationary state faster. Biodiversity delays the process because several species simultaneously compete for empty niches. On the other hand, LC is inversely correlated with S, i.e., individuals tend to be more phenotypically similar in less biodiverse communities.

Emergent neutrality

As illustrated in figure 5-3, different species with very similar trait values can coexist (e.g. yellow and orange species at the right corner of the phenotypic diagram for $\mu = 0.025$ and $\beta = 10$ in figure 5-3) even after many generations. Such a coexistence emerges spontaneously and, although it is transitory, it can last for arbitrarily long times provided that the system size is sufficiently large. From an ecological point of view, these species can be regarded as functionally equivalent as they occupy the same niche region.

It is important to underline that not all realizations lead to equivalent species coexisting in the community. However, this appears to be a significant pattern, and so, we explored it further. In particular, we decided to check the stability of the coexistence by studying the mean coexistence time of equivalent species.

As a first step we define a computational criterion to determine species equivalence: two species s_1 and s_2 are considered equivalent if their inter-specific distance (i.e. distance between their centroids) differs less than a fraction of their mean intraspecific distance (mean trait amplitude), for instance $1/4$, which produces a significant overlap of the clusters of both species in phenotypic space.

We then measured the mean number of generations ΔT between the time at which 4 species remain in the system (with two of them being equivalent, based on the previous definition) and the time at which one of such equivalent species invades the other one (as a result of demographic fluctuations). In voter models (i.e. the neutral case), the mean time to reach mono-dominance, ΔT, increases with the number of individuals in the community, N; in particular, $\Delta T \sim N \log N$ in a 2D lattice and $\Delta T \sim N$ in a well-mixed situation [46].

Figure 5-6 shows ΔT for simulations of our model, as well as the theoretical expectation for the neutral case, in $2D$. To check the robustness of coexistence to the shape of the competition kernel [85, 2, 169, 107, 9, 132] (see section 5.5), we run simulations using a linear-exponential ($e^{\beta C}$) and a quartic-exponential ($e^{\beta C^4}$) kernel, where C is the mean trait complementarity among neighbors. In both cases, our results are compatible with the neutral scenario.

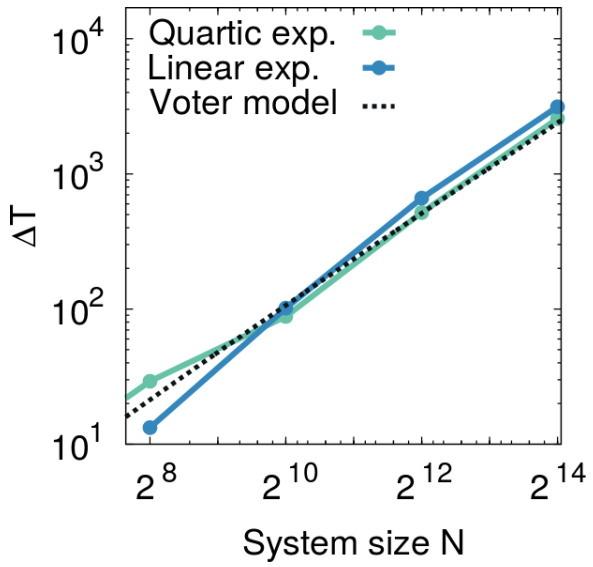

Figure 5-6: **Mean number of " coexistence"**, for different system sizes of the community. We show results using a linear-exponential ($e^{\beta C}$) and a quartic-exponential ($e^{\beta C^4}$) kernel comparing them with the theoretical expectation for a 2D voter model, $\Delta T \propto N \log N$ [46]. Parameters: $L = 64, S = 8, \beta = 10, \mu = 0.025$. Deviations from the straight line probably stem from lack of statistics (which is costly at such large sizes/times).

Surviving species

As we do not include mechanisms such as migration or speciation, the number of species actually present in the community can be reduced after several generations. The resulting change in diversity can be regarded as an important attribute, because it illustrates the limit of maximum diversity that a finite system can harbor is the absence of inmigration or speciation processes.

Figure 5-7 shows the number of surviving species in different scenarios, including different levels of competition and variability parameters, and other model variants (see section 5.5). As expected, extinctions occur more rapidly for higher levels of competition (larger values of β). The effective level of competition is enhanced in the mean-field case in which all individuals interact with each other (see section 5.5), leading to faster extinction.

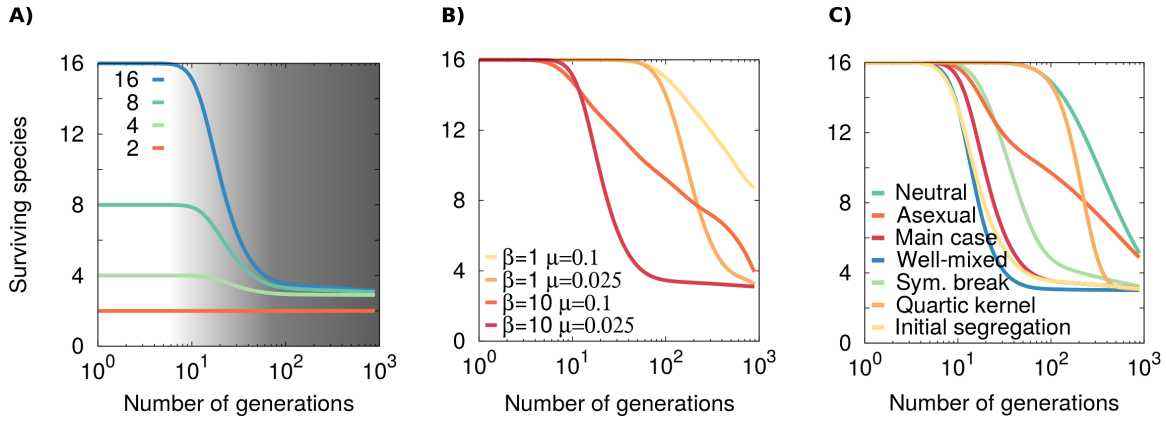

Figure 5-7: **Number of surviving species in time for different A) initial number of species, B) competition and variability parameters and C) variants of the model**. Species disappear faster in environments with high competition (higher values of β, or the mean-field). In contrast, the neutral case ($\beta = 0$) corresponds to the case in which more species survive after generations, although, due to demographic fluctuations, they still disappear on the long term. For sufficiently large numbers of generations, the system converges to a state with the same number of species than the niche dimensionality (3 in our case); these species coexist for arbitrarily long periods (provided the lattice is sufficiently large). Parameter values: $L = 64$, and $\beta = 10$, and $\mu = 0.025$ in A) and C).

In the neutral case ($\beta = 0$), species disappear at a very slow rate as there is no competition, but due to stochasticity, most of them are likely to disappear, leading to mono-dominance for sufficiently large timescales [137]. Interestingly, the stable solution in our model with competition ($\beta \neq 0$) consists of multiple species –as many as the niche dimensionality, in this case 3– coexisting for an arbitrarily large number generations. This result is congruent with the "niche dimension hypothesis", which states that a greater diversity of niches leads to a greater diversity of species [118].

5.5 Model variants and results robustness

To investigate the generality of our findings, we also explored whether the main conclusions are robust against some constraints of the implementation.

Initial phenotypic traits

In the previous section, initial conditions are given by randomly sampling the value of each individual phenotypic trait from a single distribution (Gaussian around the center of the phenotypic space), independently of species labels. After some generations, we observe that competition causes species to segregate in phenotypic space.

Although the most widely accepted definitions of species are based exclusively on the role of mating barriers, individuals belonging to the same species tend to share common trait values. Here, we approximate this kind of scenario and test the robustness of our results running simulations with partial clustering of species in phenotypic space. For this, we sampled individual traits from equal amplitude Gaussian distributions centered around different (randomly chosen) species-dependent points of the phenotypic space (see initial top panel in figure 5-8A).

As illustrated in figure 5-8B, species diversify sooner in phenotypic space (initial values for inter- and intra-specific distances are higher than in the case described in section 5.4), but after this transient, difference asymptotic results remain essentially unchanged.

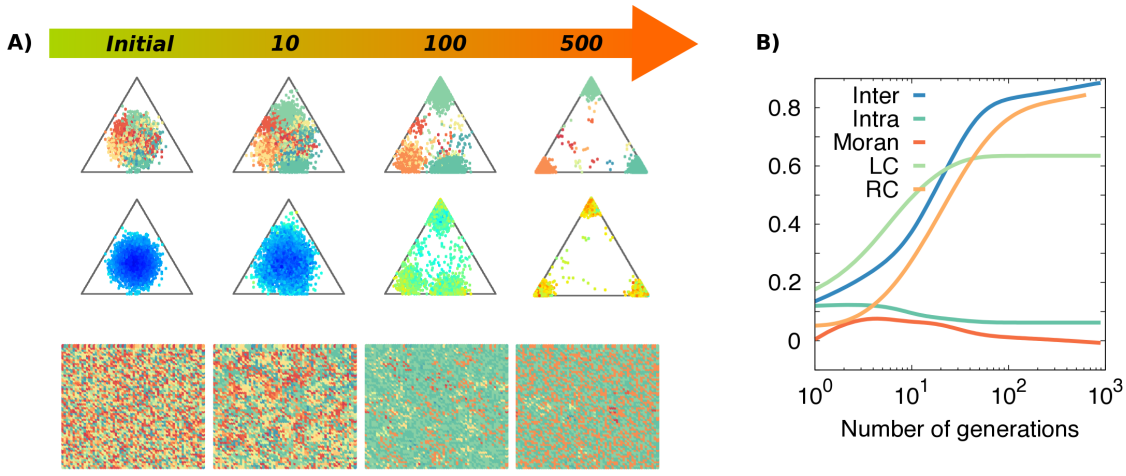

Figure 5-8: **Simulations under initial phenotypic segregation of species**. Individual traits are initially sampled from different species-dependent Gaussian distributions. Each of these Gaussians have a standard deviation equal to 0.05 and a mean value randomly selected from another Gaussian (with the same amplitude 0.05) centered at the triangle barycenter. A) From top to bottom: Tradeoff values, trait complementarities, and spatial distributions at different generations. B) Evolution of the inter and intra-specific distances, local and relative complementarity and Moran's Index. Parameters: $L = 64, S = 16, \beta = 10, \mu = 0.025$.

Effect of the competition kernel

In the implementation of our model, the reproduction probability of an individual i is proportional to $e^{\beta C_i}$, where C_i is the average trait complementarity among neighbors, $C_i = \frac{1}{K}\sum_j \frac{1}{n}\sum^k |T^k(i) - T^k(j)|$. However, the use of a non-differentiable argument (absolute value) appearing linearly in the exponential kernel may lead to spurious robust coexistence of arbitrarily similar species (at zero phenotypic distance) [85, 2, 107, 9, 132]. Kernels of the form $e^{\beta C_i^{2+\alpha}}$ with $\alpha > 0$ have been shown to avoid such artifacts [169]. For these reasons, we also considered an alternative competition kernel of the form $e^{\beta C_i^4}$ to check for the validity and robustness of our conclusions.

Results are shown in Fig 5-9. We observe that, as the quartic kernel reduces the overall competition of phenotypically similar individuals, it leads to a slower species-diversification process (as compared with the linear one for the same value of the

parameters). However, results are qualitatively similar to the linear kernel case. In particular, similar (equivalent) species continue to emerge and coexiste for very long times, as in the linear case (figure 5-6).

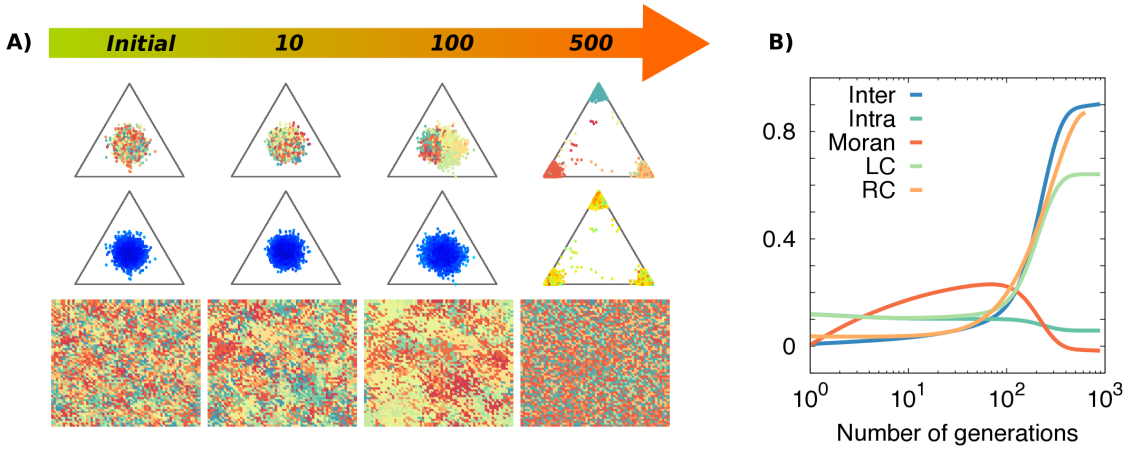

Figure 5-9: **Quartic competition kernel**. A) From top to bottom: Tradeoff values, trait complementarities, and spatial distributions at different generations. Simulations were run setting the performance of individuals proportional to $e^{\beta C^4}$ (rather than $e^{\beta C}$), where C is the average trait complementarity among neighbors. B) Inter and intra-specific distances, local and relative complementarity and Moran's Index evolution. Parameters: $L = 64, S = 16, \beta = 10, \mu = 0.025$.

Long-distance dispersal and competition

We have also studied well mixed (or "fully connected") communities, in which *i)* there is frequent long-distance dispersal (so that both progenitors of the new offspring can be located at any site in space) and, additionally, *ii)* each individual competes with the rest of the community, i.e. all individuals behave as nearest neighbors.

As illustrated in figure 5-10, all the previously reported phenomenology is still present in this ideal mean-field scenario. As a matter of fact, phenotypic differentiation seems to occur faster than when spatial distribution is conditioned by local dispersal (see figure 5-4). In other words, long-distance dispersal and global competition drive evolution faster than local dynamics. This is a consequence of enhanced

competition, which increases the relative fitness of better performing individuals. Another important difference is that, under mean field conditions, equivalent taxa cannot occupy different spatial locations and are forced to compete with each other. Consequently, coexistence of species with similar traits is much less likely than in spatially-explicit communities.

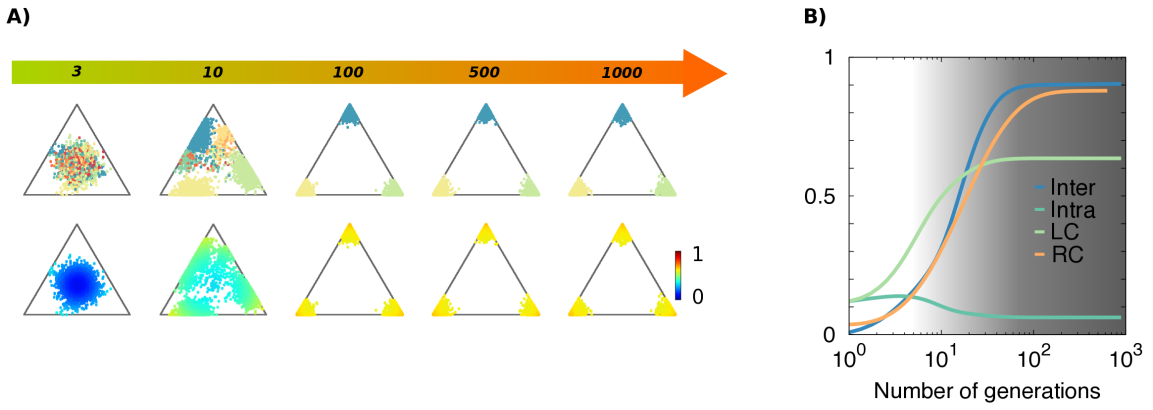

Figure 5-10: **Evolution of the community with long-distance dispersal and global competition (i.e. well-mixed or mean-field dynamics).** A) Tradeoff space and complementarity measured at different generations. B) Inter and intra-specific distances, and local complementarity and relative complementarity (RC= GC_{inter}-GC_{intra}) in time. Parameters: $L = 64$, $S = 16$, $\beta = 10$, $\mu = 0.025$.

Comparison with neutral theory ($\beta = 0$)

In the limit of no competition, $\beta = 0$, our model equates to neutral-theory [116] in which reproduction probabilities become independent of individual phenotypes. figure 5-11 reports computational results for this case, illustrating the emergence of a very different scenario with respect to the non-neutral case. Sexual reproduction still pulls species together so they aggregate in the trade-off space, but their centroids describe slow and independent random walks instead of being controlled by a relatively fast separating drift (see figure 5-12). This phenomenology is caused by the lack of an effective force pushing species away; indeed segregated species can become closer after

some generations, but on average there is only random drift allowing them to slowly diversify, so they cannot account for the empirical observations in [235]. Similarly, relative complementarities (which in the absence of competition can be regarded as the averaged difference in the level of phenotypic similarity between randomly sampled non-conspecific and conspecific individuals) start to grow later and reach low values,

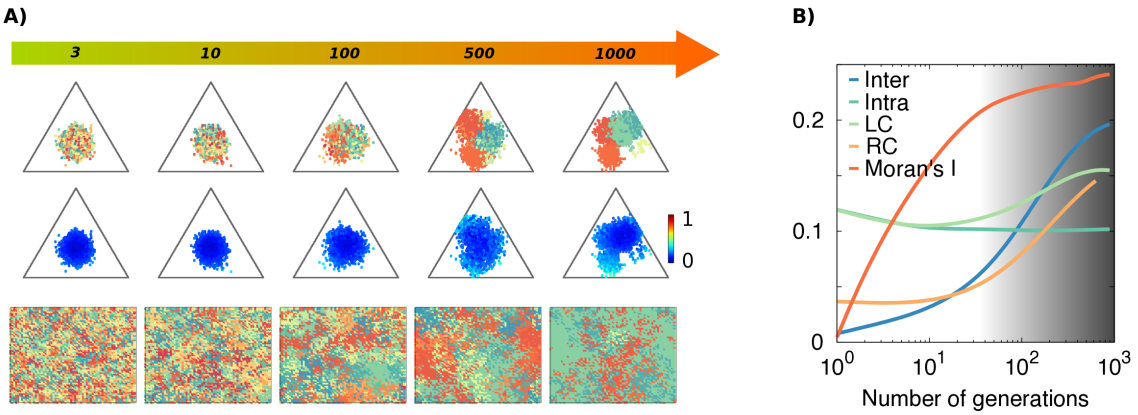

Figure 5-11: **Neutral dynamics** ($\beta = 0$), implying that all individuals have the same probability of reproduction independently of their species assignment and phenotype. A) Plots in the trade-off space illustrate that species hardly segregate in short time scales. In the physical space, local dispersal leads the the system to be clustered, i.e. positively auto-correlated rather than anti-correlated. B) Different measures illustrate that rapid evolutionary changes are much harder to observe in the neutral scenario. In particular, local complementarity (LC) and relative complementarity increase at a much slower pace. The increase in the Moran's index confirms that the system remains positively correlated (as usually is the case in neutral models) Parameters have been set to $L = 64$, $S = 16$ and $\mu = 0.025$.

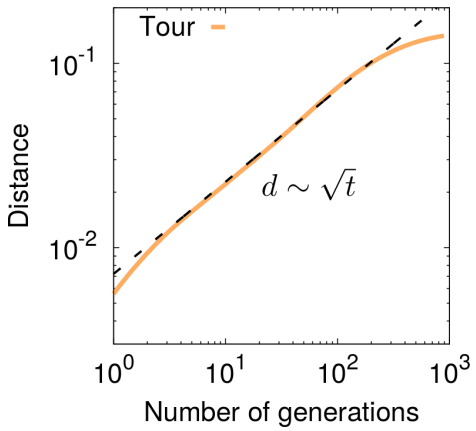

Figure 5-12: **Species diffuse in the trade-off space under neutral dynamics ($\beta = 0$):** The plot shows average distance between species centroids and the central point of the phenotypic space (i.e. the position of all species centroids at $t = 0$) as a function of time. Mutations cause a random movement of species centroids in the phenotypic space, as shown by the 0.5 slope in double logarithmic scale, characteristic of diffusive processes. Parameter values are set as in figure 5-11.

Asymmetrical resource trade-offs

In this section we consider a model variant in which positions in the trade-off space are *not* equally rewarding a priori. In particular, we chose one of the corners to be favored respect to the others: individuals whose phenotypes are closer to that vertex have a higher probability of reproduction. This could be interpreted as one particular limiting resource being more crucial, or mean that the availability of some resource scales nonlinearly with corresponding trait (e.g., a plant with a short root might not be able to reach a deep water layer. Individuals with longer root systems will have a disproportionate advantage).

In particular, we now modulate the performance of each individual i by multiplying it by a factor $R_i = r_1T^1 + r_2T^2 + r_3T^3$; where r_1, r_2 and r_3 are weights (real numbers in the interval $[0, 1]$) such that $r_1 + r_2 + r_3 = 1$. For simplicity we fix $r_1 = (1 + 2\epsilon)/3$, $r_2 = r_3 = (1 - \epsilon)/3$ in order to control the asymmetry with a single parameter (ϵ; the symmetric case is $\epsilon = 0$), while ϵ values close to 1 lead to large asymmetries. In what follows we fix $\epsilon = 0.99$.

As illustrated in figure 5-13, although most of individuals initially occupy the most favored (left) corner, after a few generations, some individuals also settle at other available (and less favorable) regions; this is a consequence of the system's tendency to reduce the level of competition. In conclusion, the main phenomenology reported in section 5.4 appears robust to asymmetrical trade-offs.

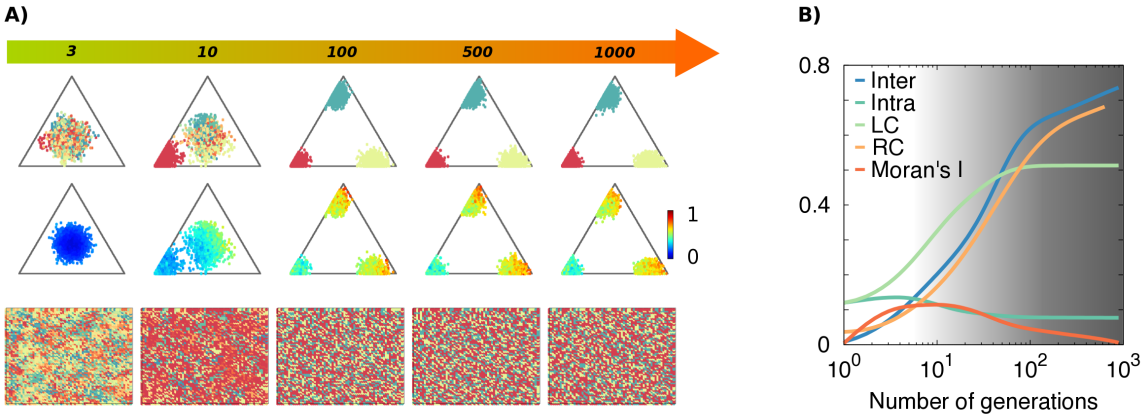

Figure 5-13: **Asymmetry among trade-offs**: A) Trade-off space and complementarity as a function of the number of generations. B) Different measurements characterizing the community in time. Local and relative complementarities confirm that rapid evolutionary changes may within a few generations. Parameters: $L = 64$, $S = 16$, $\beta = 10$, $\mu = 0.025$.

Asexual reproduction

Our main model adopts the (sexual) reproduction mechanism of the communities considered in the experiments by Zuppinger-Dingley *et al.* [235]. Here we analyze a case of asexual reproduction in which the traits are directly transmitted from an individual to its offspring (with some variability), i.e. taking $\eta = 1$ in our model.

Fig 5-14A shows the evolution of individual phenotypes (each trait value T_1, T_2, T_3 is represented by the amount of red, yellow and blue respectively), complementarity and spatial distribution. Observe that, once again, the chief phenomenology of the model, i.e. segregation toward high levels of specialization, is observed. However, in this case, the mechanism of diversification is quite different: individuals from any given species can specialize independently. Thus, in the absence of sexual reproduction, diversification occurs at an individual rather than at a species level. This type of individual differentiation fosters the presence of equivalent species (as the species label becomes completely irrelevant in this setting).

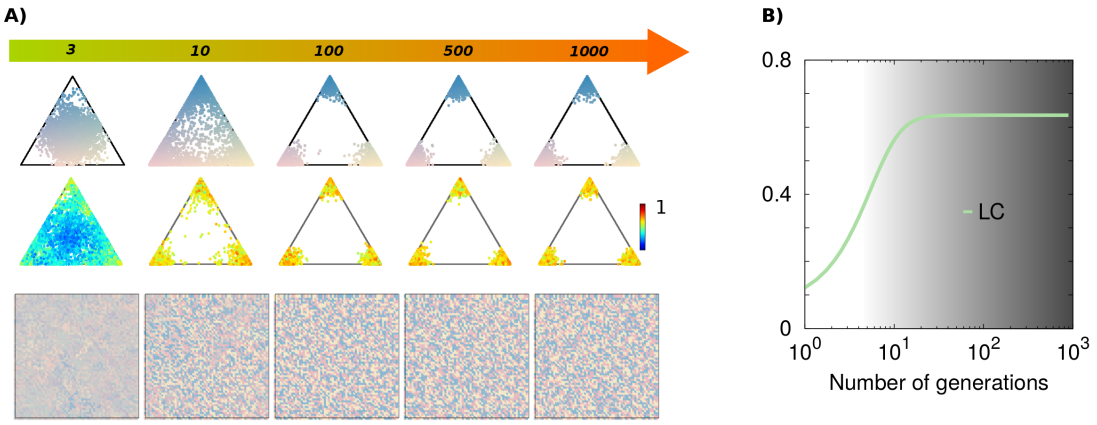

Figure 5-14: **Asexual reproduction**: A) Tradeoff space and complementarity as a function of the number of generations. Each individual traits values T_1, T_2, T_3 are represented by the amount of red, yellow and blue respectively. Parameter values: $L = 64$, $S = 16$, $\beta = 10$, $\mu = 0.025$. Competition avoidance leads individuals to segregate in the trade-off space. B) Local complementarity increases similarly to the main model.

5.6 Conclusions. *Rapid phenotypic diversification and other interesting phenomena*

In the present chapter, we have developed a parsimonious modeling approach to integrate important ecological and evolutionary processes. In particular, we focused on understanding rapid phenotypic diversification observed in complex biological communities of plants such as those recently reported by Zuppinger-Dingley *et al.* in long-term field experiments [235, 210].

Our model blends standard community processes, such as reproduction, competition or death, with evolutionary change (e.g., descent with modification); i.e. community and evolutionary dynamics are coupled together, feeding back into each other. Over the last decades, attempts to integrate ecological and evolutionary dynamics have been the goal of many studies (see e.g. [59, 60, 133, 206, 58, 62, 63, 188, 138, 37, 200, 78, 56, 40, 55, 102, 61, 50, 177]). In particular, a basic algorithm for modeling eco-evolutionary dynamics as a stochastic process of birth with mutation, interaction, and death was proposed in [59] and much work has been developed afterwards to incorporate elements such as spatial effects and different types of interspecies interactions [63].

Rather than providing a radically different framework, our model constitutes a blend of other modeling approaches in the literature of eco-evolutionary processes, and in fact it shares many ingredients with other precedent works, specially with the theory of adaptive dynamics [61, 79]. For instance, Gravel et al. [90] also considered a spatially-explicit individual-based model with trait-dependent competition. However, our work has been specifically devised to shed light on the experimental findings of Zuppinger et al. [235], and puts the emphasis on communities with arbitrarily large number of species, while usually the focus is on the (co-)evolution of pairs of species (e.g. predator-prey, host-parasite, etc.) or speciation/radiation of individual species.

Finally, our modeling approach is sufficiently general as to be flexible to be adapted to other situations with slightly different ingredients. We explored some of these possible extensions in section 5.5 (e.g long-distance dispersal, asexual reproduction, etc.), but other studies can be built upon the work laid here in a relatively simple way.

The present model relies on a number of specific assumptions, two of which are essential in that they couple community and evolutionary dynamics: i.e. (i) demographic processes are controlled by competition for resources which is mediated by phenotypic traits and (ii) successful individuals are more likely to transmit their phenotypes to the next generation with some degree of variation. These two ingredients are critical for the emerging phenomenology. For instance, in the absence of competition (i.e. $\beta = 0$) reproduction probabilities are identical for all individuals, implying that the model becomes neutral, and the evolutionary force leading to species differentiation vanishes (see section 5.5). On the other hand, variation in inherited traits is necessary to allow for the emergence of slightly different new phenotypes and the emergence of drifts in trade-off-space. Although these constraints might be regarded as limiting, we deem them biologically realistic and do not think they hamper the predictive power of our model. Most of the remaining ingredients, such as the existence of a saturated landscape, semelparity (i.e. non-overlapping generations), the specific form in which we implemented initial conditions, competition, dispersion, selection, inheritance linked to phenotypic characters rather than to a genotypic codification, etc. can be modified without substantially affecting the results. This flexibility could make the description of other type of communities possible with minimal model variations. Similarly, the model could be extended to incorporate phenotype-dependent reproductive barriers (and thus speciation) and the possibility of interspecies hybridization by making reproduction a function of phenotypic distance and relaxing its dependency on species labels.

In addition to rapid phenotypic diversification, the experiments of Zuppinger et al. found an enhancement of the overall productivity in mixtures of diverse plants with respect to monocultures of the same plants [235]. Our model cannot be used to directly quantify such "biodiversity effects" [139], as we assume a fully saturated landscape and there is no variable that accounts for total biomass production. However, in principle, under the hypothesis that larger trait complementarities correlate with greater resource capture and biomass production, the observed increase of relative complementarity in mixtures (see figure 5-4) could be used as a proxy for biodiversity effects. Observe, nonetheless, that the previous assumption might by wrong (or incomplete) as productivity can be profoundly affected by other factors such as, for instance, positive interactions between similar species, not modeled here, and more sophisticated approaches –see [113, 66, 33, 172, 87]– are necessary to validate this hypothesis. In the future we plan to modify our model to represent non-saturated landscapes and more detailed ecological dynamics, allowing for explicit analyses of biodiversity-productivity relationships.

Beyond explaining most of the empirical observations in [235], our model leads to some far-reaching predictions (some of them already shared by existing theories); one of the most remarkable ones is that optimal exploitation of resources comes about when the full community evolves into a reduced number of highly specialized species –the exact number depending on the dimensions of the trade-off space– that coexist in highly dispersed and intermixed populations. Such specialization might be unrealistic in the case in which all traits in trade-off space are essential for survival, and thus the convergence toward perfect specialization is capped. In any case, this result is congruent with the niche dimension hypothesis [118], that postulates that a greater diversity of niches entails a greater diversity of species, i.e. a larger number of limiting factors (and thus of possible trade-offs) leads to richer communities [104]. However, this outcome might be affected by perturbations (migration, environmental

variability, etc) which could be easily implemented in our model, and could prevent real communities from reaching the asymptotic steady state predicted here. It is also noteworthy that the resulting highly specialized species can be phenotypically equivalent, and a set of them can occupy almost identical locations in the trade-off space. Such species equivalence appears spontaneously, and supports the views expressed by other authors that "emergent neutrality" is a property of many ecosystems [5, 187, 10]. In future work we will explore the possibility of phase transitions separating an ecological regime based on the coexistence of multiple highly specialized species from an ecosystem dominated by generalists and the conditions under which each regime emerges.

Beyond phenotype-dependent mating, upcoming studies will extend our approach to address communities where collective diversification phenomena based on both competition and cooperation are known to emerge (see e.g. [45]), as well as investigate the evolution of communities with distinct types of interacting species such as plant-pollinator mutualistic networks. This research will hopefully complement the existing literature and help highlighting the universal and entangled nature of eco-evolutionary processes.

Chapter 6

Conclusions

For a long time, the collective emergent macroscopic behavior of many-body systems present in physics and chemistry has been the subject of study of statistical physical mechanics. In recent years, "complexity science" has emerged has as promising area for the understanding of other types of many-body systems such as those existing on biology, ecology, or socio-economic fields. In this case, the standard techniques of statistical mechanics are applied helping, among other many aspects, to identify the essential mechanisms underlying emergent phenomena of complex systems. Careful inspection is needed to infer what needs to be included into a model and how, and what can be neglected and left out. In this light, we study the role of some inherent aspects of complex systems, that are sometimes neglected in complex systems, and emphasize the importance of considering them in many cases.

Phase transitions are a remarkable feature of the above-mentioned systems. Good models that explain the mechanisms responsible of such transitions and predict its appearance are extremely important, not only in physics, but also in biology, ecology, etc. Regarding the latter, a correct understanding can help to avoid essential problems such as climate change, species extinctions, desertification, disease spreading, or market crashes, among others.

Aimed to shed light on these mechanisms, we have firstly studied a generic ecological system subjected to discontinuous/catastrophic transitions at mean-field approximation. Computational and analytical results of the simplest Langevin equation describing these systems, lead us to the conclusion that stochasticity is essential in the understanding of these systems. In particular, the presence of high demographic noise, combined with low diffusion, dramatically alters the system by forcing it to present a smoother continuous transition with a directed percolation critical point. Contrarily, in a more "mean-field" case (i.e. low-stochastic and high-diffusive systems), discontinuous transitions are recovered. A remarkable fact is that, when considering (quenched) spatial disorder, an unavoidable feature of real systems, a rounding phenomena occurs in any of the previous cases, providing the system is low-dimensional. We hope that this work helps to prevent catastrophic shifts from occurring or, at least, by identifying the mentioned mechanisms in particular systems, to know the type of transition that would be expected.

Looking for a more complete description of the effect of spatial heterogeneities, we have performed a technical and detailed analysis in a separated work. Considering the prototypical quadratic contact process, which exhibits a discontinuous phase transition from an active fluctuating phase to an inactive absorbing regime, we have performed extensive computational analysis of the "pure" and (spatially) disordered cases. While the former presents bistability, hysteresis and abrupt changes of its variables; the heterogeneous version exhibits continuous transitions features. In particular, we observe an activated-scaling critical point compatible with the quenched directed percolation universality class, and a regime of generic power-laws (also called Griffiths phase) in the vicinity of the transition point. This lead us to believe that, equilibrium (Imry-Ma-Aizenman-Wehr-Berker) arguments can be extended to non-equilibrium systems providing that a fluctuating phase exists. In that case, at least one phase is subjected to destabilizing effects of fluctuations, and as a consequence,

phase coexistence is excluded.

In this light, we ask ourselves whether, not only quenched, but also structural spatial disorder would lead to the same intriguing effect. We focus on the particular problem of neural dynamics which, in apparent contradiction to the critical features observed, is likely to be described by integrative models with discontinuous transition in mean-field approach. To that end, we consider the previous prototypical model on a hierarchical modular network that mimics the cortex structure. In particular, we consider a specific construction method that enables us to tune the topological dimension of the considered network. Similarly to the quenched version, we have shown that a rounding phenomenon, leading to criticality, appears for low-dimensional systems. In this way we explain how the activity integration that takes place in neural dynamics is compatible with critical features exhibited in the cortex.

Aiming at unraveling the role of realistic mechanisms of complex systems, adaptation cannot be ignored. In nature, individuals unavoidably changes in response to the environment in which they are embedded. However, evolution is usually extremely slow compared to community dynamics. In recent years, some examples of rapid evolutionary changes have been reported, and so, new (co-)evolutionary framework is needed. Elaborating on existing approaches, we construct an eco-evolutionary model aimed at explaining a particular system of coexisting plant-communities. By considering competition, sexual reproduction and mutation we obtain, not only the experimentally observed rapid phenotypic diversification, but also some other non-trivial results. For instance, we obtain an optimal exploitation of available resources by high specialized species efficiently distributed in space in a anti-correlated way. This result is in accordance with the niche dimension hypothesis, but may likely change when migration or environmental variability takes place. On the other hand, the appearance of emergent neutrality is remarkable, and so, studied in detail. We show that these findings are robust to a wide range of model variants as long as

competition and mutation is maintained (of course). This work contributes to the existing and extensive theory of co-evolution and paves the way for further work in this area. For instance, future studies about the conditions at which phase transition from generalists to specialist take place is a main objective on this point.

In summary, by using statistical-mechanics techniques and the theory of stochastic process –specifically, phase transitions theory, renormalization group approach and extensive computational analyses–, we have been able to simplify some complex systems to simple mathematical or computational models presenting the same (main) macroscopic behavior. Specifically, we have modeled integrative neural dynamics in cortex, ecological systems presenting catastrophic shifts and rich-species communities displaying a rapid phenotypic diversification. Besides, we have detailedly characterized absorbing non-equilibrium phase transitions existing in both, physical, and biological systems (specifically, the above-mentioned ones) in the presence of inherent aspects of real systems such as stochasticity, diffusion and spatial or structural heterogeneity. We have discussed the proper way of considering these realistic aspects in a real system and the similar results that would be encountered if they are considered in a different manner. Regarding neural systems, we have succeeded to capture essential properties of cortex networks in a simplified complex network with tunable topological dimension. Finally, apart from constructing a simple model of a eco-evolutionary system, we have been able to quantitatively characterize many aspects of the emergent diversification and check its robustness when model variations are considered.

With this, we have tried to unravel and emphasize the relevance of essential inherent aspects of real systems and its role in the way the latter behaves. Mechanisms such as stochasticity, diffusion, heterogeneities, and individuals adaptation should not be neglected carelessly, specially in the studies of phase transitions.

Conclusiones

Durante mucho tiempo, el comportamiento macroscópico emergente en sistemas de varios cuerpos, presentes en los campos de la física y química, ha sido objeto de estudio de la mecánica estadística. En los último años, "la ciencia de la complejidad" ha surgido como un área prometedora para la comprensión de otro tipo de sistemas de varios cuerpos como los que existen en biología, ecología o socio-economía. En este caso, las técnicas estándar de la mecánica estadística son aplicadas ayudando, entre otras cosas, a identificar mecanismos esenciales subyacentes a fenómenos emergentes de sistemas complejos. Un intenso trabajo es necesario para inferir lo que es necesario incluir en un modelo (y cómo) y qué puede ser despreciado. A la vista de esto, nosotros estudiamos el papel de algunos aspectos inherentes a sistemas naturales, que son a menudo ignorados, y enfatizamos la importancia de tenerlos en cuenta en el estudio de varios sistemas.

Las transiciones de fase son una característica a destacar en los sistemas mencionados anteriormente. Buenos modelos que expliquen los mecanismos responsables de dichas transiciones y que predigan su aparición, son de gran importancia, no solo en física, sino también en biología, ecología, etc. Teniendo en cuenta eso, una correcta comprensión puede ayudar a evitar problemas esenciales como el cambio climático, la extinción de especies, la desertificación, la propagación de enfermedades o caídas abruptas en la bolsa, entre otros.

Aspirando a aclarar estos mecanismos, hemos estudiado diversos problemas. En primer lugar, nos hemos centrado en un un sistema ecológico genérico sometido a una transición de fase discontinua o catastrófica en aproximación de campo medio. Resultados computacionales y analíticos a partir de la ecuación de Langevin más simple que describe a estos sistemas, nos llevan a la conclusión de que la estocasticidad es esencial para entenderlos. En particular, la presencia de ruido demográfico alto, combinado con baja difusión, altera dramáticamente el sistema forzándolo a presentar transiciones continuas con un punto crítico en la clase de universalidad de percolación dirigida. Contrariamente, en un caso más próximo a campo medio (es decir, sistemas poco fluctuantes y muy difusivos) las transiciones de fase discontinuas se recuperan. Un hecho a remarcar es que, cuando consideramos ruido espacial (congelado), inevitable en sistemas reales, un fenómeno de "redondeo" de la transición ocurre en cualquiera de los casos anteriores, siempre que el sistema sea de dimensión baja. Con este trabajo, esperamos ayudar en la prevención de los cambios catastróficos o, al menos, a identificar el tipo de transición más propicia en un sistema dado su nivel de ruido, difusión, o heterogeneidad.

Con la objetivo de hacer una descripción más completa del efecto de la heterogeneidad espacial, hemos llevado a cabo un análisis más técnico y detallado en un segundo trabajo. Considerando el proceso de "contacto cuadrático" que exhibe transiciones de fase discontinuas, entre una fase activa fluctuante y una inactiva absorbente, hemos llevado a cabo un análisis computacional extenso de los casos "puro" y desordenado. Mientras que el primer caso presenta biestabilidad, histéresis y cambios abruptos de sus variables; la versión heterogénea exhibe características de una transición de fase continua. En particular, observamos un punto crítico con "escalado-activo" compatible con la clase de universalidad de percolación dirigida congelada, y un régimen de leyes de potencia genéricas (también llamado fase de Griffit) en las vecindades del punto de transición. Esto nos lleva a pensar que los argumentos de equilibrio

de Imry, Ma, Aizenman, Wehr, y Berker, pueden ser extendidos a sistemas de no-equilibrio siempre que exista una fase fluctuante. En este caso, al menos una de las fases está sometida a los efectos desestabilizadores de las fluctuaciones, y como consecuencia, la coexistencia de fases es imposible.

A la luz de esto, nos preguntamos si, no solo desorden espacial congelado, sino estructural, conllevaría los mismos efectos. En referencia a esto, nos centramos en el problema particular de la dinámica neuronal que, en aparente contradicción con las propiedades críticas observadas, probablemente esté descrita por modelos "integrantes" con transiciones de fase discontinuas en la aproximación de campo medio. Con esto propósito, consideramos el modelo del capítulo anterior sobre una red modular jerárquica que captura la estructura del córtex. En particular, consideramos un método de construcción que nos permite ajustar la dimensión topológica de la red considerada. De forma similar al caso congelado, mostramos un fenómeno de "redondeo" hacia la criticidad para sistemas de baja dimensión, específicamente $d < 2$. De este modo explicamos cómo la dinámica integrante, que tiene lugar en la dinámica neuronal, es compatible con las propiedades críticas exhibidas en el córtex.

Si aspiramos a esclarecer el papel de mecanismos realistas en sistemas complejos, el fenómeno de adaptación no puede ser ignorado. En la naturaleza, los individuos cambian inevitablemente como respuesta al ambiente en el que están integrados. Sin embargo, la evolución es normalmente extremadamente lenta en comparación a la dinámica de comunidades. En los últimos años, algunos ejemplos de cambios evolutivos rápidos han sido observados, llevándonos a pensar que es necesario crear un nuevo marco teórico de co-evolución. Basados en las muchas teorías previas en este contexto, construimos un modelo eco-evolutivo aspirando a explicar un sistema particular de comunidades de plantas. Considerando mecanismos como competición, reproducción sexual y mutación, obtenemos, no solo la diversificación fenotípica observada, sino otros resultados no triviales. Por ejemplo, obtenemos que el sistema

consigue una explotación óptima de los recursos mediante la especialización de las especies y su distribución espacial anti-correlacionada. Aunque este resultado cumple la hipótesis de nichos, podría cambiar al considerar migraciones o variabilidad ambiental. Por otra parte, la aparición de neutralidad emergente es destacada y estudiada en detalle. Estos resultados son robustos a una gran variedad de variantes siempre que la competición y las mutaciones se mantengan. Con este trabajo intentamos contribuir a la extensa teoría existente acerca de co-evolución y nos abre un campo de trabajo futuro. De hecho, prevemos estudiar las condiciones para las cuales una transición de fase entre generalistas y especialistas tenga lugar.

En resumen, mediante el empleo de técnicas de la mecánica estadística y teoría de los procesos estocásticos (específicamente, teoría de transiciones de fase, aproximaciones del grupo de renormalización y análisis computacionales) hemos sido capaces de simplificar algunos sistemas complejos por modelos matemáticos o computacionales sencillos que presenten las mismas propiedades principales macroscópicas. Específicamente, hemos modelado la dinámica integrativa en el córtex, sistemas ecológicos sometidos a cambios catastróficos y comunidades de múltiples especies con diversificación fenotípica rápida. Además, hemos caracterizado de forma detallada transiciones de fase absorbentes de no-equilibrio existentes tanto en sistemas físicos como biológicos (específicamente los mencionados arriba) en presencia de aspectos inherentes de los sistemas reales como la estocasticidad, la difusión y la heterogeneidad espacial o temporal. Hemos discutido también la manera adecuada de considerar estos aspectos realistas y argumentado que resultados similares se obtendrían si estos aspectos se consideraran de manera distinta. En el caso de sistemas neuronales, hemos conseguido capturar las propiedades esenciales de las redes del córtex con una red simple con dimensión topológica ajustable. Finalmente, a parte de construir un modelo eco-evolutivo simple, hemos sido capaces de caracterizar cuantitativamente muchos aspectos de la diversificación emergente y probar su robustez.

Con todo esto, hemos intentado esclarecer y enfatizar la importancia de aspectos esenciales e inherentes a los sistemas reales y su papel en la manera en que estos sistemas se comportan. Mecanismos como la estocasticidad, difusión, heterogeneidad y adaptación no deben ser despreciados a la ligera, especialmente en el estudio de las transiciones de fase de dichos sistemas.

Appendix A

Langevin integration. Dornic et. al integration method

Integrating stochastic (partial) differential equations with multiplicative noise –i.e., a noise depending on the system's state– is a non-trivial task. The key problem is that standard integration techniques do lead to negative values of the activity variables ρ and, thus, to numerical instabilities. Nevertheless, an efficient and accurate numerical integration can be obtained through a split-step scheme introduced a few years back [64]. The scheme consists in separating –at each spatial site– the integration of some of the deterministic terms from that of the stochastic part (plus eventually linear and constant deterministic terms), e.g. $\partial_t \rho = a\rho + \eta$ –where the Gaussian (white) noise $\eta(\mathbf{x}, t)$ has zero mean and variance proportional to $\sigma^2 \rho(\mathbf{x}, t)$. The scheme allows us to exactly sample –at each spatial location– the time-dependent solution of the associated Fokker-Planck equation[82]:

$$P(\rho(t+\Delta t)) = \lambda e^{-\lambda(\rho(t)e^{at}+\rho)} + \left[\frac{\rho}{\rho(t)e^{at}}\right]^{\mu/2} I_\mu\left(2\lambda\sqrt{\rho(t)\rho e^{at}}\right) \qquad \text{(A.1)}$$

where, I_μ is a Bessel function of order μ, $\lambda = 2a/\sigma^2(e^{at} - 1)$ and $\mu = -1$. The most important step is to realize that this equation can be rewritten, with the help of a Taylor-series expansion, as:

$$P(\rho(t + \Delta t)) = \sum_{n=0}^{\infty} \frac{(\lambda\rho(t)e^{a\Delta t})^n e^{-\lambda\rho(t)e^{a\Delta t}}}{n!} \frac{\lambda e^{-\lambda\rho}(\lambda\rho(t))^{n+\mu}}{\Gamma(n + \mu + 1)} \tag{A.2}$$

and noticing that $\rho(t + \Delta t)$ can be obtained by a mixture of gamma and poisson probability distributions that will reconstitute, on average, all terms of the latter equation. Thus, the method alternates two steps: (i) the integration of deterministic terms employing some standard algorithm (such as an Euler or Runge-Kutta) and then (ii) using its output, Eq.(A.2) is employed to obtain the final updated value of $\rho(t + \Delta t)$ at each spatial location. More details and applications of this numerical scheme can be found in [64].

Appendix B

List of Publications

[P1] *Quenched disorder forbids discontinuous transitions in nonequilibrium low-dimensional systems*, Paula Villa Martín, Juan A. Bonachela and Miguel A. Muñoz, **Phys.Rev. E**, 89, 012145. (2014)

[P2] *Rounding of abrupt phase transitions in brain networks*, Paula Villa Martín, Paolo Moretti and Miguel A. Muñoz, **J. Stat. Phys.** 1, P01003. (2015)

[P3] *Eluding catastrophic shifts*, Paula Villa Martín, Juan A. Bonachela, Simon A. Levin and Miguel A. Muñoz, **Proc. Nat. Acad. Sci. USA**, 201414708. (2015)

[P4] *Eco-evolutionary Model of Rapid Phenotypic Diversification in Species-Rich Communities*, Paula Villa Martín, Jorge Hidalgo, Rafael Rubio de Casas, and Miguel A. Muñoz, **PLoS Comput Biol**, vol. 12, no 10, p. e1005139. (2016)

Bibliography

[1] L. F. Abbott. Lapicque's introduction of the integrate-and-fire model neuron (1907). *Brain Res. Bull.*, 50(5–6):303–304, 1999.

[2] Frederick R Adler and Julio Mosquera. Is space necessary? interference competition and limits to biodiversity. *Ecology*, 81(11):3226–3232, 2000.

[3] Michael Aizenman and Jan Wehr. Rounding of first-order phase transitions in systems with quenched disorder. *Phys. Rev. Lett.*, 62(21):2503–2506, May 1989.

[4] Réka Albert and Albert-László Barabási. Statistical mechanics of complex networks. *Reviews of modern physics*, 74(1):47, 2002.

[5] Eric Allan, Tania Jenkins, Alexander JF Fergus, Christiane Roscher, Markus Fischer, Jana Petermann, Wolfgang W Weisser, and Bernhard Schmid. Experimental plant communities develop phylogenetically overdispersed abundance distributions during assembly. *Ecology*, 94(2):465–477, 2013.

[6] Daniel J Amit and Victor Martin-Mayor. *Field theory, the renormalization group, and critical phenomena: graphs to computers*. World Scientific Publishing Co Inc, 2005.

[7] Sandro Azaele, Samir Suweis, Jacopo Grilli, Igor Volkov, Jayanth R Banavar, and Amos Maritan. Statistical mechanics of ecological systems: Neutral theory and beyond. *arXiv preprint arXiv:1506.01721*, 2015.

[8] Radu Balescu. Equilibrium and nonequilibrium statistical mechanics. *NASA STI/Recon Technical Report A*, 76, 1975.

[9] György Barabás, Rafael D'Andrea, and Annette Marie Ostling. Species packing in nonsmooth competition models. *Theoretical ecology*, 6(1):1–19, 2013.

[10] György Barabás, Simone Pigolotti, Mats Gyllenberg, Ulf Dieckmann, and Géza Meszéna. Continuous coexistence or discrete species? a new review of an old question. *Evolutionary Ecology Research*, 14(5):523–554, 2012.

[11] Hatem Barghathi and Thomas Vojta. Random Fields at a Nonequilibrium Phase Transition. *Phys. Rev. Lett.*, 109(17):170603, October 2012.

[12] Alain Barrat, Marc Barthelemy, and Alessandro Vespignani. *Dynamical processes on complex networks*. Cambridge university press, 2008.

[13] Peter W Bates, Hannelore Lisei, and Kening Lu. Attractors for stochastic lattice dynamical systems. *Stochastics and Dynamics*, 6(01):1–21, 2006.

[14] J. M. Beggs. The criticality hypothesis: How local cortical networks might optimize information processing. *Phil. Trans. R. Soc. A*, 366(1864):329–343, 2008.

[15] J. M. Beggs and .D Plenz. Neuronal avalanches in neocortical circuits. *J. Neurosci.*, 23(35):11167–11177, 2003.

[16] J. M. Beggs and D. Plenz. Neuronal avalanches are diverse and precise activity patterns stable for many hours in cortical slice cultures. *J. Neurosci.*, 24(22):5216–5229, 2004.

[17] G. Bel, A. Hagberg, and E. Meron. Gradual regime shifts in spatially extended ecosystems. *J. Theor. Ecol.*, 5:591–604, 2012.

[18] Arash Bellafard, Helmut G. Katzgraber, Matthias Troyer, and Sudip Chakravarty. Bond Disorder Induced Criticality of the Three-Color Ashkin-Teller Model. *Phys. Rev. Lett.*, 109(15):155701, October 2012.

[19] A Nihat Berker. Critical behavior induced by quenched disorder. *Phys. A*, 194(1-4):72–76, 1993.

[20] K. Binder. Theory of first-order phase transitions. *Rep. Prog. Phys.*, 50(7):783, 1987.

[21] J. J. Binney, N. J. Dowrick, A. J. Fisher, and M. E. J. Newman. *The theory of Critical Phenomena*. Clarendon Press, Oxford, 1992.

[22] C. Boettiger and A. Hastings. Early warning signals and the prosecutor's fallacy. *Proc. R. Soc. B*, 279:4734–4739, 2012.

[23] C. Boettiger and A. Hastings. Quantifying limits to detection of early warning for critical transitions. *J. R. Soc. Interface*, 9:2527–2539, 2012.

[24] J. A. Bonachela, S. de Franciscis, J. J. Torres, and M. A. Muñoz. Self-organization without conservation: are neuronal avalanches generically critical? *J. Stat. Mech.*, (02):P02015, 2010.

[25] J. A. Bonachela, M. A. Muñoz, and S. A. Levin. Patchiness and demographic noise in three ecological examples. *J. Stat. Phys.*, 148:723–739, 2012.

[26] Michael B Bonsall, Vincent AA Jansen, and Michael P Hassell. Life history trade-offs assemble ecological guilds. *Science*, 306(5693):111–114, 2004.

[27] G M Buendia and P A Rikvold. Effects of inert species in the gas phase in a model for the catalytic oxidation of CO. *Phys. Rev. E*, 85(3):31143, March 2012.

[28] A. N. Burkitt. A review of the integrate-and-fire neuron model: I. homogeneous synaptic input. *Biol. Cybern.*, 95(1):1–19, 2006.

[29] A. N. Burkitt. A review of the integrate-and-fire neuron model: Ii. inhomogeneous synaptic input and network properties. *Biol. Cybern.*, 95(2):97–112, 2006.

[30] Raffaele Cafiero, Andrea Gabrielli, and Miguel A Muñoz. Disordered one-dimensional contact process. *Phys. Rev. E*, 57(5):5060–5068, May 1998.

[31] Tomás Caraballo and Kening Lu. Attractors for stochastic lattice dynamical systems with a multiplicative noise. *Frontiers of Mathematics in China*, 3(3):317–335, 2008.

[32] Tomás Caraballo, José A. Langa, and James C. Robinson. A stochastic pitchfork bifurcation in a reaction-diffusion equation. *Proceedings of the Royal Society of London. Series A: Mathematical, Physical and Engineering Sciences*, 457(2013):2041–2061, 2001.

[33] BJ Cardinale, Emmett Duffy, Diane Srivastava, Michel Loreau, Matt Thomas, and Mark Emmerson. Towards a food web perspective on biodiversity and ecosystem functioning. *Biodiversity and human impacts*, pages 105–120, 2009.

[34] S. Carpenter and et al. Early warnings of regime shifts: A whole-ecosystem experiment. *Science*, 332:1079, 2011.

[35] S. R. Carpenter and W. A. Brock. Early warnings of regime shifts in spatial dynamics using the discrete fourier transform. *Ecosphere*, 1(10), 2010.

[36] S.R. Carpenter. *Alternate states of ecosystems: evidence and some implications*, pages 357–83. Blackwell Science, Oxford, 2001.

[37] Scott P Carroll, Andrew P Hendry, David N Reznick, and Charles W Fox. Evolution on ecological time-scales. *Functional Ecology*, 21(3):387–393, 2007.

[38] Sandra Cerrai. Stochastic reaction-diffusion systems with multiplicative noise and non-lipschitz reaction term. *Probability Theory and Related Fields*, 125(2):271–304, 2003.

[39] Sandra Cerrai, Michael Röckner, et al. Large deviations for stochastic reaction-diffusion systems with multiplicative noise and non-lipshitz reaction term. *The Annals of Probability*, 32(1B):1100–1139, 2004.

[40] Nicolas Champagnat, Régis Ferrière, and Sylvie Méléard. Unifying evolutionary dynamics: From individual stochastic processes to macroscopic models. *Theoretical Population Biology*, 69(3):297–321, 2006.

[41] Jonathan M Chase and Mathew A Leibold. *Ecological niches: linking classical and contemporary approaches*. University of Chicago Press, 2003.

[42] Peter Chesson. Mechanisms of maintenance of species diversity. *Annual review of Ecology and Systematics*, pages 343–366, 2000.

[43] D. R. Chialvo. Emergent complex neural dynamics. *Nature Phys.*, 6:744–750, 2010.

[44] Pao-Liu Chow. Stability of nonlinear stochastic-evolution equations. *Journal of Mathematical Analysis and Applications*, 89(2):400–419, 1982.

[45] Otto X Cordero and Martin F Polz. Explaining microbial genomic diversity in light of evolutionary ecology. *Nature Reviews Microbiology*, 12(4):263–273, 2014.

[46] J Theodore Cox. Coalescing random walks and voter model consensus times on the torus in zd. *The Annals of Probability*, pages 1333–1366, 1989.

[47] Jerry A Coyne and H Allen Orr. *Speciation*, volume 37. Sinauer Associates Sunderland, MA, 2004.

[48] R. Craig MaClean. Adaptive radiation in microbial microcosms. *Journal of Evolutionary Biology*, 18(6):1376–1386, 2005.

[49] Hans Crauel and Franco Flandoli. Attractors for random dynamical systems. *Probability Theory and Related Fields*, 100(3):365–393, 1994.

[50] Jonas Cremer, Anna Melbinger, and Erwin Frey. Evolutionary and population dynamics: A coupled approach. *Phys. Rev. E*, 84:051921, Nov 2011.

[51] L. Dai, K. S. Korolev, and J. Gore. Slower recovery in space before collapse of connected populations. *Nature*, 496:355, 2013.

[52] L. Dai, D. Vorselen, K. S. Korolev, and J. Gore. Generic indicators for loss of resilience before a tipping point leading to population collapse. *Science*, 336(6085):1175–1177, 2012.

[53] V. Dakos, S. Kéfi, M. Rietkerk, E. H. Van Nes, and M. Scheffer. Slowing down in spatially patterned ecosystems at the brink of collapse. *Am. Nat.*, 177:153–166, 2011.

[54] V. Dakos, E.H. van Nes, R. Donangelo, H. Fort, and Marten Scheffer. Spatial correlation as leading indicator of catastrophic shifts. *J Theor Ecol*, 3:163–174, 2010.

[55] MAM De Aguiar, M Baranger, EM Baptestini, L Kaufman, and Y Bar-Yam. Global patterns of speciation and diversity. *Nature*, 460(7253):384–387, 2009.

[56] Donald L DeAngelis and Wolf M Mooij. Individual-based modeling of ecological and evolutionary processes. *Annual Review of Ecology, Evolution, and Systematics*, pages 147–168, 2005.

[57] R. Dickman and T. Tomé. First-order phase transition in a one-dimensional nonequilibrium model. *Phys. Rev. A*, 70:046131, 2004.

[58] U Dieckmann and M On Doebeli. On the origin of species by sympatric speciation. *Nature*, 400(22):354–357, 1999.

[59] U Dieckmann, P Marrow, and R Law. Evolutionary cycling in predator-prey interactions: population dynamics and the red queen. *Journal of theoretical biology*, 176(1):91–102, sep 1995.

[60] Ulf Dieckmann and Richard Law. The dynamical theory of coevolution: a derivation from stochastic ecological processes. *Journal of mathematical biology*, 34(5-6):579–612, 1996.

[61] Michael Doebeli. *Adaptive Diversification (MPB-48)*. Princeton University Press, 2011.

[62] Michael Doebeli and Ulf Dieckmann. Evolutionary branching and sympatric speciation caused by different types of ecological interactions. *The american naturalist*, 156(S4):S77—-S101, 2000.

[63] Michael Doebeli and Ulf Dieckmann. Speciation along environmental gradients. *Nature*, 421(6920):259–264, 2003.

[64] I. Dornic, H. Chaté, and M. A. Muñoz. Integration of langevin equations with multiplicative noise and the viability of field theories for absorbing phase transitions. *Phys. Rev. Lett.*, 94:100601, 2005.

[65] J. M. Drake and B. D. Griffen. Early warning signals of extinction in deteriorating environments. *Nature*, 467:456–459, 2010.

[66] J Emmett Duffy, Bradley J Cardinale, Kristin E France, Peter B McIntyre, Elisa Thébault, and Michel Loreau. The functional role of biodiversity in ecosystems: incorporating trophic complexity. *Ecology letters*, 10(6):522–538, 2007.

[67] Santiago F Elena and Richard E Lenski. Evolution experiments with microorganisms: the dynamics and genetic bases of adaptation. *Nature Reviews Genetics*, 4(6):457–469, 2003.

[68] Vlad Elgart and Alex Kamenev. Rare event statistics in reaction-diffusion systems. *Phys. Rev. E*, 70:041106, Oct 2004.

[69] Vlad Elgart and Alex Kamenev. Classification of phase transitions in reaction-diffusion models. *Phys. Rev. E*, 74(4):041101, October 2006.

[70] Stephen P Ellner, Monica A Geber, and Nelson G Hairston. Does rapid evolution matter? measuring the rate of contemporary evolution and its impacts on ecological dynamics. *Ecology Letters*, 14(6):603–614, 2011.

[71] Suzanne Faber, Zhibing Hu, Gerard H Wegdam, Peter Schall, et al. Controlling colloidal phase transitions with critical casimir forces. *Nature communications*, 4:1584, 2013.

[72] A Fernández and H. Fort. Catastrophic phase transitions and early warnings in a spatial ecological model. *J. Stat. Mech.*, (P09014), 2009.

[73] C.E. Fiore and M.J. de Oliveira. Contact process with long-range interactions: A study in the ensemble of constant particle number. *Phys. Rev. E.*, 76:041103, 2007.

[74] Edmund Brisco Ford. *Ecological genetics*. Springer, 1975.

[75] H. Fort, N. Mazzeo, M. Scheffer, and E. Van Nes. Catastrophic shifts in ecosystems: spatial early warnings and management procedures. *Journal of Physics*, 246:012035, 2010.

[76] K. Frank, B. Petrie, J. Fisher, and W. Leggett. Transient dynamics of an altered large marine ecosystem. *Nature*, 477:86–89, 2011.

[77] Maren L Friesen, Gerda Saxer, Michael Travisano, and Michael Doebeli. Experimental evidence for sympatric ecological diversification due to frequency-dependent competition in escherichia coli. *Evolution*, 58(2):245–260, 2004.

[78] GF Fussmann, M Loreau, and PA Abrams. Eco-evolutionary dynamics of communities and ecosystems. *Functional Ecology*, 21(3):465–477, 2007.

[79] GF Fussmann, M Loreau, and PA Abrams. Eco-evolutionary dynamics of communities and ecosystems. *Functional Ecology*, 21(3):465–477, 2007.

[80] L. K. Gallos, H. A. Makse, and M. Sigman. A small world of weak ties provides optimal global integration of self-similar modules in functional brain networks. *Proc. Natl. Acad. Sci. USA*, 109:2825—-2830, 2012.

[81] J. García-Ojalvo and J. M. Sancho. *Noise in spatially extended systems*. Institute for nonlinear science. Springer, New York, 1999.

[82] C Gardiner. *Stochastic Methods: A Handbook for the Natural and Social Sciences*. Springer Series in Synergetics. Springer, 2009.

[83] S.A.H. Geritz, E. Kisdi, G. Meszéna, and J.A.J. Metz. Evolutionarily singular strategies and the adaptive growth and branching of the evolutionary tree. *Evolutionary Ecology*, (1):35–57.

[84] Stefan Geritz, J. Metz, Éva Kisdi, and Géza Meszéna. Dynamics of Adaptation and Evolutionary Branching. *Physical Review Letters*, 78(10):2024–2027, 1997.

[85] Stefan AH Geritz, Ed van der Meijden, and Johan AJ Metz. Evolutionary dynamics of seed size and seedling competitive ability. *Theoretical population biology*, 55(3):324–343, 1999.

[86] Leonardo L. Gollo, Claudio Mirasso, and Víctor M. Eguíluz. Signal integration enhances the dynamic range in neuronal systems. *Phys. Rev. E*, 85:040902, Apr 2012.

[87] James B Grace, T Michael Anderson, Eric W Seabloom, Elizabeth T Borer, Peter B Adler, W Stanley Harpole, Yann Hautier, Helmut Hillebrand, Eric M Lind, Meelis Pärtel, et al. Integrative modelling reveals mechanisms linking productivity and plant species richness. *Nature*, 529(7586):390–393, 2016.

[88] Peter R Grant and B Rosemary Grant. Evolution of character displacement in darwin's finches. *science*, 313(5784):224–226, 2006.

[89] P. Grassberger. On phase transitions in schlögl's second model. *Z. Phys. B Con. Mat.*, 47:365–374, 1982.

[90] Dominique Gravel, Charles D Canham, Marilou Beaudet, and Christian Messier. Reconciling niche and neutrality: the continuum hypothesis. *Ecology letters*, 9(4):399–409, 2006.

[91] Dominique Gravel, Charles D. Canham, Marilou Beaudet, and Christian Messier. Reconciling niche and neutrality: the continuum hypothesis. *Ecology Letters*, 9(4):399–409, 2006.

[92] Rafael L. Greenblatt, Michael Aizenman, and Joel L. Lebowitz. Rounding of first order transitions in low-dimensional quantum systems with quenched disorder. *Phys. Rev. Lett.*, 103:197201, Nov 2009.

[93] Robert B Griffiths. Nonanalytic Behavior Above the Critical Point in a Random Ising Ferromagnet. *Phys. Rev. Lett.*, 23(1):17–19, 1969.

[94] G Grinstein and A Luther. Application of the renormalization group to phase transitions in disordered systems. *Phys. Rev. B*, 13(3):1329–1343, February 1976.

[95] G. Grinstein and Miguel A. Muñoz. The statistical mechanics of absorbing states. In Pedro L. Garrido and Joaquín Marro, editors, *Fourth Granada Lectures in Computational Physics*, volume 493 of *Lecture Notes in Physics*, pages 223–270. Springer Berlin Heidelberg, 1997.

[96] Geoffrey Grinstein and Ralph Linsker. Synchronous neural activity in scale-free network models versus random network models. *Proc. Natl. Acad. Sci. USA*, 102(28):9948–9953, 2005.

[97] V. Guttal and C. Jayaprakash. Spatial variance and spatial skewness: leading indicators of regime shifts in spatial ecological systems. *J. Theor. Ecol.*, 2:3–12, 2009.

[98] Bart Haegeman and Michel Loreau. A mathematical synthesis of niche and neutral theories in community ecology. *Journal of Theoretical Biology*, 269(1):150–165, 2011.

[99] P. Hagmann, L. Cammoun, X. Gigandet, R Meuli, C. J. Honey, V. J. Wedeen, and O. Sporns. Mapping the structural core of human cerebral cortex. *PLoS Biol.*, 6(7):e159, 2008.

[100] Ariel Haimovici, Enzo Tagliazucchi, Pablo Balenzuela, and Dante R. Chialvo. Brain organization into resting state networks emerges at criticality on a model of the human connectome. *Phys. Rev. Lett.*, 110:178101, Apr 2013.

[101] Susse Kirkelund Hansen, Paul B Rainey, Janus AJ Haagensen, and Søren Molin. Evolution of species interactions in a biofilm community. *Nature*, 445(7127):533–536, 2007.

[102] Ilkka Hanski. Eco-evolutionary dynamics in a changing world. *Annals of the New York Academy of Sciences*, 1249(1):1–17, 2012.

[103] J. Von Hardenberg, E. Meron, M. Shachak, and Y. Zarmi. Diversity of vegetation patterns and desertification. *Phys. Rev. Lett.*, 87(19):198101, 2001.

[104] W Stanley Harpole and David Tilman. Grassland species loss resulting from reduced niche dimension. *Nature*, 446(7137):791–793, 2007.

[105] A Brooks Harris and T C Lubensky. Renormalization-Group Approach to the Critical Behavior of Random-Spin Models. *Phys. Rev. Lett.*, 33(26):1540–1543, 1974.

[106] Malte Henkel, Haye Hinrichsen, and Sven Lübeck. *Non-Equilibrium Phase Transitions, Volume 1*. Springer, 2008.

[107] Emilio Hernández-García, Cristóbal López, Simone Pigolotti, and Ken H Andersen. Species competition: coexistence, exclusion and clustering. *Philosophical Transactions of the Royal Society of London A: Mathematical, Physical and Engineering Sciences*, 367(1901):3183–3195, 2009.

[108] Matthew D Herron and Michael Doebeli. Parallel evolutionary dynamics of adaptive diversification in escherichia coli. *PLoS Biol*, 11(2):e1001490, 2013.

[109] J. Hidalgo, L. F. Seoane, J. M. Cortés, and M. A. Muñoz. Stochastic amplification of fluctuations in cortical up-states. *PloS ONE*, 7(8):e40710, 2012.

[110] H. Hinrichsen. Non-equilibrium critical phenomena and phase transitions into absorbing states. *Adv. in Phys.*, 49:815–958, 2000.

[111] M. Hirota, M. Holmgren, E. H. Van Nes, and M. Scheffer. Global resilience of tropical forest and savanna to critical transitions. *Science*, 334(6053):232–235, 2011.

[112] P. C. Hohenberg and B. I. Halperin. Theory of dynamic critical phenomena. *Rev. Mod. Phys.*, 49:435–479, Jul 1977.

[113] David U Hooper, FS Chapin Iii, JJ Ewel, Andy Hector, Pablo Inchausti, Sandra Lavorel, JH Lawton, DM Lodge, Michel Loreau, S Naeem, et al. Effects of biodiversity on ecosystem functioning: a consensus of current knowledge. *Ecological monographs*, 75(1):3–35, 2005.

[114] Jef Hooyberghs, Ferenc Iglói, and Carlo Vanderzande. Strong Disorder Fixed Point in Absorbing-State Phase Transitions. *Phys. Rev. Lett.*, 90(10):100601, March 2003.

[115] Fawaz Hrahsheh, José A. Hoyos, and Thomas Vojta. Rounding of a first-order quantum phase transition to a strong-coupling critical point. *Phys. Rev. B*, 86:214204, Dec 2012.

[116] Stephen P Hubbell. *The unified neutral theory of biodiversity and biogeography (MPB-32)*, volume 32. Princeton University Press, 2001.

[117] Kenneth Hui and A. Berker. Random-field mechanism in random-bond multicritical systems. *Phys. Rev. Lett.*, 62(21):2507–2510, May 1989.

[118] G.E. Hutchinson. Concluding remarks. *Cold Spring Harbor Symposia on Quantitative Biology*, 22(2):415–427, 1957.

[119] Y Imry and S K Ma. Random-Field Instability of the Ordered State of Continuous Symmetry. *Phys. Rev. Lett.*, 35:1399, 1975.

[120] Yoseph Imry and Michael Wortis. Influence of quenched impurities on first-order phase transitions. *Phys. Rev. B*, 19(7):3580–3585, 1979.

[121] VAA Jansen and GSEE Mulder. Evolving biodiversity. *Ecology Letters*, 2(6):379–386, 1999.

[122] H. K. Janssen. On the nonequilibrium phase transition in reaction-diffusion systems with an absorbing stationary state. *Z. Phys. B*, 42:151, 1981.

[123] Marc TJ Johnson and John R Stinchcombe. An emerging synthesis between community ecology and evolutionary biology. *Trends in Ecology & Evolution*, 22(5):250–257, 2007.

[124] M. Kaiser and C. C. Hilgetag. Optimal hierarchical modular topologies for producing limited sustained activation of neural networks. *Front. Neuroinform.*, 4:14, 2010.

[125] M Kaiser, Görner M, and C C Hilgetag. Criticality of spreading dynamics in hierarchical cluster networks without inhibition. *New Journal of Physics*, 9:110, 2007.

[126] Marcus Kaiser, Robert Martin, Peter Andras, and Malcolm P. Young. Simulation of robustness against lesions of cortical networks. *Eur. J. Neurosci.*, 25(10):3185–3192, 2007.

[127] S. Kéfi, M. Rietkerk, C. L. Alados, Y. Pueyo, V. P. Papanastasis, A. Elaich, and P. C. de Ruiter. Spatial vegetation patterns and imminent desertification in mediterranean arid ecosystems. *Nature*, 449:213–217, 2007.

[128] S. Kéfi, M. Rietkerk, M. van Baalen, and Michel Loreau. Local facilitation, bistability and transitions in arid ecosystems. *Theor. Popul. Biol.*, 71:367–379, 2007.

[129] O. Kinouchi and M. Copelli. Optimal dynamical range of excitable networks at criticality. *Nature Phys.*, 2(5):348–351, 2006.

[130] S. J. Lade and T. Gross. Early warning signals for critical transitions: a generalized modeling approach. *PLoS Comput. Biol.*, 8(2):e1002360, 2012.

[131] S. J. Lade, A. Tavoni, S. A. Levin, and M. Schlüter. Regime shifts in a social-ecological system. *Theoretical Ecology*, 6(3):359–372, 2013.

[132] Adam Lampert and Alan Hastings. Sharp changes in resource availability may induce spatial nearly periodic population abundances. *Ecological Complexity*, 19:80–83, 2014.

[133] Richard Law, Paul Marrow, and U Dieckmann. On evolution under asymmetric competition. *Evolutionary Ecology*, 11(4):485–501, 1997.

[134] SA Levin. The problem of scale and pattern in ecology. *Ecology*, 73(1943):1967, 1992.

[135] S.A. Levin and S.W. Pacala. *Theories of simplification and scaling of spatially distributed processes*, pages 271–296. Princeton University, 1997.

[136] A. Levina, J. M. Herrmann, and T. Geisel. Dynamical synapses causing self-organized criticality in neural networks. *Nature Phys.*, 3(12):857–860, 2007.

[137] T M Liggett. *Interacting Particle Systems*. Classics in Mathematics. Springer, 2004.

[138] Nicolas Loeuille and Michel Loreau. Nutrient enrichment and food chains: can evolution buffer top-down control? *Theoretical population biology*, 65(3):285–298, 2004.

[139] Michel Loreau and Andy Hector. Partitioning selection and complementarity in biodiversity experiments. *Nature*, 412(6842):72–76, 2001.

[140] D. Ludwig, D. D. Jones, and C. S. Holling. Qualitative analysis of insect outbreak systems: the spruce budworm and the forest. *J. Anim. Ecol.*, 47:315–332, 1978.

[141] G. Sartoni M. Kardar, A.L. Stella and B. Derrida. Unusual universality of branching interfaces in random media. *Phys. Rev. E.*, 52:R1269, 1995.

[142] Robert MacArthur and Richard Levins. The limiting similarity, convergence, and divergence of coexisting species. *American Naturalist*, pages 377–385, 1967.

[143] Robert H MacArthur. *Geographical ecology: patterns in the distribution of species*. Princeton University Press, 1984.

[144] A. Manor and N. M. Shnerb. Facilitation, competition, and vegetation patchiness: From scale free distribution to patterns. *J. Theor. Biol.*, 253:838–842, 2008.

[145] Alon Manor and Nadav M. Shnerb. Origin of pareto-like spatial distributions in ecosystems. *Phys. Rev. Lett.*, 101:268104, 2008.

[146] J. Marro and R. Dickman. *Nonequilibrium Phase Transition in Lattice Models*. Cambridge University Press, 1999.

[147] Naoki Masuda, N. Gibert, and S. Redner. Heterogeneous voter models. *Phys. Rev. E*, 82(1):010103, July 2010.

[148] R. M. May, S. A. Levin, and G. Sugihara. Complex systems - ecology for bankers. *Nature*, 451(7181):893–895, 2008.

[149] Robert M May and Robert H Mac Arthur. Niche overlap as a function of environmental variability. *Proceedings of the National Academy of Sciences*, 69(5):1109–1113, 1972.

[150] M. A. McPeek and R. D. Holt. The evolution of dispersal in spatially and temporally varying environments. *Am. Nat.*, 140(6):1010–1027, 1992.

[151] Baruch Meerson and Pavel V. Sasorov. Extinction rates of established spatial populations. *Phys. Rev. E.*, 83:011129, 2011.

[152] D. Meunier, R. Lambiotte, A Fornito, K. Ersch, and E.T. Bullmore. Hierarchical modularity in human brain functional networks. *Front. Neuroinform.*, 3:37, 2009.

[153] Kaisa Miettinen. *Nonlinear multiobjective optimization*, volume 12. Springer Science & Business Media, 1999.

[154] S. Millman, D. Mihalas, A. Kirkwood, and E. Niebur. Self-organized criticality occurs in non-conservative neuronal networks during up states. *Nature Phys.*, 6(10):801–805, 2010.

[155] Patrick AP Moran. Notes on continuous stochastic phenomena. *Biometrika*, pages 17–23, 1950.

[156] Paolo Moretti and Miguel A. Muñoz. Griffiths phases and the stretching of criticality in brain networks. *Nat. Commun.*, 4:2521, 2013.

[157] M. A. Muñoz, R. Dickman, A. Vespignani, and S. Zapperi. Avalanche and spreading exponents in systems with absorbing states. *Phys. Rev. E*, 59(5):6175, 1999.

[158] M. A. Muñoz, R. Juhász, C. Castellano, and G. Ódor. Griffiths phases on complex networks. *Phys. Rev. Lett.*, 105:128701, 2010.

[159] J. D. Murray. *Mathematical Biology: I. An Introduction.* Springer-Verlag, New York, 2002.

[160] E. H. Van Nes and M. Scheffer. Implications of spatial heterogeneity for catastrophic regime shifts in ecosystems. *Ecology*, 86(7):1797–1807, 2005.

[161] Géza Ódor. *Universality in nonequilibrium lattice systems.* World Scientific, 2008.

[162] T. Ohtsuki and T. Keyes. Nonequilibrium critical phenomena in one-component reaction-diffusion systems. *Phys. Rev. A*, 35:2697, 1987.

[163] E. Ott. *Chaos in Dynamical Systems.* Cambridge University Press, 2002.

[164] M. Pal, A. K. Pal, S. Ghosh, and I. Bose. Early signatures of regime shifts in gene expression dynamics. *Phys. Biol.*, 10(3):036010, 2013.

[165] Giorgio Parisi. *Statistical field theory.* Frontiers in Physics. Addison-Wesley, Redwood City, CA, 1988.

[166] T. Petermann, T. A. Thiagarajan, M. Lebedev, M. Nicolelis, D. R. Chialvo, and D. Plenz. Spontaneous cortical activity in awake monkeys composed of neuronal avalanches. *Proc. Natl. Acad. Sci. USA*, 106(37):15921–15926, 2009.

[167] Eric R Pianka. Niche overlap and diffuse competition. *Proceedings of the National Academy of Sciences*, 71(5):2141–2145, 1974.

[168] Simone Pigolotti and Massimo Cencini. Coexistence and invasibility in a two-species competition model with habitat-preference. *Journal of Theoretical Biology*, 265(4):609 – 617, 2010.

[169] Simone Pigolotti, Cristóbal López, and Emilio Hernández-García. Species clustering in competitive lotka-volterra models. *Physical review letters*, 98(25):258101, 2007.

[170] D. Plenz and T. C. Thiagarajan. The organizing principles of neuronal avalanches: cell assemblies in the cortex? *Trends. Neurosci.*, 30(3):101–110, 2007.

[171] Paul B Rainey and Michael Travisano. Adaptive radiation in a heterogeneous environment. *Nature*, 394(6688):69–72, 1998.

[172] Julia Reiss, Jon R Bridle, Jose M Montoya, and Guy Woodward. Emerging horizons in biodiversity and ecosystem functioning research. *Trends in ecology & evolution*, 24(9):505–514, 2009.

[173] M. Rietkerk, S. C. Dekker, P. C. de Ruiter, and J. Van de Koppel. Self-organized patchiness and catastrophic shifts in ecosystems. *Science*, 305:1926–1929, 2004.

[174] Michael L Rosenzweig. *Species diversity in space and time*. Cambridge University Press, 1995.

[175] James Rosindell, Stephen P Hubbell, and Rampal S Etienne. The unified neutral theory of biodiversity and biogeography at age ten. *Trends in ecology & evolution*, 26(7):340–348, 2011.

[176] Mikail Rubinov, Olaf Sporns, Jean-Philippe Thivierge, and Michael Breakspear. Neurobiologically realistic determinants of self-organized criticality in networks of spiking neurons. *PLoS Comput. Biol.*, 7(6):e1002038, 2011.

[177] Steffen Rulands, David Jahn, and Erwin Frey. Specialization and bet hedging in heterogeneous populations. *Physical review letters*, 113(10):108102, 2014.

[178] T. M. Scanlon, K. K. Caylor, S. A. Levin, and I. Rodriguez-Iturbe. Positive feedbacks promote power-law clustering of kalahari vegetation. *Nature*, 449:209–213, 2007.

[179] T.M. Scanlon, K.K. Caylor, S. Manfreda, S.A. Levin, and I. Rodriguez-Iturbe. Dynamic response of grass cover to rainfall variability: implications for the function and persistence of savanna ecosystems. *Adv. Water Resour.*, 28(3):291–302, 2005.

[180] M. Scheffer. *The Ecology of Shallow Lake*. Chapman and Hall, London, 1998.

[181] M Scheffer. *Critical transitions in nature and society*. Princeton Studies in Complexity. Princeton University Press, 2009.

[182] M. Scheffer, J. Bascompte, W. A. Brock, V. Brovkin, S. R. Carpenter, V. Dakos, H. Held, E. H. van Nes, M. Rietkerk, and G. Sugihara. Early-warning signals for critical transitions. *Nature*, 461:53–59, 2009.

[183] M. Scheffer, S. Carpenter, J. A. Foley, C. Folke, and B. Walkerk. Catastrophic shifts in ecosystems. *Nature*, 413 (6856):591–596, 2001.

[184] M. Scheffer and S. R. Carpenter. Catastrophic regime shifts in ecosystems: linking theory to observation. *Trends Ecol. Evol.*, 18(12):648–656, 2003.

[185] M. Scheffer, S. R. Carpenter, T. M. Lenton, J. Bascompte, W. Brock, J. van de Koppel V. Dakos, I. A. van de Leemput, S. A. Levin, E. H. van Nes, M. Pascual, and J. Vandermeer. Anticipating critical transitions. *Science*, 338:344, 2012.

[186] Marten Scheffer and Egbert H van Nes. Self-organized similarity, the evolutionary emergence of groups of similar species. *Proceedings of the National Academy of Sciences*, 103(16):6230–6235, 2006.

[187] Marten Scheffer and Egbert H. van Nes. Self-organized similarity, the evolutionary emergence of groups of similar species. *Proc Natl Acad of Sci USA*, 103(16):6230–6235, 2006.

[188] Dolph Schluter. *The ecology of adaptive radiation*. Oxford University Press, 2000.

[189] Thomas W Schoener. The newest synthesis: understanding the interplay of evolutionary and ecological dynamics. *science*, 331(6016):426–429, 2011.

[190] Montogemery Slatkin. Ecological character displacement. *Ecology*, 61(1):163–177, 1980.

[191] R. Solé. Ecology: Scaling laws in the drier. *Nature*, 449:151–153, 2007.

[192] R. V. Solé. *Phase transitions*. Princeton University Press, 2011.

[193] R. V. Solé and J. Bascompte. *Self-Organization in Complex Ecosystems*. Princeton University Press, 2006.

[194] Christine C Spencer, Melanie Bertrand, Michael Travisano, and Michael Doebeli. Adaptive diversification in genes that regulate resource use in escherichia coli. *PLoS Genet*, 3(1):e15, 2007.

[195] O. Sporns, C. J. Honey, and R. Kötter. Identification and classification of hubs in brain networks. *PLoS ONE*, 2(10):e1049, 2007.

[196] O. Sporns, G. Tononi, and R. Kötter. The human connectome: A structural description of the human brain. *PLoS Comput. Biol.*, 1(4):e42, 2005.

[197] H Eugene Stanley. Phase transitions and critical phenomena. *Clarendon, Oxford*, page 9, 1971.

[198] A. C. Staver, S. Archibald, and S. A. Levin. The global extent and determinants of savanna and forest as alternative biome states. *Sciences*, 334(6053):230–232, 2011.

[199] A. C. Staver and S. A. Levin. Integrating theoretical climate and fire effects on savanna and forest systems. *Am. Nat.*, 180:211–224, 2012.

[200] Sharon Y Strauss, Jennifer A Lau, Thomas W Schoener, and Peter Tiffin. Evolution in ecological field experiments: implications for effect size. *Ecology Letters*, 11(3):199–207, 2008.

[201] Y. E. Stuart, T. S. Campbell, P. A. Hohenlohe, R. G. Reynolds, L. J. Revell, and J. B. Losos. Rapid evolution of a native species following invasion by a congener. *Science*, 346(6208):463–466, 2014.

[202] Enzo Tagliazucchi, Pablo Balenzuela, Daniel Fraiman, and Dante R Chialvo. Criticality in large-scale brain fmri dynamics unveiled by a novel point process analysis. *Front. Physiol.*, 3(15), 2012.

[203] Mark L Taper and Ted J Case. Models of character displacement and the theoretical robustness of taxon cycles. *Evolution*, pages 317–333, 1992.

[204] C. M. Taylor and A. Hastings. Allee effects in biological invasions. *Ecol. Lett.*, 8:895–908, 2005.

[205] R. Thom. Topological models in biology. *Topology*, 8:313–335, 1969.

[206] John N Thompson. Rapid evolution as an ecological process. *Trends in Ecology & Evolution*, 13(8):329–332, 1998.

[207] David Tilman. *Plant strategies and the dynamics and structure of plant communities*. Number 26. Princeton University Press, 1988.

[208] David Tilman. Niche tradeoffs, neutrality, and community structure: a stochastic theory of resource competition, invasion, and community assembly. *Proceedings of the National Academy of Sciences of the United States of America*, 101(30):10854–10861, 2004.

[209] David Tilman, Peter B Reich, and Johannes MH Knops. Biodiversity and ecosystem stability in a decade-long grassland experiment. *Nature*, 441(7093):629–632, 2006.

[210] David Tilman and Emilie C Snell-Rood. Ecology: Diversity breeds complementarity. *Nature*, 515:44–45, 2014.

[211] Jabus Tyerman, Naomi Havard, Gerda Saxer, Michael Travisano, and Michael Doebeli. Unparallel diversification in bacterial microcosms. *Proceedings of the Royal Society of London B: Biological Sciences*, 272(1570):1393–1398, 2005.

[212] Sorin Tănase-Nicola and David K. Lubensky. Exchange of stability as a function of system size in a nonequilibrium system. *Phys. Rev. E.*, 86:040103, 2012.

[213] NG Van Kampen. *Stochastic Processes in Physics and Chemistry*, volume 1. Elsevier, 1992.

[214] F. Vazquez, J.A. Bonachela, C. López, and M.A Muñoz. Temporal griffiths phases. *Phys. Rev. Lett.*, 106:235702, 2011.

[215] F. Vazquez, C. López, J. M. Calabrese, and M. A. Muñoz. Dynamical phase coexistence: a simple solution to the "savanna problem". *J. Theor. Biol.*, 264(2):360–366, 2010.

[216] Mart Verwijmeren, Max Rietkerk, Martin J Wassen, and Christian Smit. Interspecific facilitation and critical transitions in arid ecosystems. *Oikos*, 122(3):341–347, 2013.

[217] Paula Villa Martín, Juan A. Bonachela, and Miguel A. Muñoz. Quenched disorder forbids discontinuous transitions in nonequilibrium low-dimensional systems. *Phys. Rev. E*, 89:012145, Jan 2014.

[218] T. Vojta, , and M. Y. Lee. Nonequilibrium phase transition on a randomly diluted lattice. *Phys. Rev. Lett.*, 96:035701, 2006.

[219] Thomas Vojta. Disorder-Induced Rounding of Certain Quantum Phase Transitions. *Phys. Rev. Lett.*, 90(10):107202, March 2003.

[220] Thomas Vojta. Rare region effects at classical, quantum and nonequilibrium phase transitions. *Journal of Physics A: Mathematical and General*, 39(22):R143, 2006.

[221] Thomas Vojta and Mark Dickison. Critical behavior and Griffiths effects in the disordered contact process. *Phys Rev E*, 72(3 Pt 2):36126, 2005.

[222] Thomas Vojta, Adam Farquhar, and Jason Mast. Infinite-randomness critical point in the two-dimensional disordered contact process. *Phys. Rev. E*, 79(1):11111, 2009.

[223] I. Volkov, J.I. Banavar, S.P. Hubbell, and A. Maritan. Neutral theory and relative species abundance in ecology. *Nature*, 424:1035–1037, 2003.

[224] Sheng-Jun Wang, Claus C Hilgetag, and Changsong Zhou. Sustained activity in hierarchical modular neural networks: self-organized criticality and oscillations. *Frontiers in computational neuroscience*, 5(June):30, 2011.

[225] Sheng-Jun Wang and Changsong Zhou. Hierarchical modular structure enhances the robustness of self-organized criticality in neural networks. *New Journal of Physics*, 14(2):23005, 2012.

[226] Haim Weissmann and Nadav M. Shnerb. Stochastic desertification. *Europhys. Lett.*, 106(2):28004, 2014.

[227] K. G. Wilson. Confinement of quarks. *Phys. Rev. D*, 10:2445, 1974.

[228] A. Windus and H.J Jensen. Phase transitions in a lattice population model. *J. Phys. A: Math. Theor.*, 40:2287–2297, 2007.

[229] Alastair Windus and Henrik J. Jensen. Change in order of phase transitions on fractal lattices. *Physica A*, 388:3107–3112, 2009.

[230] Da-Jiang Liu Xiaofang Guo and J. W. Evans. Generic two-phase coexistence, relaxation kinetics, and interface propagation in the quadratic contact process: Simulation studies. *Phys. Rev. E.*, 75:061129, 2007.

[231] Takehito Yoshida, Laura E Jones, Stephen P Ellner, Gregor F Fussmann, and Nelson G Hairston. Rapid evolution drives ecological dynamics in a predator–prey system. *Nature*, 424(6946):303–306, 2003.

[232] G. Zamora-López, C. Zhou, and J. Kurths. Cortical hubs form a module for multisensory integration on top of the hierarchy of cortical networks. *Front. Neuroinform.*, 4:1, 2010.

[233] Robert Ziff, Erdagon Gulari, and Yoav Barshad. Kinetic Phase Transitions in an Irreversible Surface-Reaction Model. *Phys. Rev. Lett.*, 56(24):2553–2556, June 1986.

[234] R. S. Zucker and W. G. Regehr. Short-Term Synaptic Plasticity. *Annu. Rev. Physiol*, 64:355–405, 2002.

[235] Debra Zuppinger-Dingley, Bernhard Schmid, Jana S Petermann, Varuna Yadav, Gerlinde B De Deyn, and Dan FB Flynn. Selection for niche differentiation in plant communities increases biodiversity effects. *Nature*, 515(7525):108–111, 2014.